



Virginia Commonwealth University
VCU Scholars Compass

Theses and Dissertations

Graduate School

2012

Impact of Post-Synthesis Modification of Nanoporous Organic Frameworks on Selective Carbon Dioxide Capture

Timur İslamoğlu
Virginia Commonwealth University

Follow this and additional works at: <https://scholarscompass.vcu.edu/etd>

 Part of the [Chemistry Commons](#)

© The Author

Downloaded from

<https://scholarscompass.vcu.edu/etd/454>

This Thesis is brought to you for free and open access by the Graduate School at VCU Scholars Compass. It has been accepted for inclusion in Theses and Dissertations by an authorized administrator of VCU Scholars Compass. For more information, please contact libcompass@vcu.edu.

© COPYRIGHT BY

Timur İslamođlu

2013

All Rights Reserved

**IMPACT OF POST-SYNTHESIS MODIFICATION OF NANOPOROUS ORGANIC
FRAMEWORKS ON SELECTIVE CARBON DIOXIDE CAPTURE**

A thesis submitted in partial fulfillment of the requirements for the degree of Master of Science at Virginia Commonwealth University.

by

Timur İslamoğlu

Bachelor of Science, Chemistry, Dumlupınar University, 2008

Bachelor of Science, Mathematics, Dumlupınar University, 2009

Director: Hani M. El-Kaderi,

Assistant Professor, Department of Chemistry

Virginia Commonwealth University

Richmond, Virginia

January, 2013.

Acknowledgement

I would like to acknowledge the support and guidance of Professor Dr. Hani M. El-Kaderi whose ideas and talents helped to make this work possible. I would also like to acknowledge my committee members Professor Dr. Scott Gronert, Professor Dr. Indika Arachiche, and Professor Dr. Purusottam Jena for their input in pursuit of a degree. I am very thankful to the members of the El-Kaderi Group who have been a pleasure to work beside. I would also like to thank the Department of Chemistry at Virginia Commonwealth University for giving me the chance to pursue a master degree. I would also like to acknowledge the Republic of Turkey Ministry of National Education for graduate fellowship at Virginia Commonwealth University. I would especially like to thank my family for all their love and care. My parents, İbrahim and Saniye İslamođlu have been, and continue to be, a true inspiration for what a good person can be. I would certainly like to thank my wonderful wife Ülkü İslamođlu as well. She is my other half and my better half. Without her by my side, I would not be close to the man that I am today.

Table of Contents

List of Tables.....	v
List of Figures	vi
List of Schemes	ix
List of Abbreviations.....	x
Abstract.....	xii
Chapter 1 Introduction.....	1
1.1 Global CO ₂ Concerns.....	1
1.2 CO ₂ Capture Technologies	2
1.3 Porous Solid Adsorbents for CO ₂ Capture	6
1.4 Synthesis of Porous Organic Materials	8
1.5 Post-Synthesis Modification of NPOFs	13
1.6 Thesis Problem	15
Chapter 2 Synthesis and Characterization of a Novel Nanoporous Organic Framework and its Post-Synthesis Modification.....	16
2.1 Introduction	16
2.2 Synthesis	17
2.2.1 Synthesis of Building Block.....	17
2.2.2 Synthesis of Nanoporous Organic Framework (NPOF-4).....	19
2.2.3 Post-Synthesis Nitration of NPOF-4	19

2.2.4	Post-Synthesis Reduction of NPOF-4-NO ₂	20
2.3	Characterization of Building Block and NPOFs.....	20
2.4	Results and Discussion.....	30
Chapter 3	Gas Storage Capabilities for Nanoporous Organic Frameworks	34
3.1	Introduction	34
3.2	Surface Area and Pore Size Characterization.....	37
3.3	Hydrogen, Carbon Dioxide, and Methane Sorption of Nanoporous Organic Frameworks	49
Chapter 4	Isosteric Heat of Adsorption of Carbon Dioxide, Methane, and Hydrogen with Nanoporous Organic Frameworks	58
4.1	Introduction	58
4.2	Experimental Calculations for the Isosteric Heat of Adsorption of Carbon Dioxide, Methane, and Hydrogen.....	60
Chapter 5	Gas Separation and Selectivity Capabilities for Nanoporous Organic Frameworks	69
5.1	Introduction	69
5.2	Results and Discussion.....	71
Chapter 6	Concluding Remarks	81
	List of References	83
	Vita.....	97

List of Tables

Table 3.1: Surface areas, pore size distributions and pore volumes for NPOF networks.	38
Table 4.1: Gas uptakes for NPOFs. Gas uptake in mg g^{-1} and the isosteric enthalpies of adsorption (Q_{st}) in kJ mol^{-1}	60
Table 5.1: Selectivity results for NPOFs.....	73
Table 5.2: CO_2 and N_2 uptakes at 273 and 298 K for CO_2/N_2 selectivity studies by using Equation 1.	80
Table 5.3: CO_2 and CH_4 uptakes at 273 and 298 K for CO_2/CH_4 selectivity studies by using Equation 1.	80

List of Figures

Figure 1.1: Different technologies and associated materials for CO ₂ separation and capture.	4
Figure 1.2: Schematic representation of pre-synthesis modification	12
Figure 1.3: Schematic representation of post-synthesis modification.....	12
Figure 2.1: ¹ H NMR for 1,3,5,7-tetrakis(4-acetylphenyl)adamantane in CDCl ₃	22
Figure 2.2: ¹³ C NMR for 1,3,5,7-tetrakis(4-acetylphenyl)adamantane in CDCl ₃	23
Figure 2.3: FT-IR spectra of TAPA, NPOF-4, NPOF-4-NO ₂ and NPOF-4-NH ₂	24
Figure 2.4: SEM images of NPOF-4, NPOF-4-NO ₂ and NPOF-4-NH ₂	25
Figure 2.5: TGA traces of NPOF-4, NPOF-4-NO ₂ and NPOF-4-NH ₂	26
Figure 2.6: XRD-patterns for NPOF-4, NPOF-4-NO ₂ and NPOF-4-NH ₂	27
Figure 2.7: Solid state ¹³ C CP-MAS NMR spectra of NPOF-4.	28
Figure 2.8: Solid state ¹³ C CP-MAS NMR spectra of NPOF-NO ₂	29
Figure 2.9: Solid state ¹³ C CP-MAS NMR spectra of NPOF-NH ₂	30
Figure 3.1: Image of Autosorb-1C with essential components labeled.	36
Figure 3.2: Argon uptake isotherms for NPOFs.	39
Figure 3.3: Pore size distribution for NPOF-4, NPOF-4-NO ₂ and NPOF-4-NH ₂	40
Figure 3.4: NLDFT calculated isotherm for NPOF-4 overlaid with the experimental Argon isotherm.	41
Figure 3.5: Multipoint BET plot for NPOF-4 calculated from the Argon adsorption in the range 0.04-0.16 P/P ₀	42

Figure 3.6: Langmuir plot for NPOF-4 calculated from the Argon adsorption in the range 0.05-0.25 P/P ₀	43
Figure 3.7: NLDFT calculated isotherm for NPOF-4-NO ₂ overlaid with the experimental Argon isotherm.....	44
Figure 3.8: Multipoint BET plot for NPOF-4-NO ₂ calculated from the Argon adsorption in the range 0.04-0.16 P/P ₀	45
Figure 3.9: Langmuir plot for NPOF-4-NO ₂ calculated from the Argon adsorption in the range 0.05-0.25 P/P ₀	46
Figure 3.10: NLDFT calculated isotherm for NPOF-4-NH ₂ overlaid with the experimental Argon isotherm.....	47
Figure 3.11: Multipoint BET plot for NPOF-4-NH ₂ calculated from the Argon adsorption in the range 0.04-0.16 P/P ₀	48
Figure 3.12: Langmuir plot for NPOF-4-NH ₂ calculated from the Argon adsorption in the range 0.05-0.25 P/P ₀	49
Figure 3.13: Carbon dioxide isotherms for NPOFs at 273 K.	50
Figure 3.14: Carbon dioxide isotherms for NPOFs at 298 K.	51
Figure 3.15: Methane isotherms for NPOFs at 273 K.	52
Figure 3.16: Methane isotherms for NPOFs at 298 K.	53
Figure 3.17: Hydrogen isotherms for NPOFs at 77 K.....	54
Figure 3.18: Hydrogen isotherms for NPOFs at 87 K.....	55
Figure 4.1: Carbon dioxide isosteric heat of adsorption curves of NPOFs.	63
Figure 4.2: Methane isosteric heat of adsorption curves of NPOFs.	64
Figure 4.3: Hydrogen isosteric heat of adsorption curves of NPOFs.....	65

Figure 4.4: Virial analysis curve fitting of CO ₂ adsorption isotherms for NPOF-4, NPOF-4-NO ₂ and NPOF-4-NH ₂	66
Figure 4.5: Virial analysis curve fitting of CH ₄ adsorption isotherms for NPOF-4, NPOF-4-NO ₂ and NPOF-4-NH ₂	67
Figure 4.6: Virial analysis curve fitting of H ₂ adsorption isotherms for NPOF-4, NPOF-4-NO ₂ and NPOF-4-NH ₂	68
Figure 5.1: Gas uptake selectivity studies for NPOF-4 at 273 K.	74
Figure 5.2: Gas uptake selectivity studies for NPOF-4 at 298 K.	75
Figure 5.3: Gas uptake selectivity studies for NPOF-4-NO ₂ at 273 K.....	76
Figure 5.4: Gas uptake selectivity studies for NPOF-4-NO ₂ at 298 K.....	77
Figure 5.5: Gas uptake selectivity studies for NPOF-4-NH ₂ at 273 K.....	78
Figure 5.6: Gas uptake selectivity studies for NPOF-4-NH ₂ at 298 K.....	79

List of Schemes

Scheme 1.1: Yamamoto coupling formation of PAF-1 and PPN-4.	9
Scheme 1.2: A representative route for the synthesis of BILPs.	10
Scheme 1.3: Cyclotrimerization of acetyl groups to construct porous framework.	11
Scheme 1.4: Post-synthesis modification of Porous Polymer Networks.....	14
Scheme 2.1: Reaction scheme for synthesis of TAPA, NPOF-4, NPOF-4-NO ₂ , and NPOF-4-NH ₂	18

List of Abbreviations

BET	Brunauer–Emmett–Teller
BILP	Benzimidazole-Linked Polymer
BLP	Borazine-Linked Polymer
CCS	Carbon Capture and Sequestration
CMP	Conjugated Microporous Polymer
COF	Covalent Organic Framework
DCM	Dichloromethane
DFT	Density Functional Theory
FT-IR	Fourier Transform-Infrared Spectroscopy
IAST	Ideal Adsorbed Solution Theory
MEA	Monoethanolamine
MOF	Metal-Organic Framework
NLDFT	Non-Local Density Functional Theory
NMR	Nuclear Magnetic Resonance Spectroscopy
NPOF	Nanoporous Organic Framework
PAF	Porous Aromatic Framework
PECONF	Porous Electron-Rich Covalent Organo Nitridic Framework
PIM	Polymers of Intrinsic Microporosity
POP	Porous Organic Polymer

PPN.....Porous Polymer Network
PSM Post-Synthesis Modification
SEMScanning Electron Microscopy (Microscope)
TGA Thermogravimetric Analysis
XRD..... X-Ray Diffraction

Abstract

IMPACT OF POST-SYNTHESIS MODIFICATION OF NANOPOROUS ORGANIC FRAMEWORKS ON SELECTIVE CARBON DIOXIDE CAPTURE

By Timur İslamoğlu, M.Sc.

A thesis submitted in partial fulfillment of the requirements for the degree of Master of Science at Virginia Commonwealth University

Virginia Commonwealth University, 2013

Director: Hani M. El-Kaderi, Assistant Professor, Department of Chemistry

Porous organic polymers containing nitrogen-rich building units are among the most promising materials for selective CO₂ capture and separation applications that impact the environment and the quality of methane and hydrogen fuels. The work described herein describes post-synthesis modification of Nanoporous Organic Frameworks (NPOFs) and its impact on gas storage and selective CO₂ capture. The synthesis of NPOF-4 was accomplished via a catalysed cyclotrimerization reaction of 1,3,5,7-tetrakis(4-acetylphenyl)adamantane in Ethanol/Xylenes mixture using SiCl₄ as a catalyst. NPOF-4 is microporous and has high surface area ($SA_{BET} = 1249 \text{ m}^2 \text{ g}^{-1}$). Post-synthesis modification of NPOF-4 by nitration afforded (NPOF-4-NO₂) and subsequent reduction resulted in an amine-functionalized framework (NPOF-4-NH₂) that exhibits improved gas storage capacities and high CO₂/N₂ (139) and CO₂/CH₄ (15) selectivities compared to NPOF-4 under ambient conditions. These results demonstrate the impact

of nitro- and amine- pore decoration on the function of porous organic materials in gas storage and separation application.

Chapter 1

Introduction

1.1 Global CO₂ Concerns

The increase in CO₂ concentration in the atmosphere is an urgent global problem that needs to be addressed immediately. Over the last fifty years, CO₂ concentration has increased from about 310 ppm to over 390 ppm and CO₂ emission from power plants has been identified as one of major contributors.¹ Currently, ~85% of the world's energy comes from fossil fuel sources and realistically, this situation will not change until sustainable and cleaner energy sources and technologies become widely available at a reasonable cost which will take time.² An alternative way to reduce CO₂ emission is switching from coal-fired power plants to natural gas-fired power plants since natural gas has a lower carbon footprint. For the same reason, the use of natural gas in automotive applications is highly desired; however, natural gas found in reservoirs has tangible amounts of CO₂, N₂, and H₂S that need to be minimized before transport and use. Natural gas purification processes involve CO₂ and H₂S removal to prevent pipeline corrosion and to increase the energy density of this methane-rich gas making its onboard storage and use more effective. As a result of the economical and environmental impacts of gaseous impurities, selective CO₂ capture and sequestration (CCS) have attained great attention over the past decades. Particularly, the selective separation of CO₂ from N₂, CH₄, and H₂ has gained interest since carbon dioxide is the

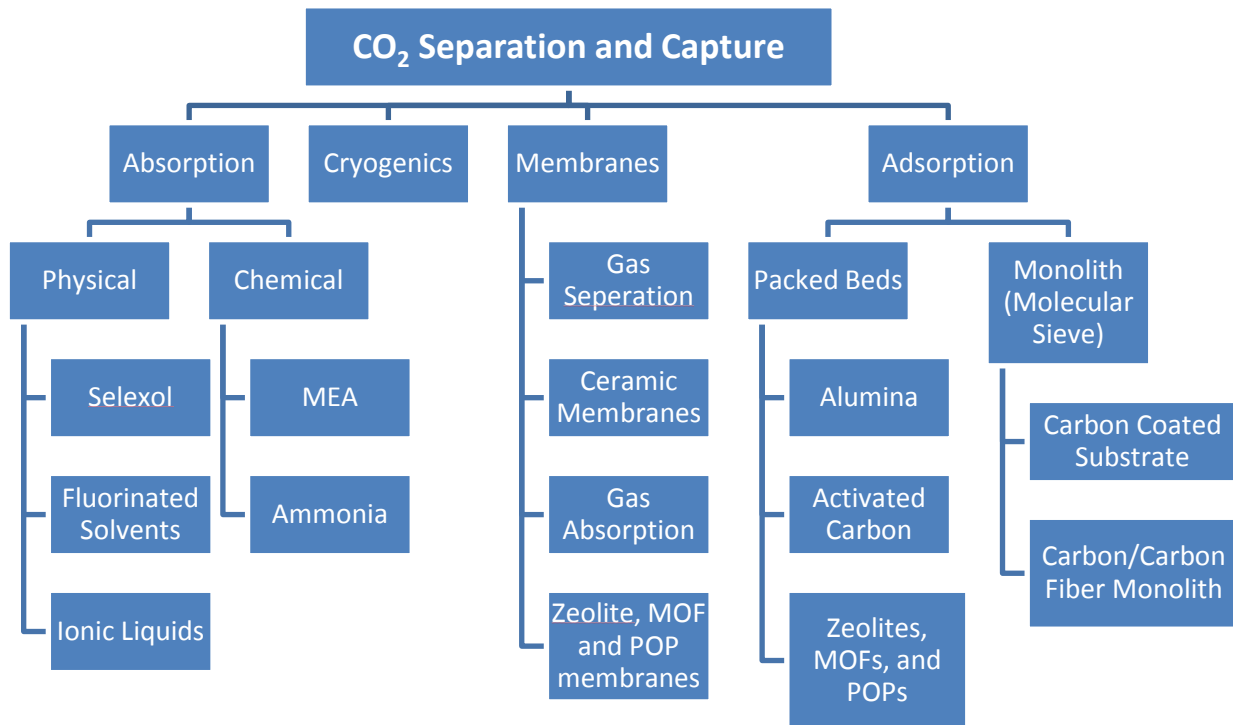
main impurity in flue gases (gases that exit to the atmosphere via an exhaust port such as smoke stacks from power plants) as well as natural gas. Advancements in this area by the scientific and industrial communities can limit the release of this greenhouse gas to the atmosphere and can lead to the production of high purity natural gas in a more economically and friendly manner.³⁻⁵

1.2 CO₂ Capture Technologies

Different technologies and associated materials exist for CO₂ separation and captures as schematically illustrated in Figure 1.1. With the current technology, the most widely employed method to capture CO₂ from flue gas is by chemisorption where CO₂ is chemically absorbed by solutions that contain amine organic solvent (typically 30 wt% in water) such as monoethanolamine (MEA) which is the most common amine compound used. In such systems, the flue gas is scrubbed with an amine solution, where up to 98% of CO₂ can be captured.⁶ The CO₂-laden solvent is then pumped to a second vessel where heat is applied to regenerate the amine solution by releasing absorbed CO₂. Even though this process is the current state-of-the-art technology, there are several concerns because of the enormous energy required for solvent regeneration. This concern stems from the fact that the regeneration of amine solutions consumes great amount of energy due to the high heat capacity of water. Moreover, the volatile nature of amines in addition to their decomposition during regeneration processes result in the loss of absorbent over time. In addition, amine sorbents themselves are corrosive, not stable in the presence of sulfur containing compounds, and during regeneration when the sorbent is heated, they can be oxidized by oxygen present in the gas stream.⁷ Recent studies have indicated that electricity cost would increase by ~80% if CO₂ were

to be captured by aqueous MEA absorption processes that eliminate CO₂ from the flue gas of coal-fired power plants and such processes can consume about 40% of the energy output of the plant.⁸ The expected properties of an ideal liquid absorbent can be summarized as high capture capacity and selectivity towards the targeted gas, regeneration with a minimal amount of input energy, thermal and chemical stability, and a straightforward synthetic route from accessible precursors. Today's inventories of adsorbents for carbon dioxide capture application, unfortunately, are far from combining two or more of these properties together.⁹

Figure 1.1: Different technologies and associated materials for CO₂ separation and capture.



Membrane-based CO₂ separation has also been studied extensively as an efficient way to capture CO₂. Membranes can be prepared from a wide range of materials such as organic polymers, zeolites, ceramics and they can be porous or non-porous. The driving force for CO₂ in the system can be achieved by having higher partial pressure on one side of the membrane relative to the other side which can be obtained by pressurizing the one side and/or applying vacuum on the other side. Membranes cannot be optimized for large volume of gas separation since they cannot usually achieve high degree of separation.¹⁰ Therefore, multiple treatments are

necessary and also they suffer from sulfur and other trace contaminants. In addition, their feasibility decreases when CO₂ concentration in the feed stream are below 20%.¹¹

Another approach to capture CO₂ from flue gas is the use of porous solids. With this approach, the regeneration energy penalty is greatly reduced compared to MEA solution process because water is no longer part of the capturing process. The development of efficient systems with solid adsorbents depends on the design of new materials with high stability, reversible and high adsorption capacity, and high selectivity under industrial conditions. Zeolites and activated carbon have also been extensively studied for CO₂ capture.^{12,13} Even though zeolites, porous alumina silicate materials, perform better than MEA absorbents, their low CO₂ capacity and instability in the presence of water limit their usage.¹⁴ Activated carbon shows better CO₂ adsorption capacity compared to zeolites, but it generally suffers from low selectivity of CO₂ over N₂ and CH₄.⁶ Among the emerging alternatives that can mitigate the aforementioned problems are Metal-Organic Frameworks (MOFs). MOFs are crystalline hybrid materials that combine organic ligands (linkers) and metal ions (nodes) and they have attracted intense research interest due to their tunable chemical and physical properties. Their extremely high surface area, permanent porosity, thermal stability, well-defined structures, and tunable pore functionality have made them plausible adsorbents for CO₂ and other gases such as methane and hydrogen. However, the limited chemical stability of MOFs under practical conditions due to non-covalent nature of framework significantly limits their application to CO₂ capture and separation processes. To address this limitation, porous organic polymers (POPs), have been identified as alternatives for carbon capture from flue gas as well as natural gas sweetening. POPs

are highly cross-linked, amorphous polymers possessing nanopores with high surface area. Unlike MOFs, POPs are metal-free purely organic frameworks linked by covalent bonds and display remarkable physicochemical stability. Due to their stable covalent nature, POPs are in general not subject to hydrolysis in the presence of water and remain intact under acidic or basic conditions. Under thermodynamic and kinetic controls, POPs can be designed to form crystalline networks known as covalent-organic frameworks (COFs) such as those linked by B-O, C-N, and B-N bonds.¹⁵⁻¹⁷ It should be mentioned that these COFs have limited stability under aqueous conditions and lose their porosity. In contrast, POPs' physical and chemical stability allow for their chemical modification, a process that imparts desirable properties such as pore hydrophobicity which is central for gas separation and storage, sensing, and catalysis.

1.3 Porous Solid Adsorbents for CO₂ Capture

Porous materials, including POPs, are classified depending on the size of the pores. According to IUPAC classification, microporous solids have pore width not exceeding 2 nm; mesoporous materials are materials that exhibit pore width ranging from 2 - 50 nm, and macroporous materials having pores larger than 50 nm.¹⁸

Synthetic porous materials (MOFs, COFs, POPs, etc) have attracted considerable attention due to their tunable chemical and physical nature that is not accessible for other porous materials such as zeolites, porous silica, and activated carbon. They can be processed easily; for instance, they can be produced in a molded monolithic form that makes them very attractive for use in a wide range of applications. In addition, some soluble porous polymers can be processed by solvent-based

techniques without losing their porosity, in contrast to those of naturally occurring porous materials listed above.¹⁹

The list for synthetic porous organic materials includes those developed by El-Kaderi such as Benzimidazole-Linked Polymers (BILP),²⁰ Borazine-Linked Polymers (BLPs),^{21,22} and Nanoporous Organic Frameworks (NPOF),²³ and many other systems: Porous Aromatic Framework (PAF),²⁴ Porous Polymer Networks (PPN),²⁵ Polymer Intrinsic Microporosity (PIM),²⁶ Covalent Triazine Frameworks (CTZ)²⁷ and Conjugated Microporous Polymers (CMP).²⁸ Almost all synthetic strategies to obtain porous materials employ either ditopic or polytopic functional organic linkers in order to attain extended frameworks. Desired textural properties such as extremely high surface area, permanent porosity, and narrow pore size distribution can be achieved by varying the molecular building units during synthesis. Combined together, these parameters dictate the structure-function relationship in POPs and determine their effectiveness in CO₂ capture applications.

In order for a porous organic polymer to be useful for carbon capture from flue gas as well as natural gas stock, the following criteria must be met.⁶

- The adsorbent needs to have high CO₂ adsorption capacity in order to make adsorbent column smaller.
- The adsorbent needs to have high selectivity toward CO₂. Since CO₂ is not the major component, highly selective adsorbent will increase the quality of CO₂ capture.
- The adsorbent needs to be chemically stable since reactive chemicals such as oxygen and sulfur are also present as contaminants.

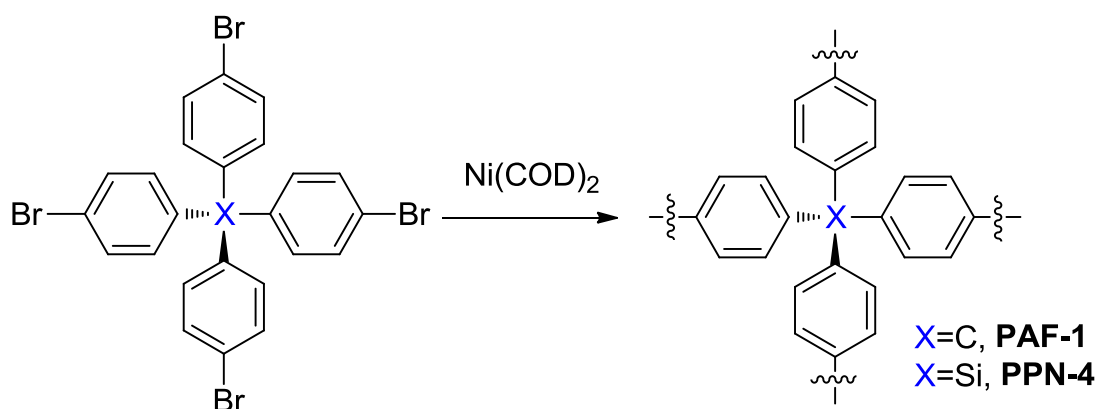
- The adsorbent needs to have mechanical stability in order to be densely packed for maximum volumetric capacity.
- The adsorbent itself and building blocks should be readily synthesized from abundant and accessible chemicals to make the process cost-effective.
- The regeneration of adsorbent should be achieved with minimal additional energy input to decrease the energy penalty of the total system.
- The mass and heat transfer of adsorbent should be good. Densely packed adsorbent should allow the adsorption and desorption of the guest molecules. In addition, heat conductivity is needed since temperature can be used to regenerate the adsorbents.

1.4 Synthesis of Porous Organic Materials

Several synthetic methods have been reported for the synthesis of porous organic materials and they mainly entail metal catalysts. Other methods are metal-free processes and represent a more “economical” way for the mass production of porous adsorbents. Probably, having many different routes to synthesize POPs is one of the most attractive features of this field. These synthetic routes include Yamamoto coupling,²⁴ Suzuki coupling,²⁹ imidazole ring formation,³⁰ Friedel-Crafts alkylation,³¹ dibenzo-dioxane formation,³² imidization,³³ amidation,³³ Sonogashira-Hagihara coupling,²⁸ imine formation,³⁴ nitrile cyclotrimerization²⁷ and acetyl cyclotrimerization.³⁵ In the following section, representative synthetic methodologies of porous organic materials are presented to highlight some of their advantages and shortcomings. One of the most extensively used methods for the synthesis of POPs is metal catalyzed cross-coupling reactions. In 2009, Qiu *et al.* reported a new class of POPs referred as PAF-1

(Porous Aromatic Framework).²⁴ PAF-1 was synthesized by Yamamoto coupling (Scheme 1.1) using tetra(bromo phenyl)methane as building block and it has an exceptionally high BET surface area of $5600 \text{ m}^2 \text{ g}^{-1}$ and remarkable gas uptake capacity (H_2 , CH_4 , CO_2) under high pressure. Due to its robust covalent nature, PAF-1 showed high thermal and chemical stability. However, carbon-based PAFs do not perform well in gas storage applications at low pressure (1.0 bar) due to their uniform and non-functionalized pore walls that lead to low isosteric heats of adsorption for small gases.

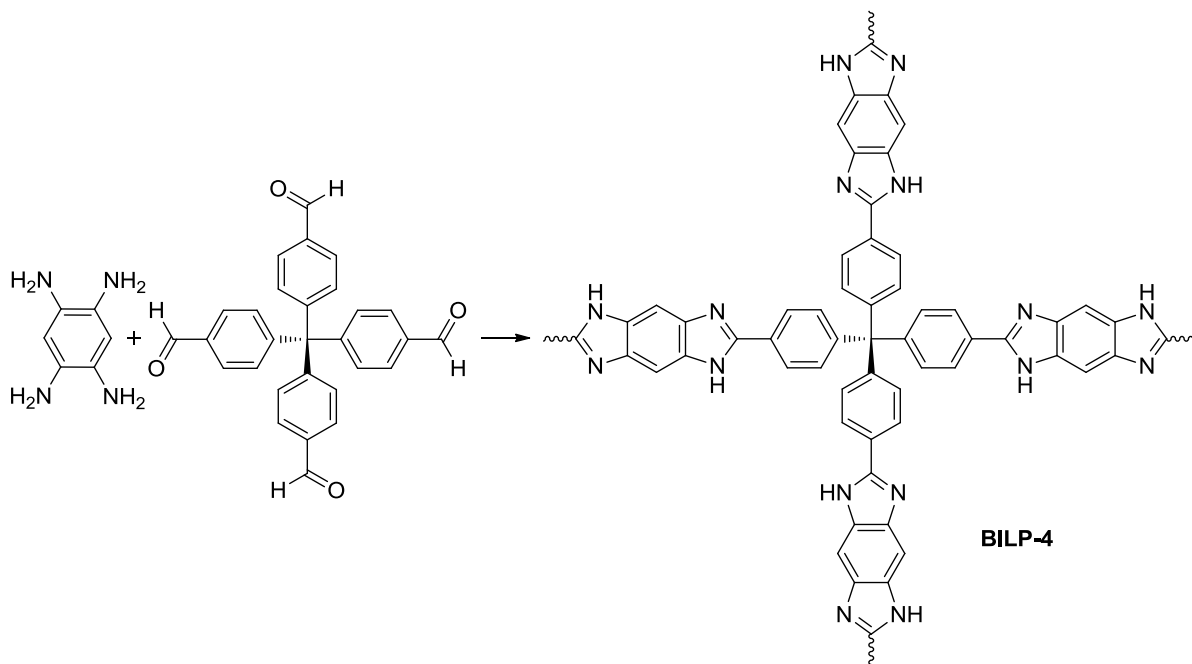
Scheme 1.1: Yamamoto coupling formation of PAF-1 and PPN-4.



Zhou and coworkers have synthesized several PPNs by employing the same method. They have extended the library of PAFs and modified their synthetic procedures that resulted in one of the highest surface area ($\text{SA}_{\text{BET}} = 6461 \text{ m}^2 \text{ g}^{-1}$) known to date as reported for PPN-4 (Scheme 1.1).³⁶ The very high surface area of PAF-1 and PPN-4 was attributed to the diamond-like framework topology which provides accessible pores with highly cross-linked structures. Another key point in the synthesis of PPN-4 was that the C-C coupling was carried out at room temperature to slow down the kinetic of the reaction and hence the overall network growth.

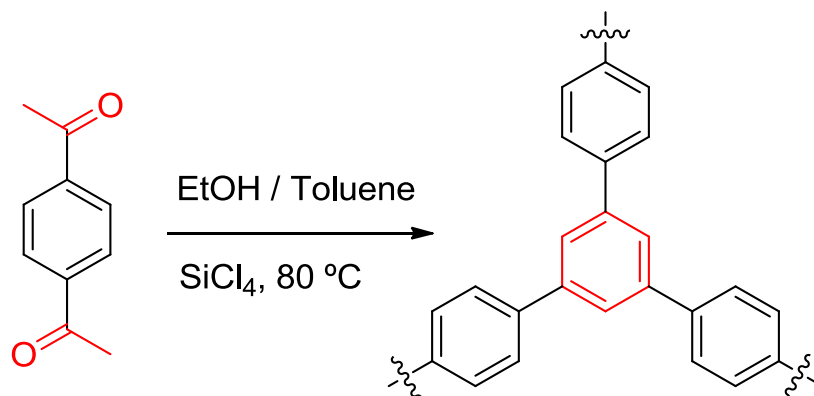
Very recently, El-Kaderi and coworkers introduced a new class of porous organic material called Benzimidazole-Linked Polymers (BILPs),²⁰ prepared by metal-free catalyzed condensation of aryl-o-diamine and arylaldehyde that resulted imidazole-ring formation (Scheme 1.2). Both experimental and theoretical studies have proven that having polar functional groups on pore surfaces increases the CO₂ uptake dramatically, especially at low pressures, and makes the material more selective for CO₂ over N₂ and CH₄. As such, the imidazole-functionalized pore walls in BILPs make this type of material one of the most attractive candidates for CO₂ capture application due to their selective nature and high CO₂ capacity. BILPs showed CO₂ uptake as high as 5.4 mmol g⁻¹ at 273 K and 1 bar and very good selectivity as high as 113 for CO₂ over N₂ and 17 for CO₂ over CH₄.³⁷

Scheme 1.2: A representative route for the synthesis of BILPs.



Kaskel and coworkers published a report where cyclotrimerization of bifunctional acetyl compounds were employed to synthesize porous organic polymers as illustrated in Scheme 1.3.³⁵

Scheme 1.3: Cyclotrimerization of acetyl groups to construct porous framework.



The polymers reported by Kaskel are hydrophobic in nature and exhibit only moderate surface area (up to 865 m² g⁻¹). Unlike PAFs, PPNs, and CMPs where cross-coupling reactions were used for the construction of the frameworks, Kaskel's polymerization strategy does not employ expensive or precious catalysts and therefore, is more viable for large-scale production processes. However, non-functional carbon based frameworks are less desirable for CO₂ capture due to their low affinity and low selectivity at ambient settings.

As mentioned above, selective CO₂ capture and capacity are the most important features for CO₂ adsorbents. High surface area materials do not necessarily lead to high CO₂ uptake since gas uptake capacity depends on the favorable interactions between pore walls and guest gas molecules. Among the new directions for enhancing these factors has been pore functionalization with polar groups such as -OH, -NH₂, -

SO₃, etc. Incorporation of these functionalities into the framework can be achieved by pre-synthesis modification (Figure 1.2) of the building blocks wherein CO₂-philic moieties are attached to building blocks before framework formation, automated functionalization as in the case of imidazole ring formation, or through post-synthesis modification (PSM) (Figure 1.3) processes in which functional groups are tethered to the pore walls after framework assembly.³⁸

Figure 1.2: Schematic representation of pre-synthesis modification. Adopted from reference 38.

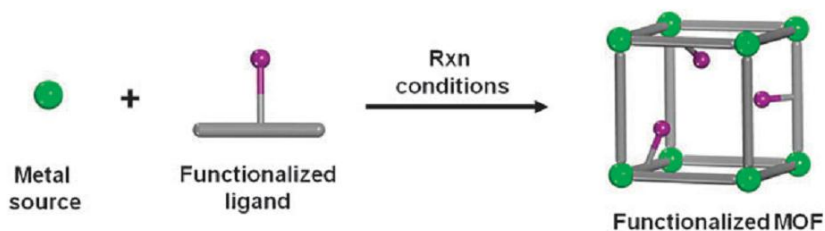
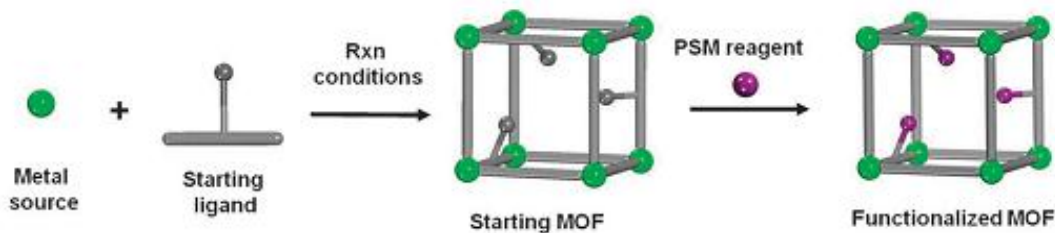


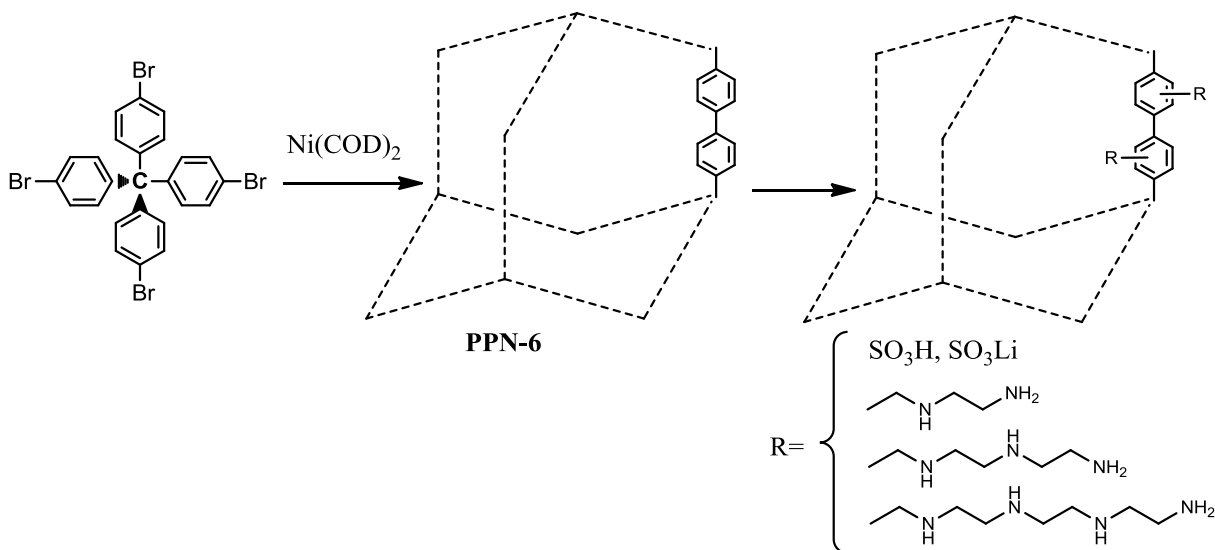
Figure 1.3: Schematic representation of post-synthesis modification. Adopted from reference 38.



1.5 Post-Synthesis Modification of NPOFs

Significant efforts have been devoted to the development of functional porous materials for use in gas storage and separation applications. Post-synthesis modification (PSM) is one way of synthesizing these functional NPOFs. The chemical and thermal stability of NPOFs have allowed researchers to introduce heterogeneity to the surface of the pores by PSM even under harsh reaction conditions in order to enhance the CO₂ uptake capacity as well as selectivity. Even though PSM of NPOFs have been studied more recently it is still in its early stage compared to MOFs. As stated above, targeted framework functionalities within the pores can be engineered through the functionalization of building block before the network formation which is known as pre-synthesis functionalization. However, there are some problems associated with this method. First, functionalization of building blocks often necessitates alternate reaction conditions (i.e. protection of some functional groups), and these reactions are often time consuming and non-trivial. In addition, the synthesis of NPOFs typically requires harsh conditions such as high temperature, acidic or basic media wherein the functional groups on the building blocks may not survive or lead to side reactions. Therefore, developing new methods for PSM of NPOFs is highly desirable.

Scheme 1.4: Post-synthesis modification of Porous Polymer Networks.



Zhou and coworkers have shown the successful incorporation of sulfonic acid and its lithium salt within the pores of PPN-6 (Scheme 1.4).^{39,40} PPN-6- SO_3H and PPN-6- SO_3Li exhibited significant increase in isosteric heat of adsorption and showed a substantial increase in the uptakes of H_2 and CO_2 .³⁹ This dramatic increase in the heat of adsorption and CO_2 uptake capacity is attributed to strong electrostatic interactions between sulfonic acid/ CO_2 and lithium/ CO_2 . The same group reported another study on PSM of PPNs. The latter work described PPN-6 functionalization with alkyl amine chains and the modified networks resulted in an excellent CO_2 uptake (4.3 mmol g^{-1}) and selectivity of CO_2/N_2 (442, calculated by Ideal Adsorbed Solution Theory) at 1 bar and 295 K (Scheme 1.4).⁴⁰

1.6 Thesis Problem

A significant need exists for improving CO₂ capture from flue gas as CO₂ emission from power plants is the main cause for increasing CO₂ concentration in the atmosphere. Employing porous solid adsorbents to capture CO₂ is one of the most promising techniques; however, selective adsorption of CO₂ may not be possible if the framework does not have functional groups within the pores to attract CO₂. In addition, integrating these functionalities into the pores to engineer their chemical and physical environment is not always possible by using pre-functionalized building blocks. With these concerns in mind, the specific aims of the work described herein are summarized below:

1) To prepare highly porous networks that are chemically and physically robust, using viable and cost effective methods. The chemical nature of these materials should enable PSM processes to improve gas binding and selectivity.

2) Post-synthesis modification of the frameworks described above should offer moderate binding affinities that lead to high CO₂ capacity while permitting adsorbent regeneration without energy input in the form of heating.

3) Establish experimental methods to investigate the physical and textural properties of the frameworks before and after PSM and evaluate their performance in small gas uptake and selective binding.

Chapter 2

Synthesis and Characterization of a Novel Nanoporous Organic Framework and its Post-Synthesis Modification

2.1 Introduction

For a porous solid to be employed in flue gas CO₂ capture application, chemical and physical stability is also as important as CO₂ capture capacity because a typical flue gas sample is composed of 73-77% N₂, 7.4-15% CO₂, 6.2-14.6% H₂O, ~420 ppm SO₂, 50-300 ppm CO, 60-70 ppm NO_x, and ~4.45 ppm O₂ which depends on whether it is from gas-fired or coal-fired flue gas.⁴¹ Therefore, adsorbents are expected to maintain their porosity in the presence of these gases. In this regard, purely organic porous polymers are superior to MOFs because of their chemical stability under harsh conditions due to their covalent nature. By taking these concerns into consideration we chose tetraphenyl adamantane (TPA) as the starting building unit to synthesize NPOF-4 because of the rigid nature of the TPA core. TPA then was acetylated to afford 1,3,5,7-tetrakis(4-acetylphenyl)adamantane (TAPA). The latter was used to construct NPOF-4 through acetyl groups' cyclotrimerization. The tetrahedral structure of TPA can lead to the formation of 3-D frameworks that possess high accessible free volume for gas storage and separation. Post-synthesis modification of NPOF-4 was needed in order to improve selective CO₂ capture and storage. NPOF-4 functionalization was successfully

achieved by nitration of the benzene rings directly attached to the adamantane core, and by subsequent reduction of the nitro groups to amines.

2.2 Synthesis

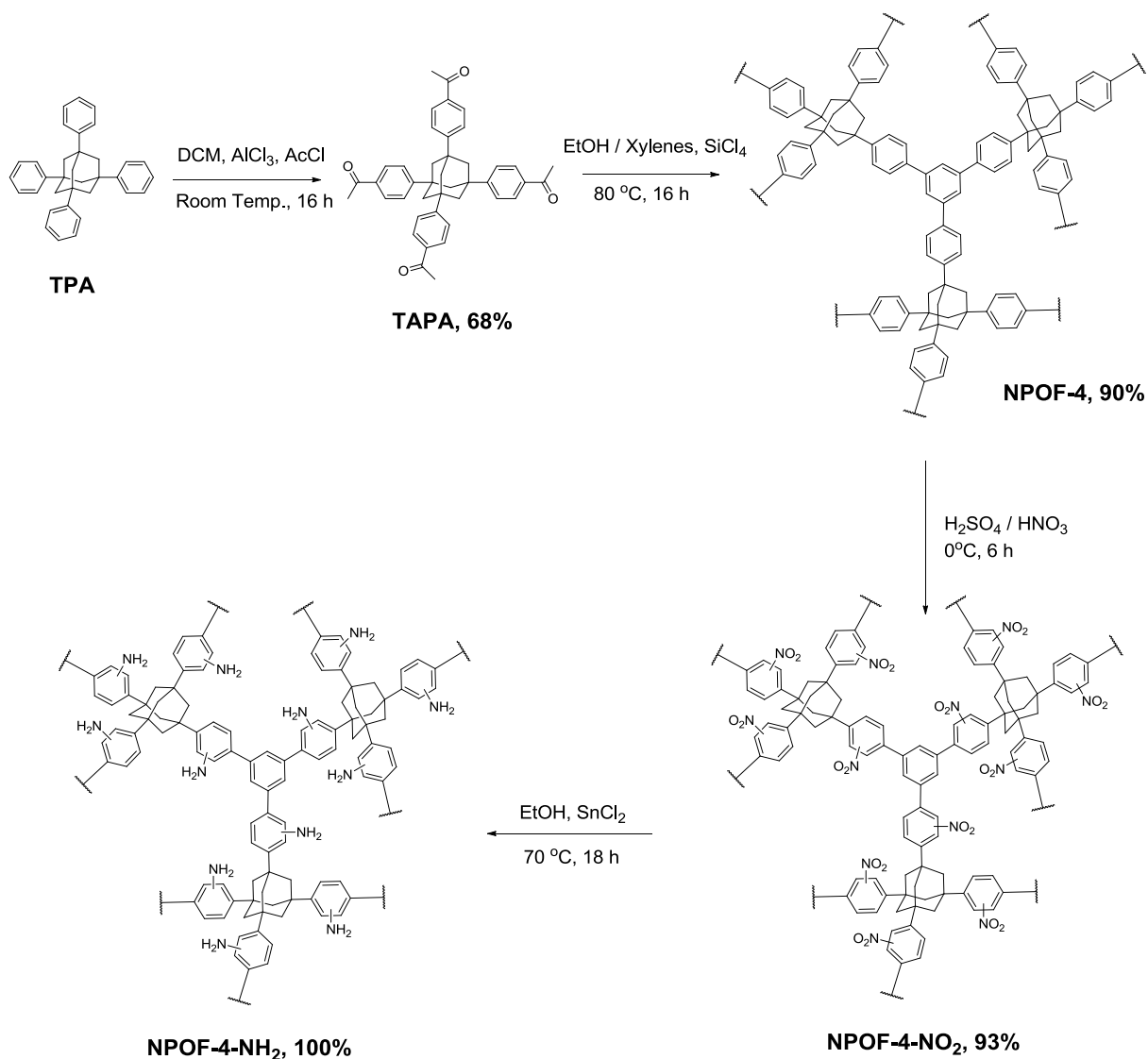
Starting materials and solvents, unless otherwise noted, were obtained from Acros Organics and used without further purification. 1,3,5,7-Tetraphenyladamantane was synthesized according to published method.⁴² SiCl_4 was purchased from Sigma-Aldrich. SnCl_2 was purchased from MP Biomedicals, LLC. Absolute ethanol was purchased from Pharmaco Products. Solvents were dried by distillation from Na (Xylenes) or Na/benzophenone (THF). Air-sensitive samples and reactions were handled under an inert atmosphere of nitrogen using either glovebox or Schlenk line techniques.

2.2.1 Synthesis of Building Block

The synthetic strategy for the preparation of TAPA is summarized in Scheme 2.1. A 250 mL reaction flask was charged with AlCl_3 (16.4 g, 123 mmol), placed in an ice bath and 90 mL of acetyl chloride (AcCl) was added to afford a colorless solution. A mixture of tetraphenyl adamantane (2.50 g, 5.67 mmol) and freshly distilled DCM (100 mL) was added to this solution at 0 °C and stirred for 10 minutes at 0 °C, and then it was allowed to warm to room temperature and stirred for 16 h. The reaction mixture was slowly poured into ice (200 mL) while stirring and then was stirred further for 30 minutes at room temperature. The organic layer was extracted with DCM, and wash with 10 % NaHCO_3 solution. The resulting yellow solution was dried over MgSO_4 , and filtered over glass frit. Excess DCM was removed by evaporation under reduced pressure. The resulting product was crystallized from Chloroform/Ethanol mixture to

afford off-white crystals in 68% yield (2.35 g, 3.86 mmol) upon concentration. ^1H NMR (CDCl_3 , 300 MHz) δ (ppm) 7.98 (d, $J_{\text{HH}} = 6.0$, 8H), 7.595 (d, $J_{\text{HH}} = 9.0$, 8H), 2.61 (s, 12H), 2.24 (s, 12H). ^{13}C NMR (CDCl_3 , 75 MHz) δ (ppm) 197.9, 154.0, 135.7, 128.9, 125.5, 46.8, 39.8, 26.9. Anal. Calcd. for $\text{C}_{42}\text{H}_{40}\text{O}_4 \cdot 0.5\text{CHCl}_3$: C, 76.36; H, 6.11. Found: C, 76.12; H, 6.07. TOF MS ES+ m/z for $\text{C}_{42}\text{H}_{40}\text{O}_4$ Calcd 609.30, $[\text{M}+\text{H}]^+$ 609.35. ⁴³

Scheme 2.1: Reaction scheme for synthesis of TAPA, NPOF-4, NPOF-4- NO_2 , and NPOF-4- NH_2 .



2.2.2 Synthesis of Nanoporous Organic Framework (NPOF-4)

The synthetic strategy for the preparation of NPOF-4 is summarized in Scheme 2.1. A 100 mL reaction flask was charged with TAPA (300 mg, 0.493 mmol), 60 mL absolute Ethanol and 60 mL Xylenes (dried over Na). The colorless solution was cooled to 0 °C, and SiCl₄ (18.3 mL, 157.8 mmol) was added dropwise. The solution was allowed to stir for 30 minutes at 0 °C, and then 1 hour at room temperature giving a black colored solution which was further refluxed at 80 °C for 16 h. The solution was allowed to cool down to room temperature and then was filtered over a glass frit. The bright yellow powder was washed with Ethanol, 2.0 M HCl, 2.0 M NaOH, water, and DCM, and then dried at 70 °C in the oven to afford NPOF-4 (240 mg, 90% yield) as a yellow powder. Anal. Calcd. for C₁₂₆H₉₆: C, 93.99; H, 6.01. Found: C, 83.09; H, 6.11.³⁵

2.2.3 Post-Synthesis Nitration of NPOF-4

The synthetic strategy for the post-synthesis nitration of NPOF-4 is summarized in Scheme 2.1. A 50 mL round bottom flask was charged with 12.5 mL of concentrated H₂SO₄, and then cooled to 0 °C. To this solution, 180 mg NPOF-4 was added in small portions followed by a dropwise addition of 9 mL 70% HNO₃, and was stirred for 6 h at 0 °C. The mixture was then poured into 100 mL ice. The resulting mixture was stirred for 30 minutes at room temperature, and then washed with water and EtOH. The resulting brown powder was soaked in ethanol/water mixture for 16 h and then was filtered and dried in air at 80 °C for 12 h to give NPOF-4-NO₂ (225 mg, 93% yield) as a brown powder. Anal. Calcd. for C₁₂₆H₈₄N₁₂O₂₄: C, 70.39; H, 3.94; N, 7.82. Found: C, 67.52; H, 4.61; N, 7.84.⁴⁴

2.2.4 Post-Synthesis Reduction of NPOF-4-NO₂

The synthetic strategy for the post-synthesis reduction of NPOF-4-NO₂ is summarized in Scheme 2.1. A 100 mL reaction flask was charged with 210 mg NPOF-4-NO₂, 50 mL Ethanol, and 3.0 g SnCl₂. The mixture was refluxed at 70 °C for 18 h. The resulting green suspension was filtered, then suspended in 20 mL concentrated HCl and stirred for 16 h at room temperature. Then HCl was replenished and stirring continued for 5 h at room temperature. The mixture was filtered and washed with 2 M NaOH solution, then sufficient amount of water. The resulting polymer was washed with EtOH, dried in air at 80 °C for 6 h to give NPOF-4-NH₂ (180 mg, 100% yield) as a dark brown powder. Anal. Calcd. for C₁₂₆H₁₀₈N₁₂: C, 84.53; H, 6.08; N, 9.39. Found: C, 65.55; H, 4.96; N, 8.39.⁴⁴

Note: the low carbon content may be due to several issues that still need to be addressed; among these issues are partial reduction of the nitro groups, residual tin chloride, or trapped HCl.

2.3 Characterization of Building Block and NPOFs

The chemical composition and structural aspects of these nanoporous frameworks were investigated by spectral and analytical methods. Elemental microanalyses were performed at the Midwest Microlab, LLC. Liquid ¹H and ¹³C NMR spectra were obtained on a Varian Mercury-300 MHz NMR spectrometer (75 MHz carbon frequency). Solid-state ¹³C cross-polarization magic angle spinning (CP-MAS) NMR spectra for solid samples were taken at Spectral Data Services, Inc. Spectra were obtained using a Tecmag-based NMR spectrometer operating at a H-1 frequency of 363

MHz, using a contact time of 1 ms and a delay of three seconds for the CPMAS experiment. All samples were spun at 7.0 kHz. Thermogravimetric analysis (TGA) were carried out using a TA Instruments Q-5000IR series thermal gravimetric analyzer with samples held in 50 μ L platinum pans under an atmosphere of air (heating rate 5 $^{\circ}$ C /min). For Scanning Electron Microscopy imaging (SEM), samples were prepared by dispersing the material onto a sticky carbon surface attached to a flat aluminum sample holder. The samples were then coated with platinum at 1×10^{-5} mbar of pressure in a nitrogen atmosphere for 90 seconds before imaging. Images were taken on a Hitachi SU-70 Scanning Electron Microscope. Powder X-ray diffraction data were collected on a Panalytical X'pert pro multipurpose diffractometer (MPD). Samples were mounted on a sample holder and measured using Cu K α radiation with a 2θ range of 1.5-35. FT-IR spectra were obtained on a Nicolet-Nexus 670 spectrometer furnished with an attenuated total reflectance accessory. Porosity and gas sorption experiments were collected using a Quantachrome Autosorb 1-C volumetric analyzer using adsorbates of UHP grade. In a typical experiment, a sample of polymer (~ 60 mg) was loaded into a 9 mm large bulb cell (from Quantachrome) of known weight and then hooked up to the Autosorb 1-C and degassed at 120 $^{\circ}$ C for 12 hours. The degassed sample was refilled with helium, weighed precisely, and then transferred back to the analyzer. The temperatures for adsorption measurements were controlled by using a refrigerated bath of liquid nitrogen (77 K), liquid Argon (87 K), or temperature controlled water bath (273 and 298 K).

Figure 2.1: ^1H NMR for 1,3,5,7-tetrakis(4-acetylphenyl)adamantane in CDCl_3 .

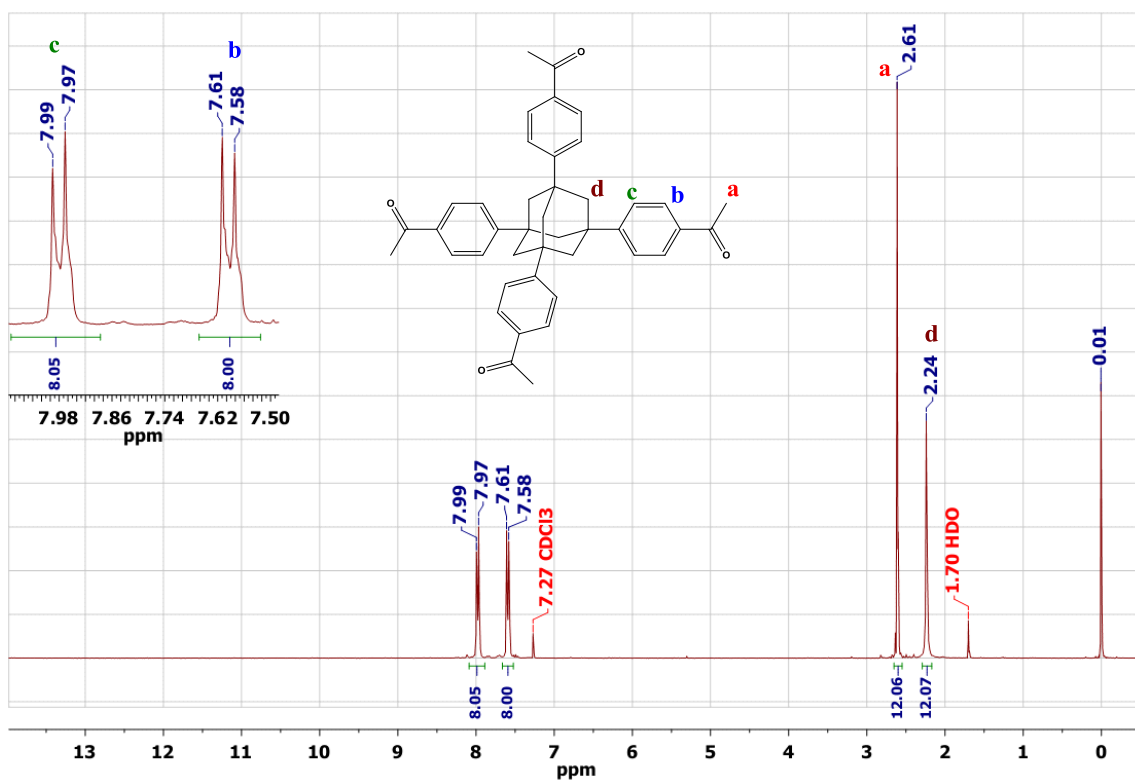


Figure 2.2: ^{13}C NMR for 1,3,5,7-tetrakis(4-acetylphenyl)adamantane in CDCl_3 .

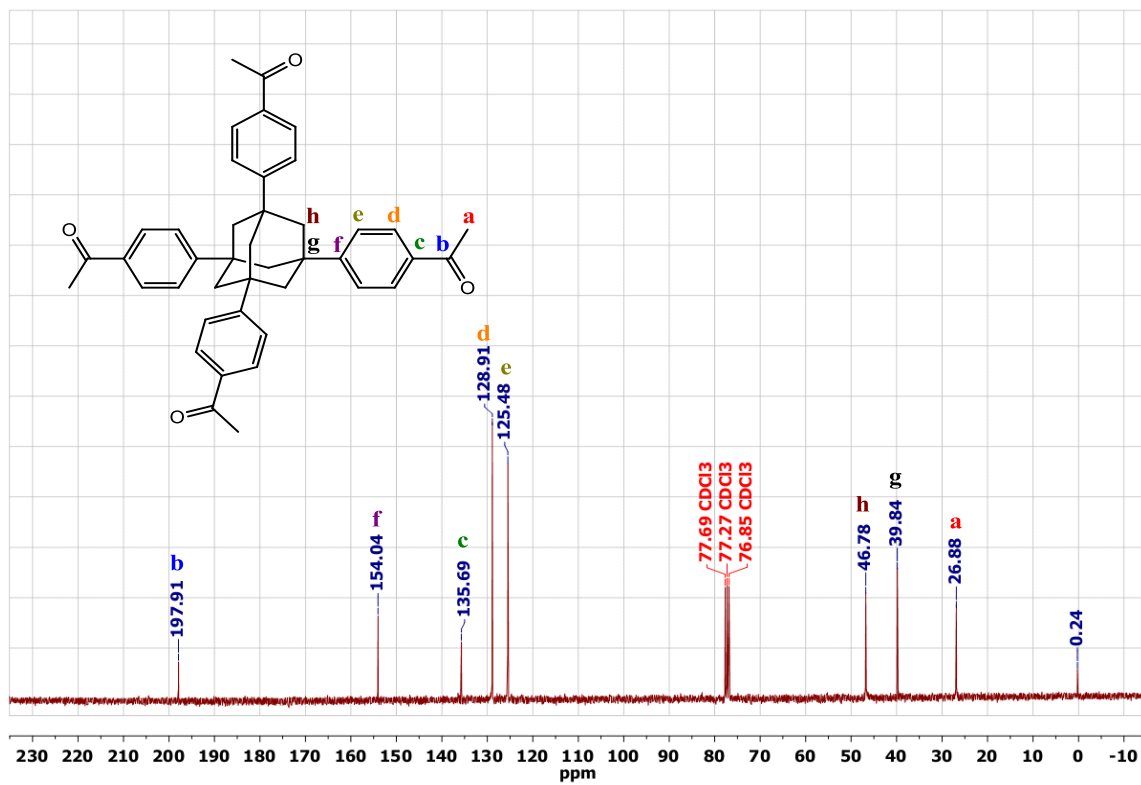


Figure 2.3: FT-IR Spectra of TAPA, NPOF-4, NPOF-4-NO₂ and NPOF-4-NH₂.

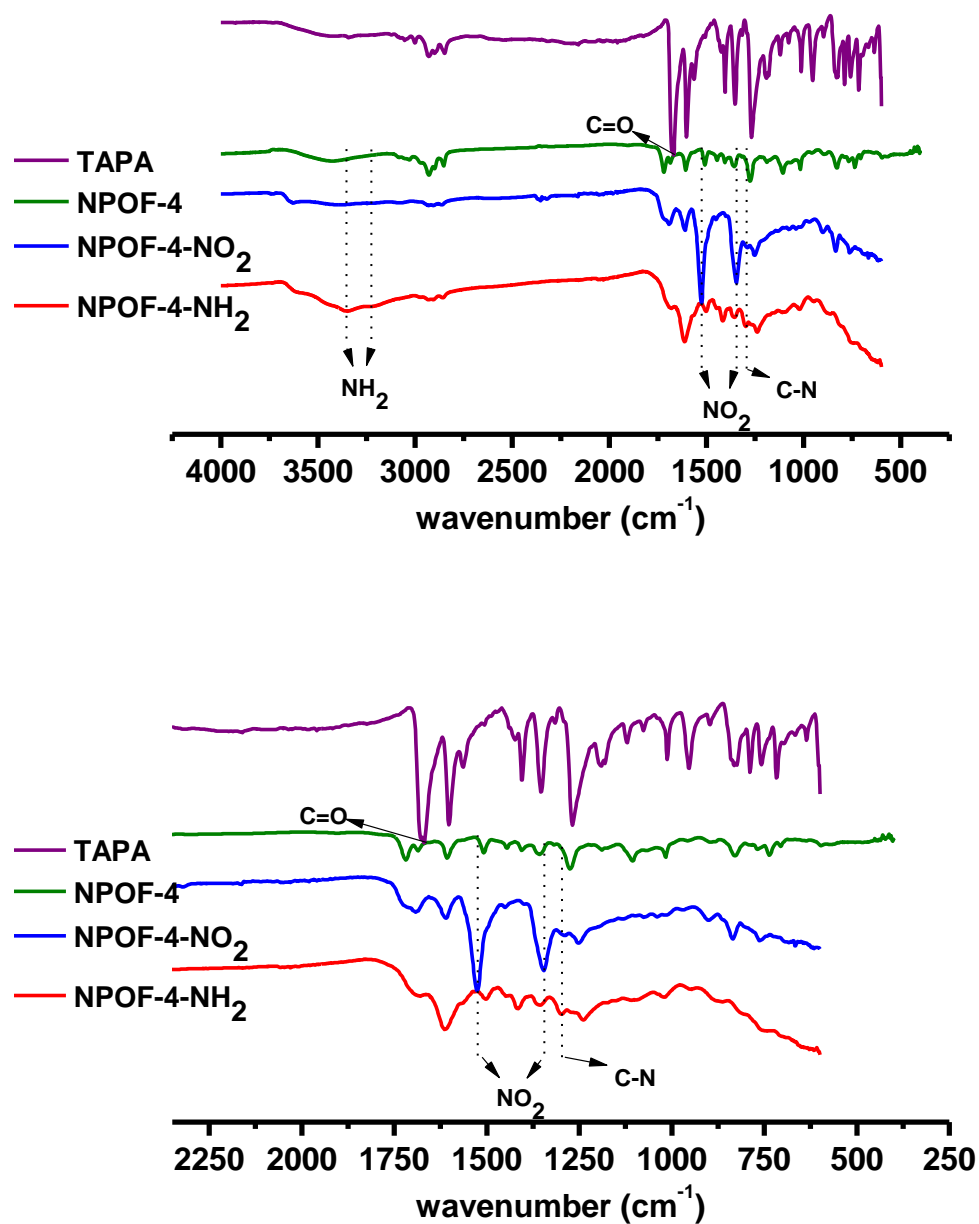
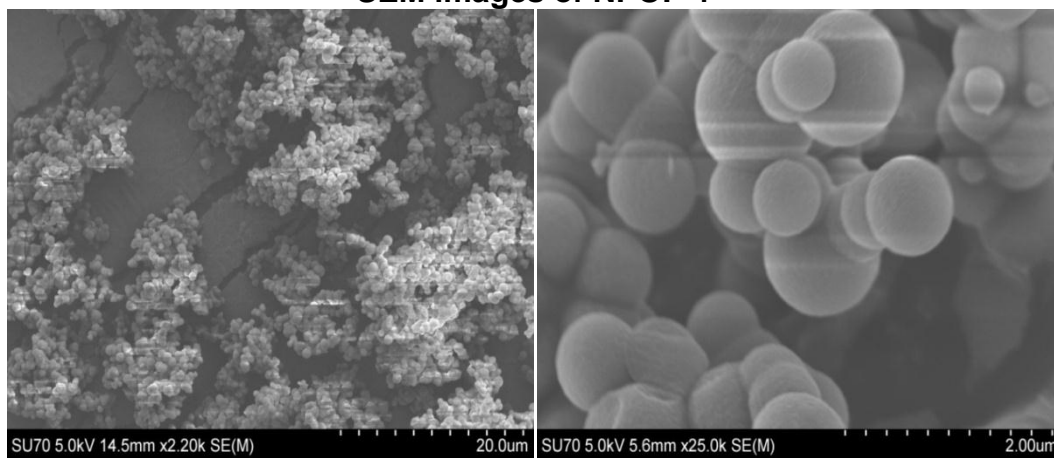
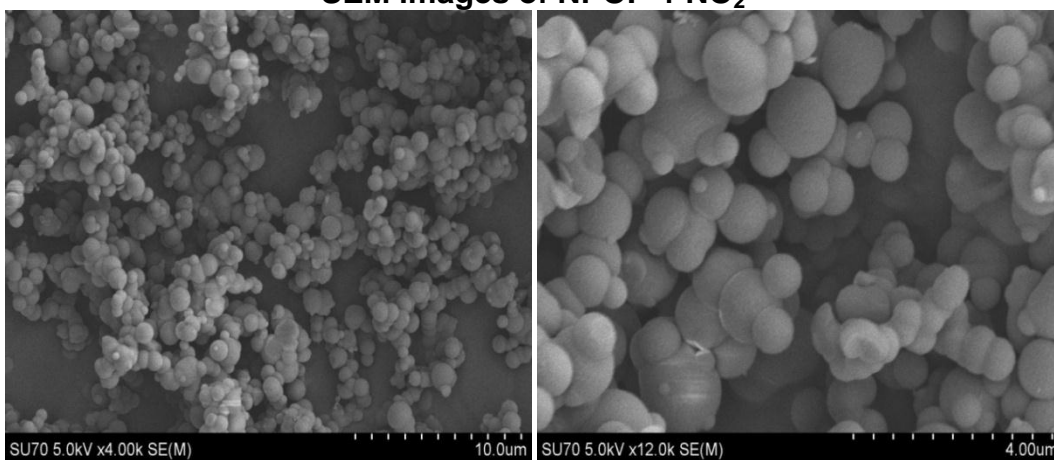


Figure 2.4: SEM images of NPOF-4, NPOF-4-NO₂ and NPOF-4-NH₂.

SEM images of NPOF-4



SEM images of NPOF-4-NO₂



SEM images of NPOF-4-NH₂

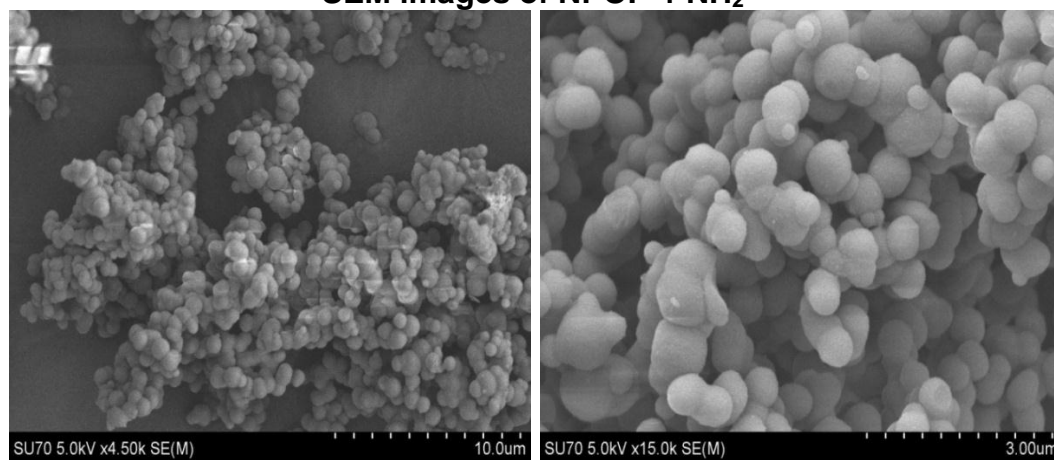


Figure 2.5: TGA Traces of NPOF-4, NPOF-4-NO₂ and NPOF-4-NH₂.

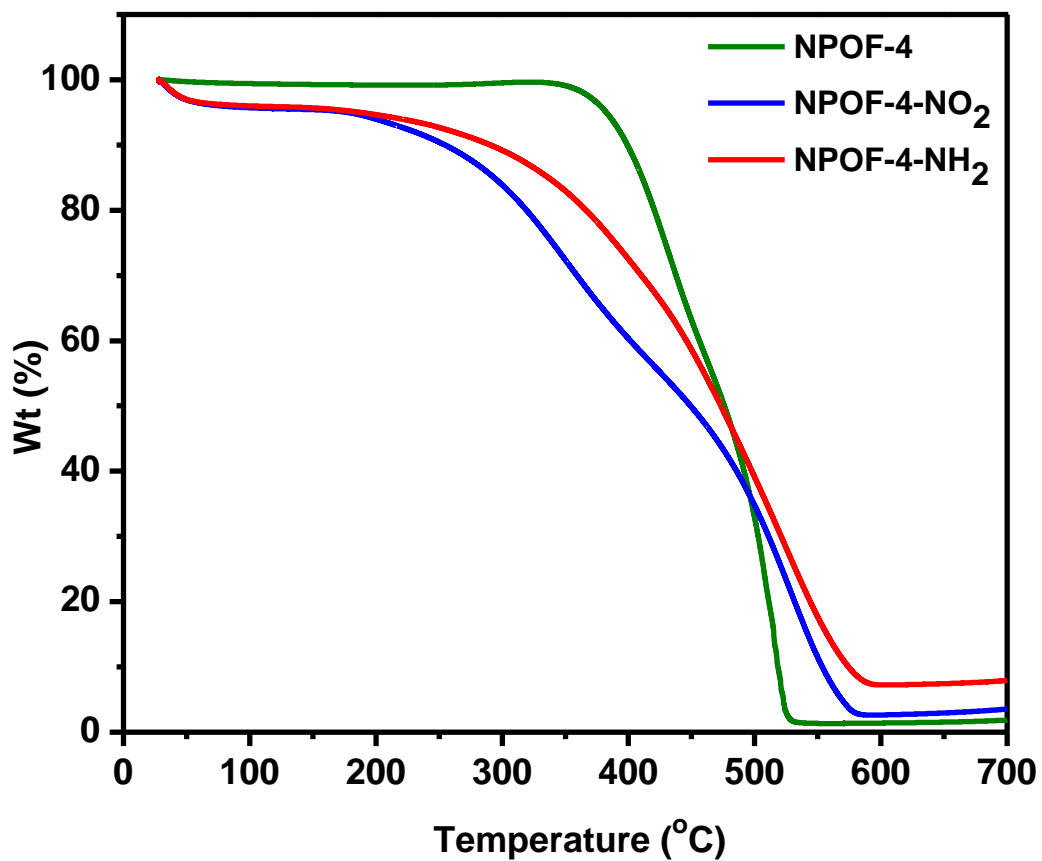


Figure 2.6: XRD Patterns for NPOF-4, NPOF-4-NO₂ and NPOF-4-NH₂.

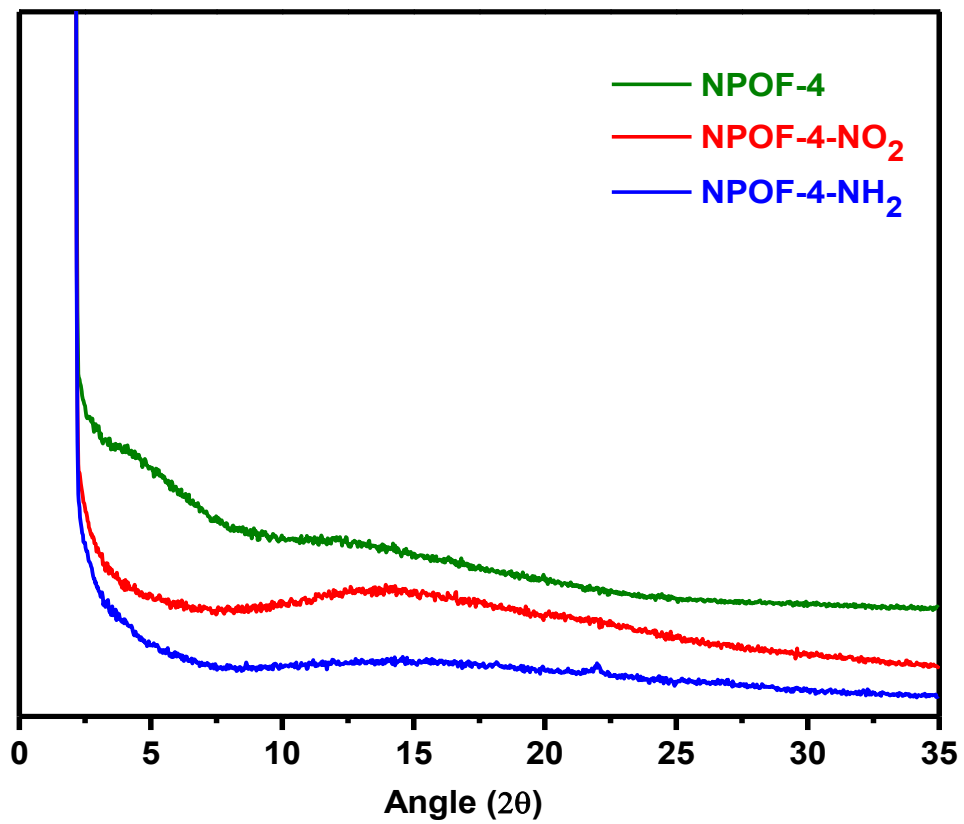


Figure 2.7: Solid state ^{13}C CP-MAS NMR spectra of NPOF-4.

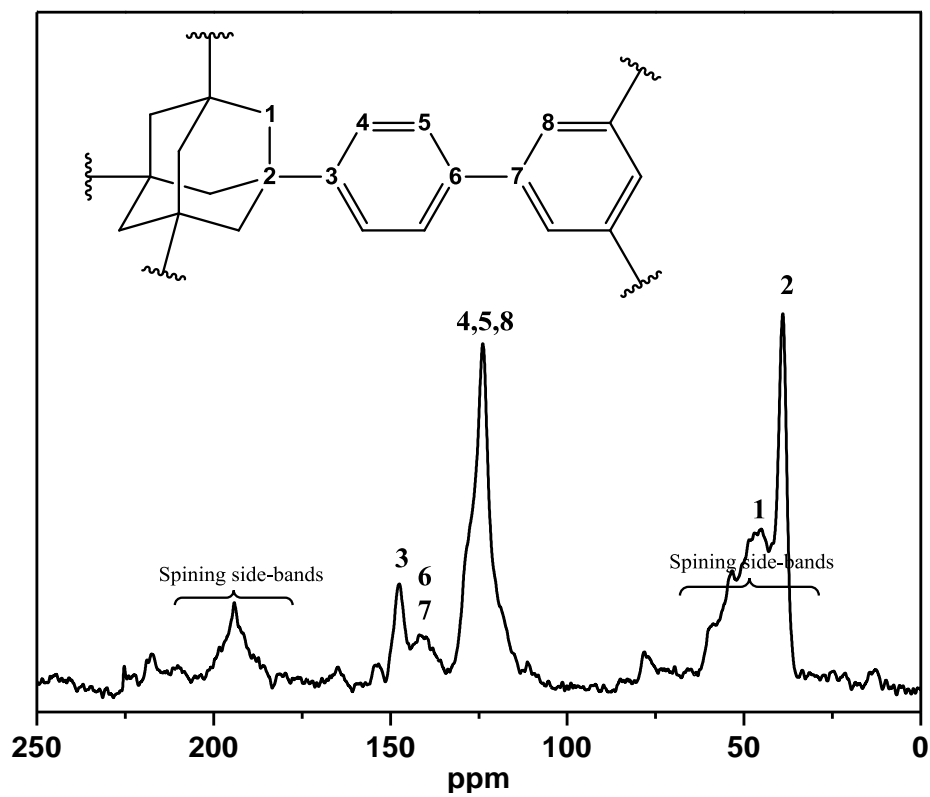


Figure 2.8: Solid state ^{13}C CP-MAS NMR spectra of NPOF- NO_2 .

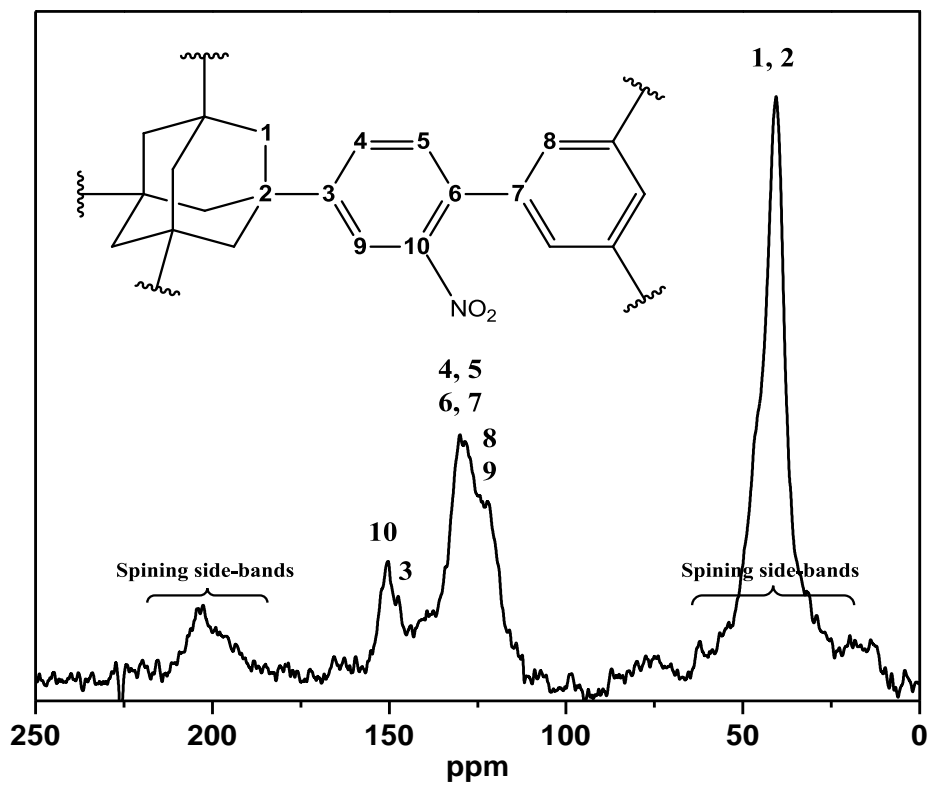
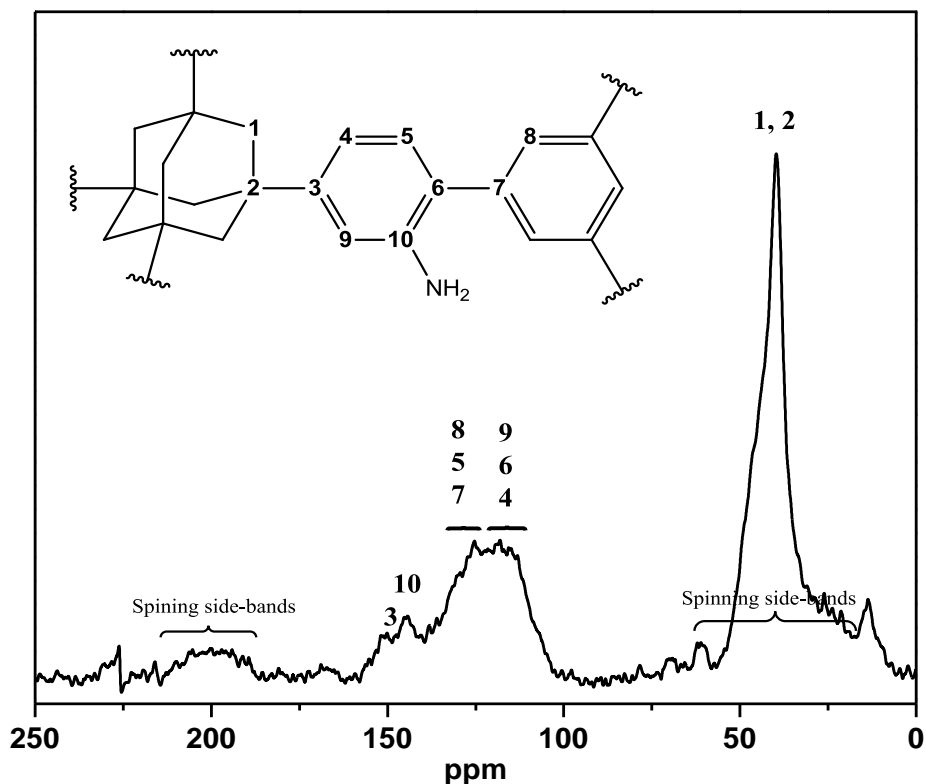


Figure 2.9: Solid state ^{13}C CP-MAS NMR spectra of NPOF-NH₂.



2.4 Results and Discussion

Cyclotrimerization of acetyl functional groups which is frequently used to construct macromolecules through benzene ring formation has been employed here for synthesizing the adamantane-based nanoporous organic polymers (Scheme 2.1). Acid catalyzed cyclotrimerization of three acetyl groups results in the formation of a 1,3,5-substituted benzene units and the elimination of three water molecules.

NPOF-4 was synthesized in good yields following a modified procedure reported recently by Kaskel as depicted in Scheme 2.1.³⁵ The slow addition of SiCl_4 at 0 °C

prevents rapid premature oligomers formation and leads to a more controlled pore formation and enhanced porosity. Although there are reports describing room temperature cyclotrimerization of acetylated aromatic molecules to generate isolated molecules, high temperatures are frequently used to either accelerate the rate of reactions or to overcome the steric and electronic effects of substituents. NPOP-4 is insoluble in common organic solvents such as DMF, THF, toluene, ethanol, etc, and remains intact upon washing with aqueous HCl and NaOH as evidenced by spectral and physical studies. Its high chemical stability enables post-synthesis modification particularly to introduce new functional groups that are known to enhance gas storage and separation properties. For example, pore surface chemical modification of organic frameworks with amino groups has significantly enhanced CO₂ binding in PPNs and POPs. There has been considerable interest recently in the synthesis of amino functionalized porous materials because of their interactions with small gas molecules consisting of polar bonds, particularly to CO₂ capture and selective separation of CO₂ from gas mixtures. Consequently, we have first modified NPOF-4 by nitration (NPOF-4-NO₂) then reduced the resulting network to the corresponding amino-functionalized framework (NPOF-4-NH₂).

Nitration was performed through the use of concentrated HNO₃/H₂SO₄ mixture to yield brown powder in a quantitative yield. The nitrated polymer NPOF-4-NO₂ was then reduced to NPOF-4-NH₂ using SnCl₂ in ethanol under refluxing at 70 °C for 18 h which resulted in a dark brown powder in 100% yield after drying at 80 °C. While the synthesis of NPOF-4-NO₂ and NPOF-4-NH₂ under harsh acidic conditions attests the chemical robustness of the resultant polymers, the thermal stabilities were examined by thermo

gravimetric analysis (TGA). The parent NPOP-4 is stable up to 400 °C, while the nitrated and reduced forms NPOF-4-NO₂ and NPOF-4-NH₂ showed a lower thermal stability (~200 °C, Figure 2.5). Scanning electron microscopy (SEM) of the polymers revealed aggregated particle morphology in the range of 0.4-1.1 μm (Figure 2.4) which seem to remain intact under nitration and reduction steps. As expected, NPOFs are amorphous as evidenced by powder X-ray diffraction studies (Figure 2.6).

The chemical functionalization of the polymers were investigated by FT-IR and solid state ¹³C NMR spectroscopic methods. Figure 2.3 shows the FT-IR spectra of the monomer and the synthesized polymers. Upon polymerization, the intensity of the band at 1680 cm⁻¹ (C=O) of TAPA is substantially decreased in NPOF-4 as a result of acetyl groups cyclotrimerization. This was further supported by the disappearance of 26 ppm ¹³C NMR peak of TAPA in NPOF-4 (Figure 2.7). Successful incorporation of nitro groups were confirmed by the appearance of new FT-IR bands at 1532 and 1350 cm⁻¹ (Figure 2.3) which have been assigned to asymmetrical and symmetrical stretching of NO₂, respectively, in NPOF-4-NO₂. Upon reduction, these bands disappear and new bands at 3350 and 3230 cm⁻¹ appear which confirm the conversion of the nitro groups to the amine functionality (Figure 2.3). Solid-state ¹³C NMR spectra showed the broadening of the peaks at around 150 ppm upon nitration and reduction probably due to the overlap of peaks of substituted carbons (Figure 2.8 and Figure 2.9). The chemical composition of the functionalized networks was investigated by elemental analysis that indicated the content of nitrogen by mass to be 7.84% for NPOF-4-NO₂ (~0.54 N per phenyl directly attached to adamantane) as illustrated in Scheme 2.1. The nitrogen content, as expected, increased to 8.39% upon reduction. Notably, this method seems

to be more effective than the previous methods reported for PAFs which resulted in only 0.25-0.3 N per phenyl rings).⁴⁰

Chapter 3

Gas Storage Capabilities for Nanoporous Organic Frameworks

3.1 Introduction

Great interest has been expressed in the gas storage capabilities of many porous media. Recently, the storage of carbon dioxide has received great attention because of its greenhouse nature and impact on the environment. Additionally, the use of argon gas to examine porosity can provide useful information about the textural properties of gas adsorbents and very reliable data on surface area and pore size distribution.

Nitrogen is the probe gas most commonly used for surface area and pore size distribution (PSD) analysis because it is inexpensive, readily available, inert, and well-studied in the adsorption literature. The nitrogen isotherm at 77 K (liquid nitrogen temperature), which is again convenient since liquid nitrogen is inexpensive, is widely used as a standard for micro and mesopore size analysis, however, it is also generally accepted that nitrogen adsorption is not satisfactory for quantitative assessment of the ultramicropores (pore widths <0.7 nm).⁴⁵ Although the kinetic diameter of nitrogen and argon are similar (0.36, 0.34 nm, respectively) the adsorption behavior of these probe gases is different because argon is a monoatomic and spherical molecule without a quadrupole moment. On the other hand, the nitrogen adsorption and the orientation of the adsorbate molecules on the surface is affected by interactions between functional groups on the surface and the quadrupole moment of the nitrogen molecule (4.7×10^{-40} Cm²).⁴⁶ Therefore, argon has been extensively used for characterizing the pore

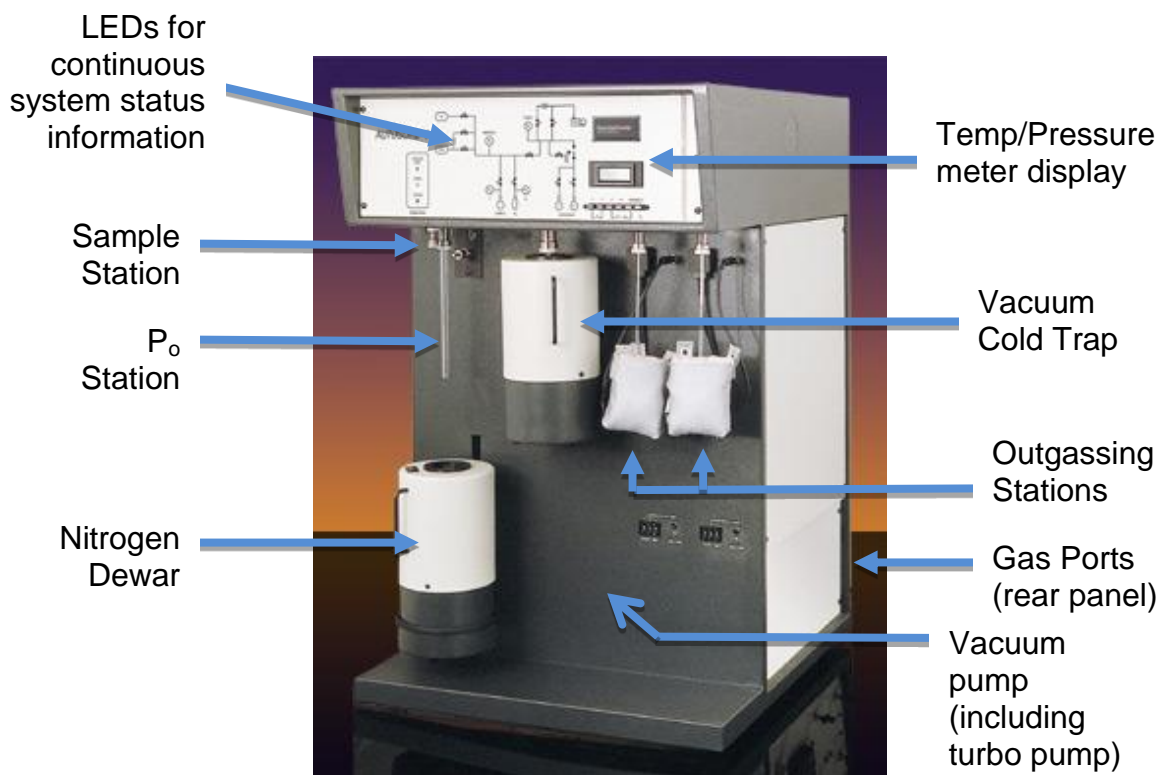
structure of heterogeneous adsorbents to avoid the abovementioned problems. Thus, we have decided to use Argon isotherms at 87 K to characterize the porosity of our materials because of their heterogeneous surfaces especially after the incorporation of functional groups within the pores.⁴⁷

To assess gas storage capabilities, sorption equipment is employed. The pressure range that dedicated low pressure sorption equipment can reach is typically around 10^{-6} to 1 bar. Gas storage by high pressure gas sorption measurements is beyond the scope of the research described herein.

For the present work, all sorption isotherms were determined in an automated low pressure volumetric gas adsorption instrument (Quantachrome Autosorb 1-C). An image of the instrument with essential components labeled is shown in Figure 3.1. Sorption isotherms were collected at constant temperatures which typically range from 77 K to 298 K. The temperature choice within this range is determined by the achievability and maintainability of the desired temperature. For example, submerging a sample in liquid nitrogen bath will keep the temperature at 77 K until all of the nitrogen boils off. Similarly, ice-water bath is used to maintain the temperature at 273 K. In order to test the applicability of materials to real life conditions isotherms are also collected at higher temperatures *i.e.* 25 °C which can be achieved and maintain by a thermal circulator bath compatible with the sorbent analyzer instrument. The result of an isothermal experiment is a graph with pressure on the x-axis and volumetric gas uptake (cc g^{-1}) on the y-axis then the uptake can be converted to desired units. The instrument measures the amount of gas adsorbed onto (or desorbed from) a solid surface at pre-requested equilibrium vapor pressure. The instrument admits or removes a known

volume of gas at a constant temperature and measure the corresponding pressure. The pressure in the sample cell changes as the instrument admits or removes gas in repetitive small quantities until the threshold around the requested pressure is reached. Then the amount of gas adsorbed or desorbed calculated by the difference between the amount of gas admitted or removed and the amount required to fill the void space.

Figure 3.1: Image of Autosorb-1C with essential components labeled.



3.2 Surface Area and Pore Size Characterization

To investigate the permanent porosity of NPOFs, Argon sorption data was acquired using a Quantachrome Autosorb 1-C at 87 K. Pore size distributions were calculated using the Non-Local Density Functional Theory (NLDFT)⁴⁸ on the adsorption branch with a cylindrical/spherical pore model for all NPOFs. This model was used in conjunction with a similar model on the adsorption branch of the carbon dioxide isotherm at 273 K as has been reported previously in literature to obtain lower level pore size distributions.^{49,50} The choice of one model over another is generally determined by the shapes of the theoretical computer-generated models. Argon sorption studies were performed on activated samples. The activation process for all samples involved removing guest molecules by heating at 120 °C for 18 hours under vacuum (10^{-5} torr). Porous textural properties of NPOFs are summarized in Table 3.1. The rapid argon uptakes at very low pressure (below 0.1×10^{-2} bar) are indicative of microporosity and applying the Brunauer-Emmett-Teller (BET) model within the pressure range of $P/P_0=0.01-0.15$ resulted in apparent surface areas SA_{BET} of $1249 \text{ m}^2 \text{ g}^{-1}$ (NPOF-4), $337 \text{ m}^2 \text{ g}^{-1}$ (NPOF-4-NO₂), and $554 \text{ m}^2 \text{ g}^{-1}$ (NPOF-4-NH₂). The surface area decreased significantly upon pore functionalization with nitro groups which can restrict pore accessibility by Argon. Further modification upon nitro group reduction resulted in a surface area value that is intermediate between those of NPOF-4 and NPOF-4-NO₂. Pore size distribution was estimated by fitting the argon uptake branch of the isotherms with NLDFT (cylindrical/spherical pore geometry with zeolites/silica model) and found to be in a broad range of $\sim 8.0-16.8 \text{ \AA}$ for NPOF-4, $\sim 7.7-10.8 \text{ \AA}$ for NPOF-4-NO₂ and $\sim 7.7-15.2 \text{ \AA}$ for NPOF-4-NH₂ (Figure 3.3). Pore volumes were calculated from single-point

measurements ($P/P_0 = 0.95$) and found to be 0.78, 0.21, and 0.28 cc g^{-1} for NPOF-4, NPOF-4- NO_2 , and NPOF- NH_2 , respectively. The porous properties of NPOF-4 and its functionalized derivatives are comparable to those of porous organic networks and the chemical nature of the latter can be advantageous for small gas storage and separation applications as described below.

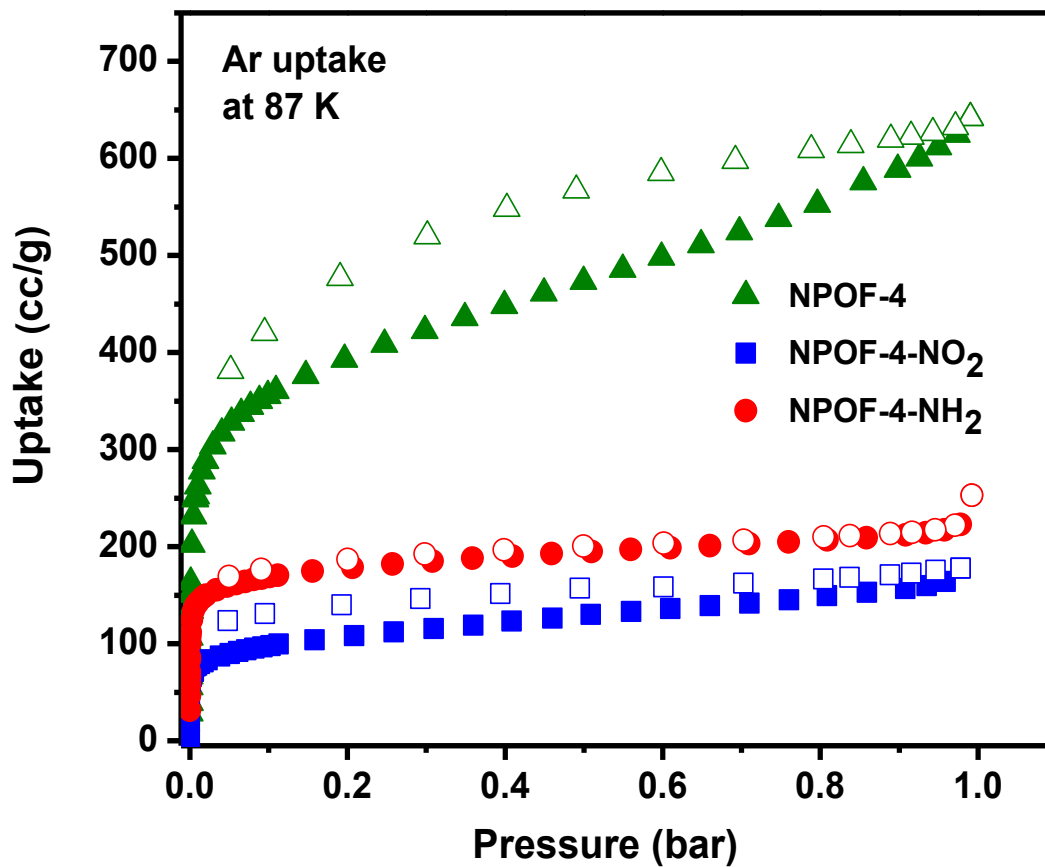
Table 3.1: Surface areas, pore size distributions and pore volumes for NPOF networks.

^aCalculated by BET method. ^bCalculated by Langmuir method. ^cCalculated from Argon adsorption at $P/P_0 = 0.95$. ^dCalculated from NLDFT.

Network	$\text{SA}_{\text{BET}} (\text{m}^2 \text{g}^{-1})^{\text{a}}$	$\text{SA}_{\text{Lang}} (\text{m}^2 \text{g}^{-1})^{\text{b}}$	PSD (\AA) ^c	$\text{V}_{\text{total}} (\text{cm}^3 \text{g}^{-1})^{\text{d}}$
NPOF-4	1249	1685	8.0-16.8	0.78
NPOF-4- NO_2	337	461	7.7-10.8	0.21
NPOF-4- NH_2	554	719	7.7-15.2	0.28

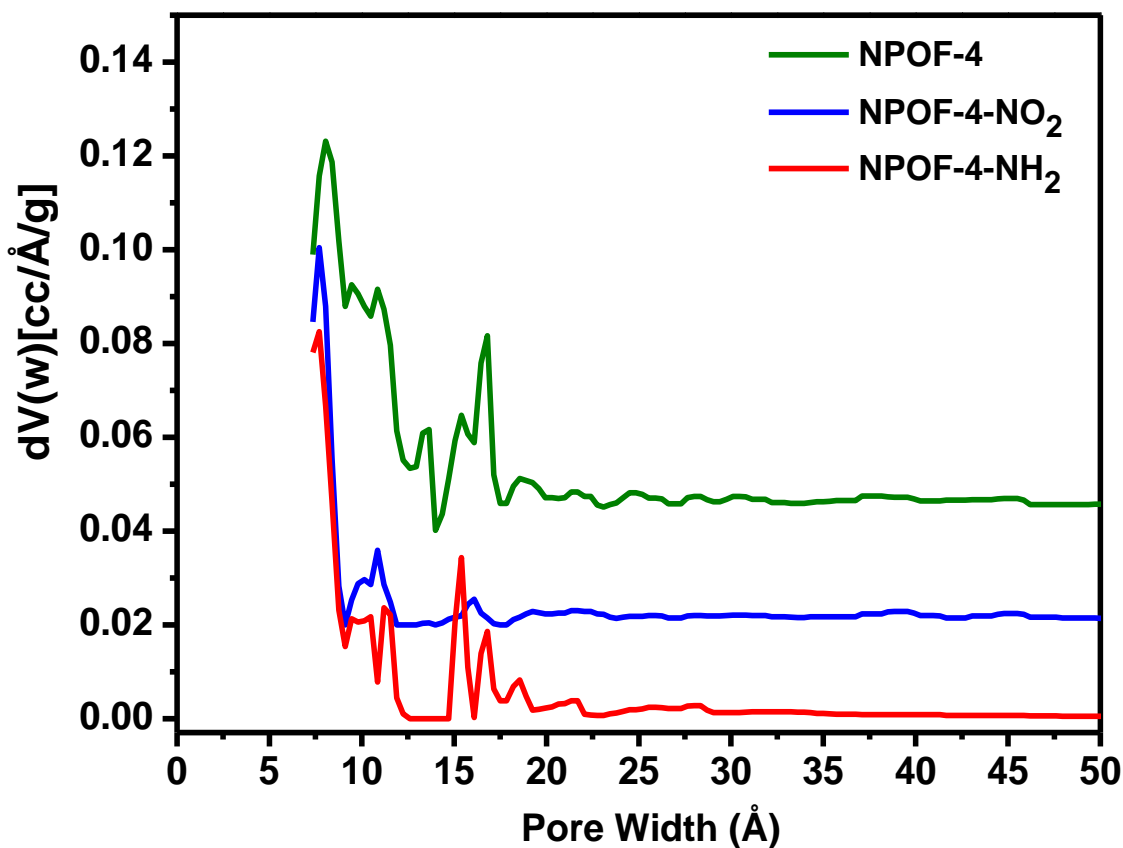
Figure 3.2 shows the argon adsorption/desorption isotherms for NPOF-4, NPOF-4- NO_2 , and NPOF- NH_2 at 87 K. All isotherms are fully reversible and exhibit hysteresis that is well pronounced for NPOF-4 most likely due to the flexible nature of the framework as documented for numerous porous organic materials.³⁵

Figure 3.2: Argon uptake isotherms for NPOFs; adsorption (filled) and desorption (empty) data points were taken at 87 K and 0-1 bar.



In spite of their amorphous nature, the surface area of the networks under investigation, particularly for NPOF-4, are considerably high and comparable with a wide range of porous organic networks such as PIMs ($618\text{-}1760\text{ m}^2\text{ g}^{-1}$),⁵¹ cage compounds ($1375\text{ m}^2\text{ g}^{-1}$),⁵² imine-linked microporous polymer organic frameworks (POFs, $466\text{-}1521\text{ m}^2\text{ g}^{-1}$),⁵³ covalent organic frameworks (COF-300, $1360\text{ m}^2\text{ g}^{-1}$),⁵⁴ diimide-based polymers ($750\text{-}1407\text{ m}^2\text{ g}^{-1}$),⁵⁵ functionalized conjugated microporous polymer (CMP) networks ($522\text{-}1043\text{ m}^2\text{ g}^{-1}$)⁵⁶ and porous electron-rich covalent organo nitridic frameworks (PECONFs, $499\text{-}851\text{ m}^2\text{ g}^{-1}$).⁵⁷

Figure 3.3: Pore size distribution for NPOF-4, NPOF-4-NO₂ and NPOF-4-NH₂.



Pore size distribution by NLDFT are based on fitting the sorption experimental data to mathematical functions. As such, the graphical comparison for the fitting method of the NLDFT calculations as well as the curves for the BET calculations are shown in the following figures.

Figure 3.4: NLDFT calculated isotherm for NPOF-4 overlaid with the experimental Argon isotherm. A fitting error less than 1% indicates validity of the model.

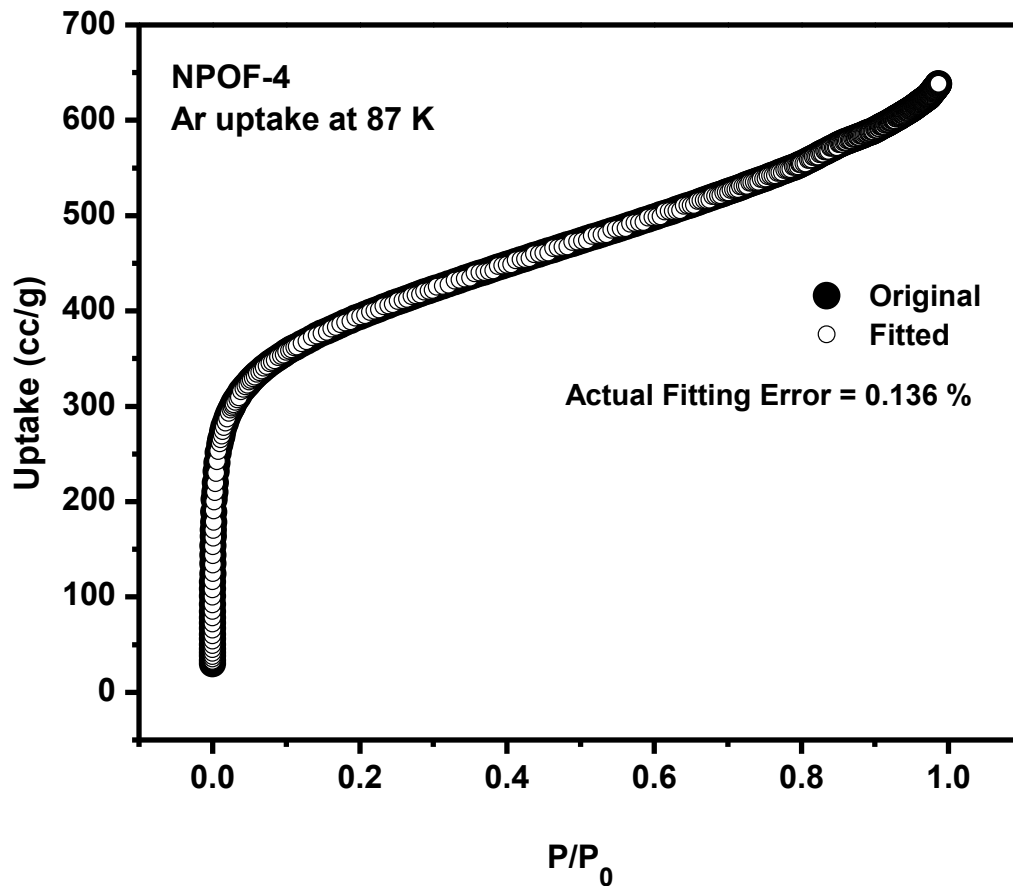


Figure 3.5: Multipoint BET plot for NPOF-4 calculated from the Argon adsorption in the range 0.04-0.16 P/P_o.

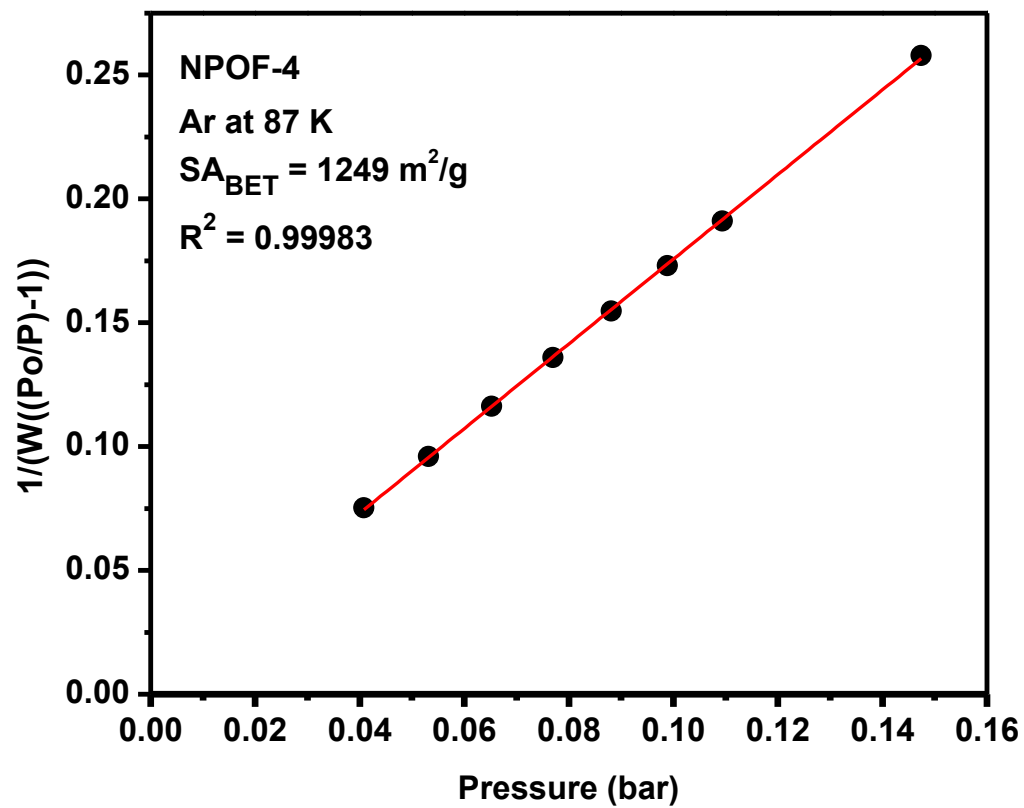


Figure 3.6: Langmuir plot for NPOF-4 calculated from the Argon adsorption in the range 0.05-0.25 P/P₀.

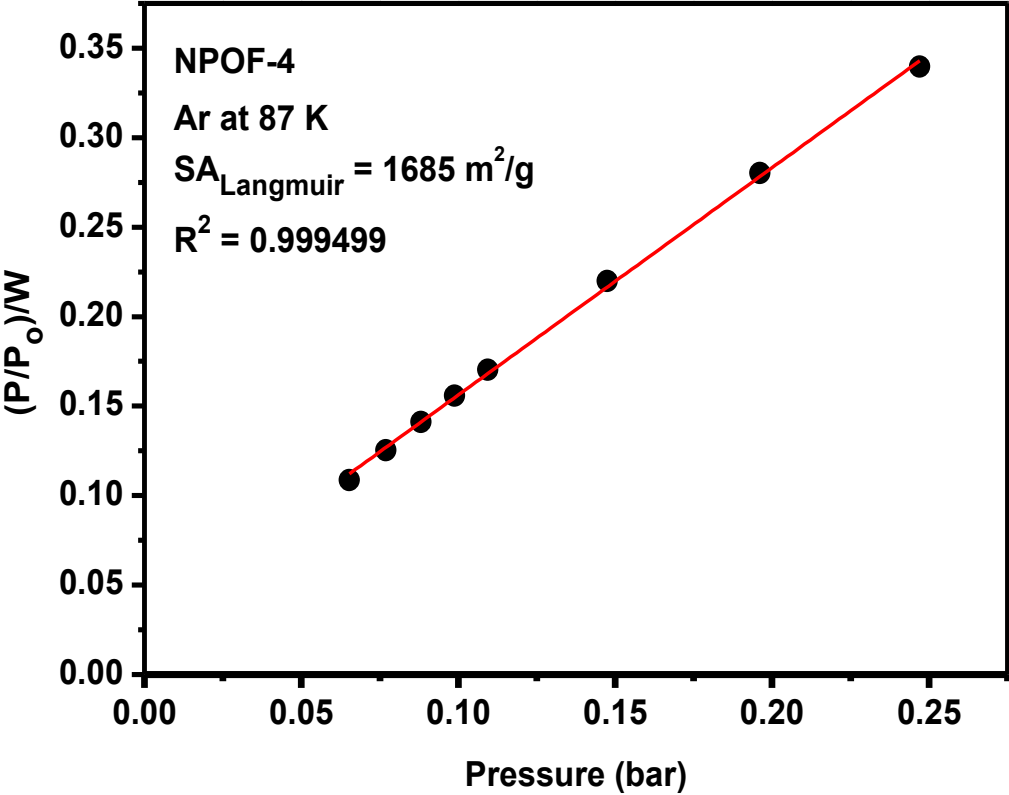


Figure 3.7: NLDFT calculated isotherm for NPOF-4-NO₂ overlaid with the experimental Argon isotherm. A fitting error less than 1% indicates validity of the model.

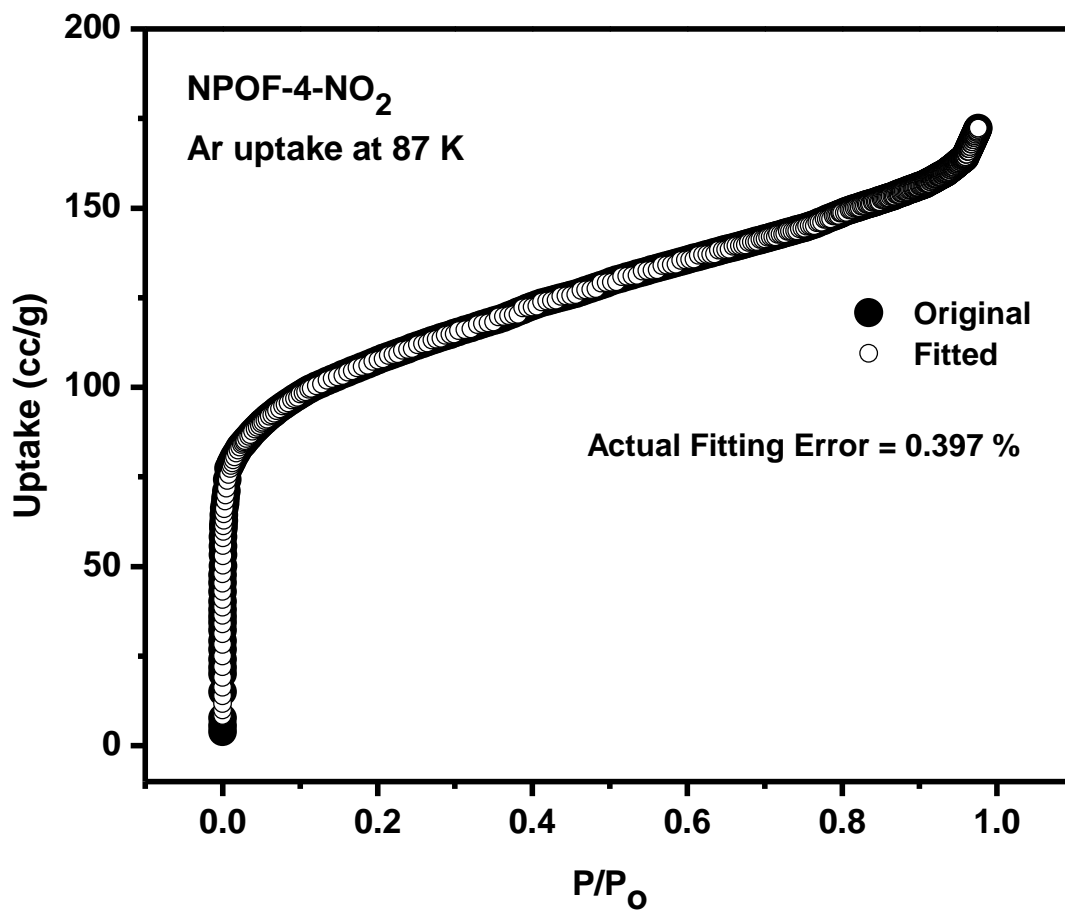


Figure 3.8: Multipoint BET plot for NPOF-4-NO₂ calculated from the Argon adsorption in the range 0.04-0.16 P/P_o.

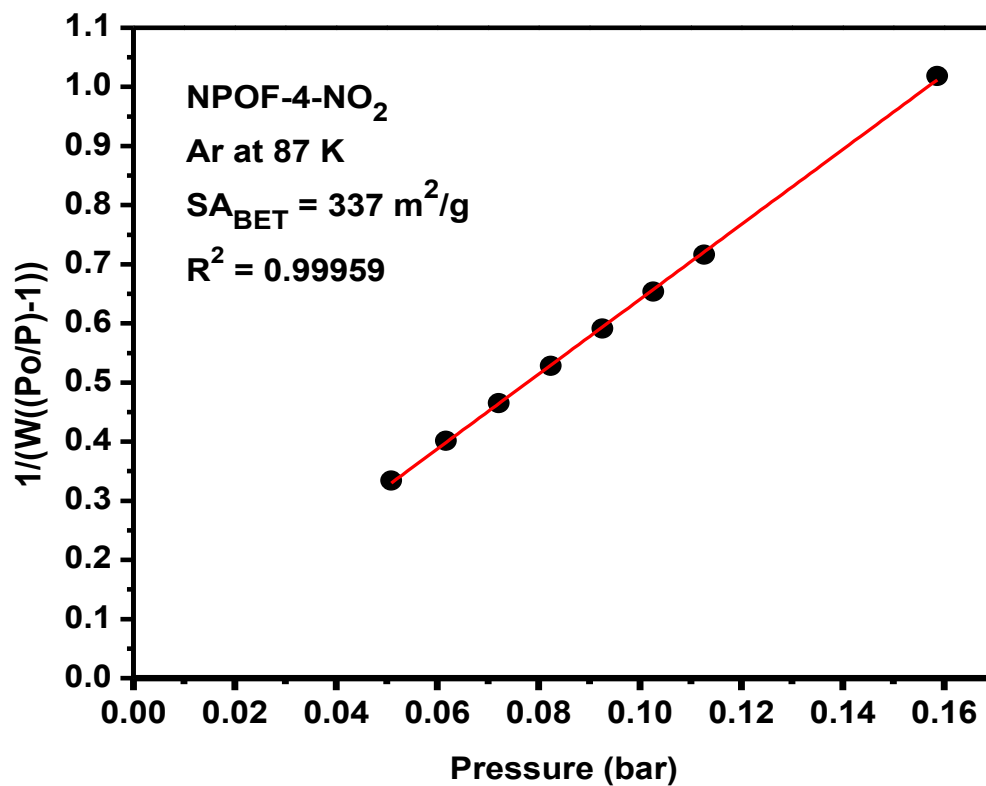


Figure 3.9: Langmuir plot for NPOF-4-NO₂ calculated from the Argon adsorption in the range 0.05-0.25 P/P₀.

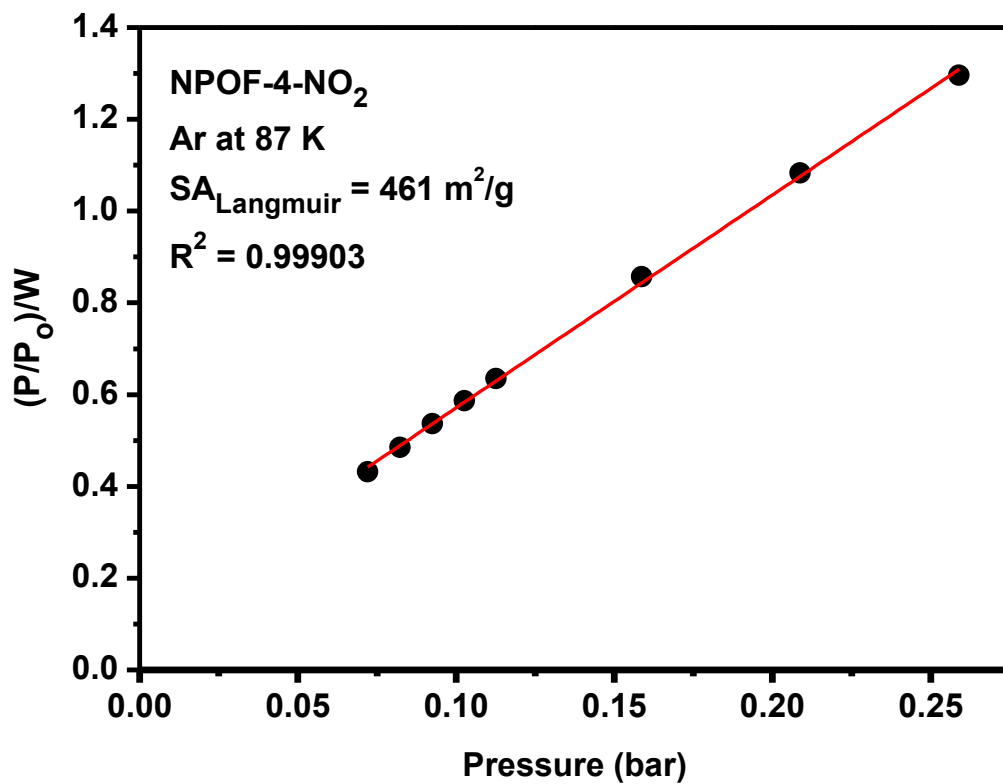


Figure 3.10: NLDFT calculated isotherm for NPOF-4-NH₂ overlaid with the experimental Argon isotherm. A fitting error less than 1% indicates validity of the model.

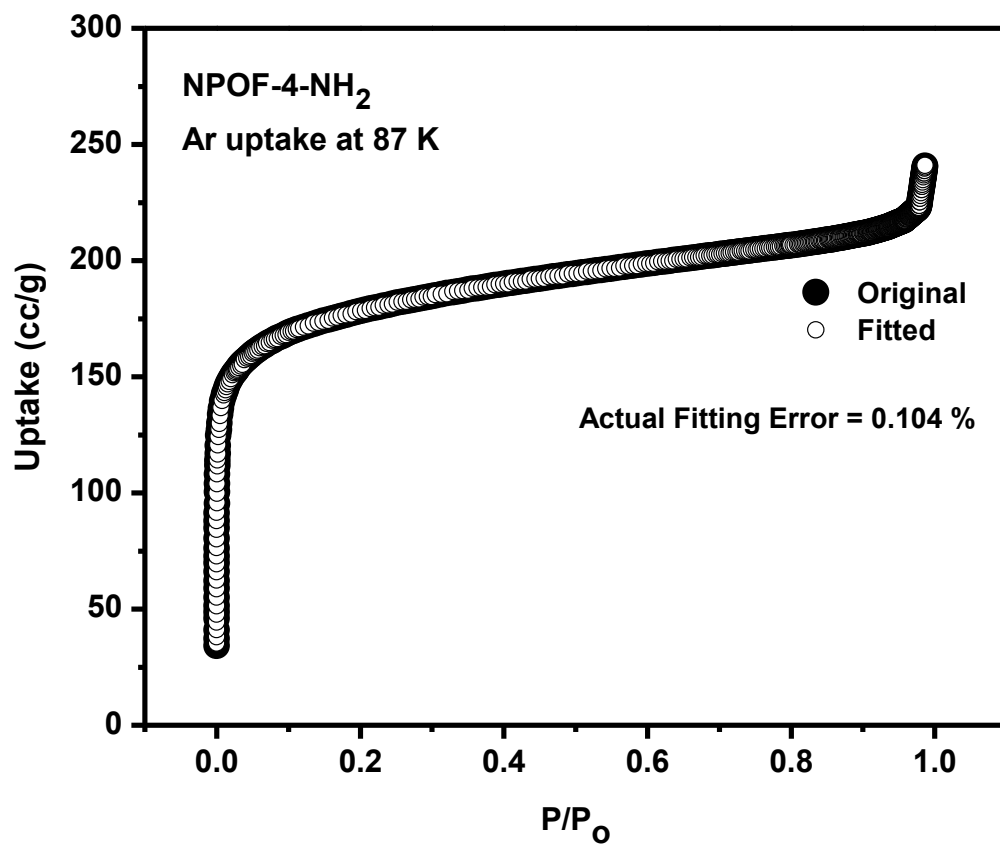


Figure 3.11: Multipoint BET plot for NPOF-4-NH₂ calculated from the Argon adsorption in the range 0.04-0.16 P/P_o.

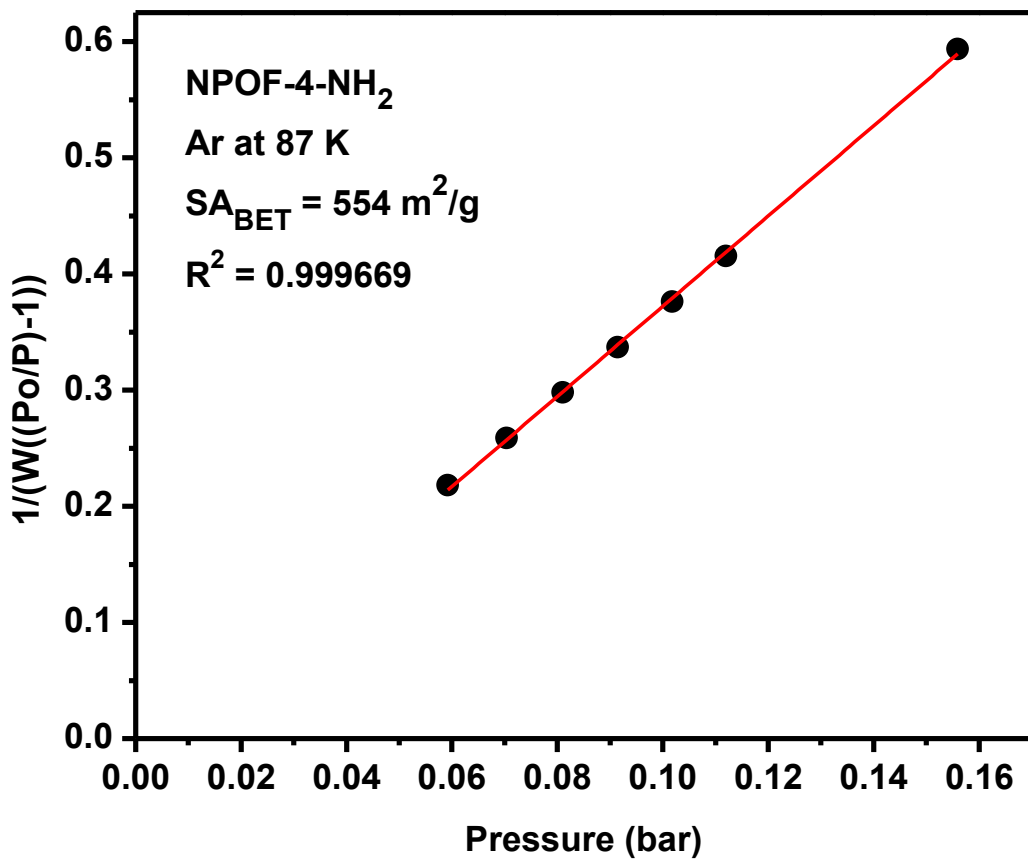
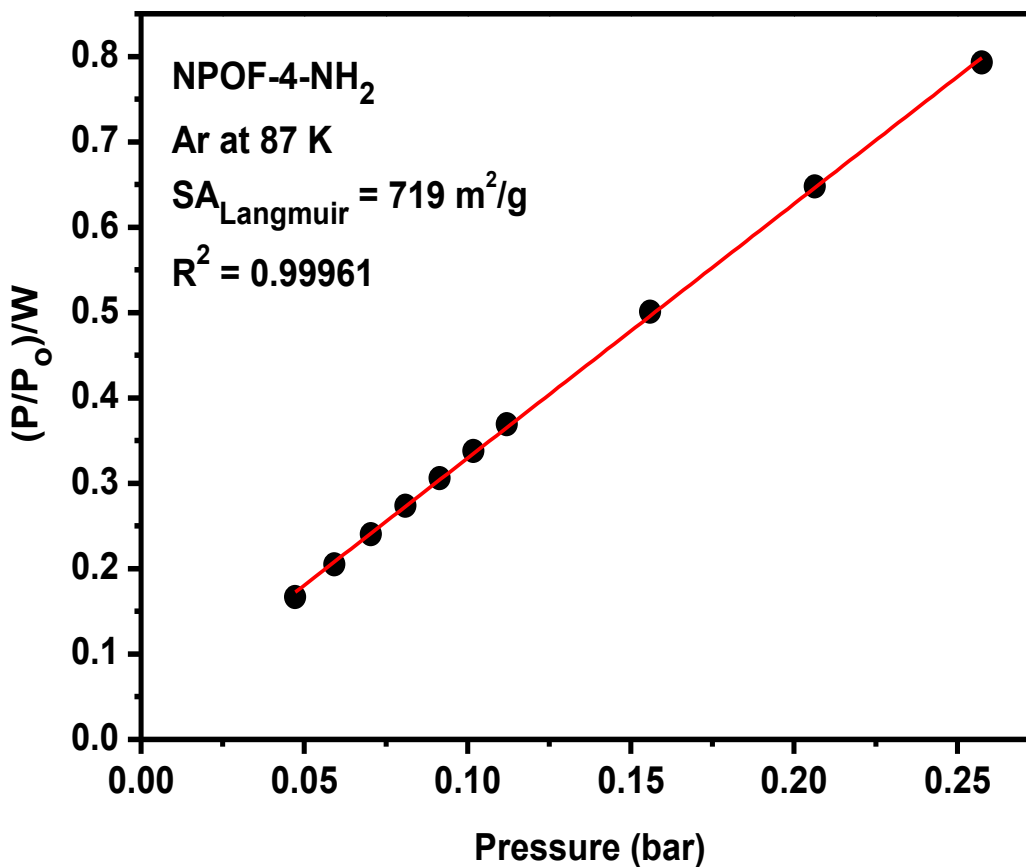


Figure 3.12: Langmuir plot for NPOF-4-NH₂ calculated from the Argon adsorption in the range 0.05-0.25 P/P₀.



3.3 Hydrogen, Carbon Dioxide, and Methane Sorption of Nanoporous Organic Frameworks

To investigate the performance of NPOFs in the capture of different gases, sorption experiments on activated samples for carbon dioxide, methane, and hydrogen were performed. Hydrogen isotherms were performed at 77 and 87 K whereas carbon dioxide and methane isotherms were performed at 273 and 298 K. The combined isotherms for CO₂ (Figure 3.13 and Figure 3.14), CH₄ (Figure 3.15 and Figure 3.16), and H₂ (Figure 3.17 and Figure 3.18) are all fully reversible illustrating the facile gas

release typical for organic polymers which makes them energetically attractive for gas storage and separation applications.

Figure 3.13: Carbon dioxide isotherms for NPOFs at 273 K: adsorption (filled symbols) and desorption (empty symbols).

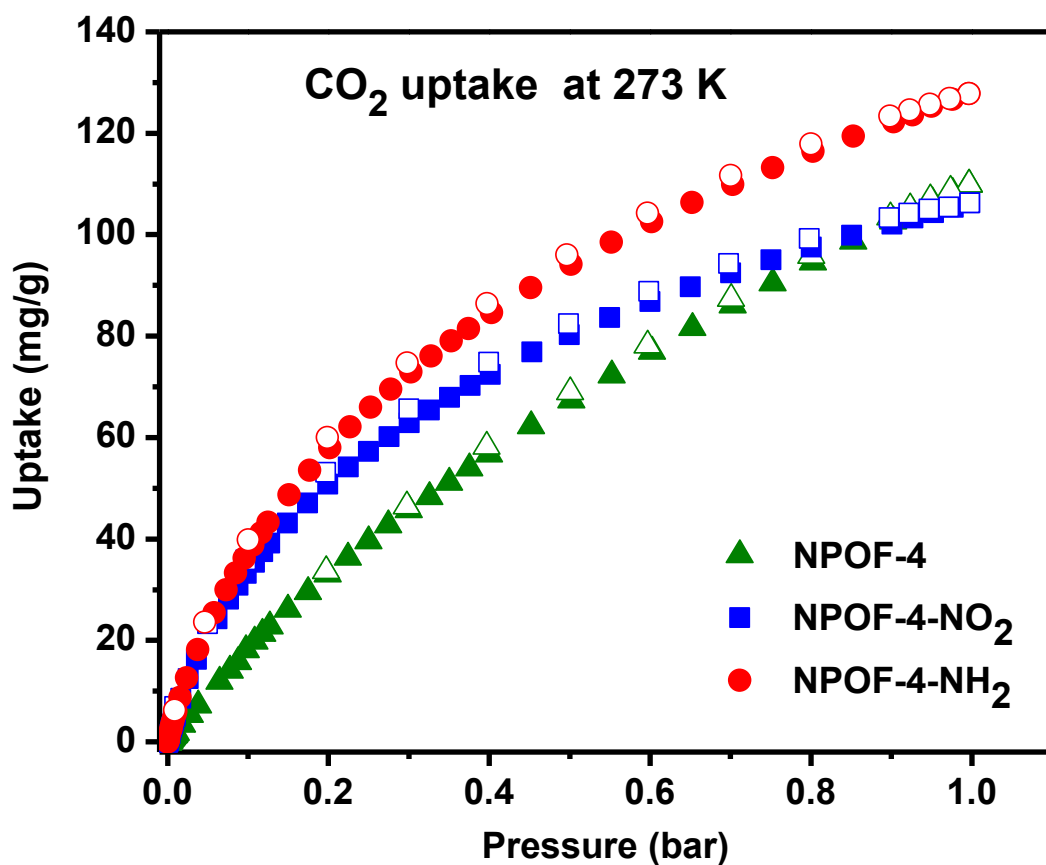


Figure 3.14: Carbon dioxide isotherms for NPOFs at 298 K: adsorption (filled symbols) and desorption (empty symbols).

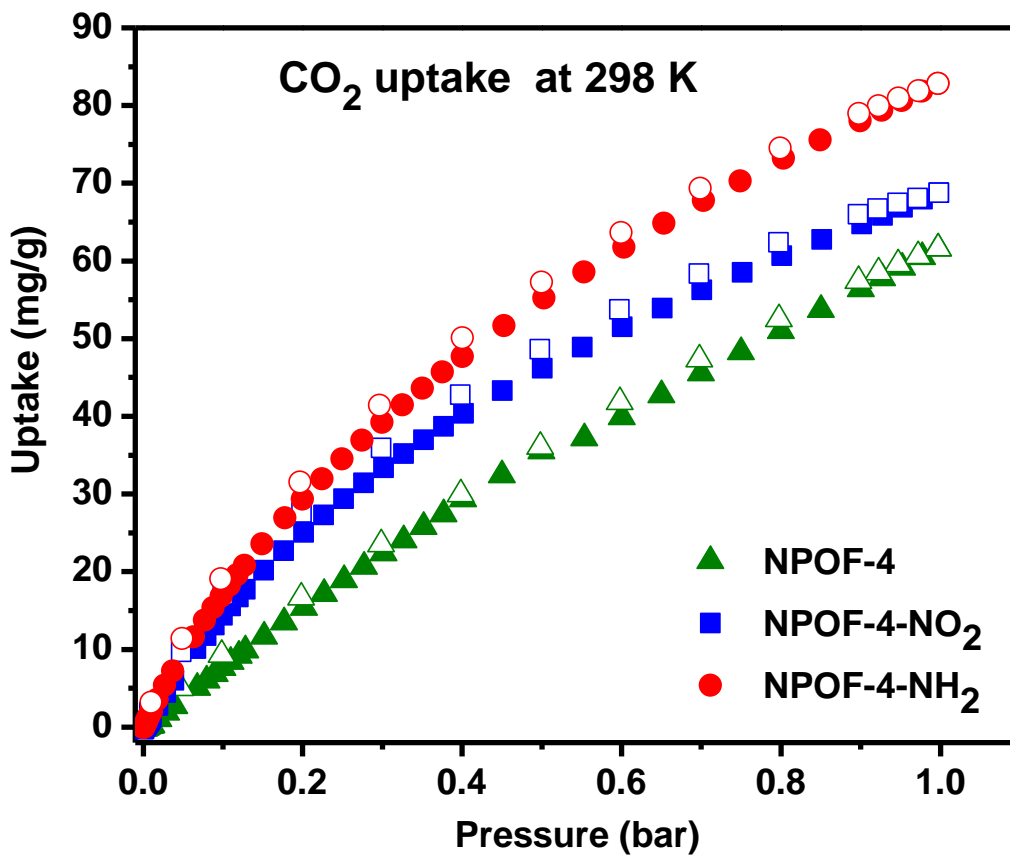


Figure 3.15: Methane isotherms for NPOFs at 273 K: adsorption (filled symbols) and desorption (empty symbols).

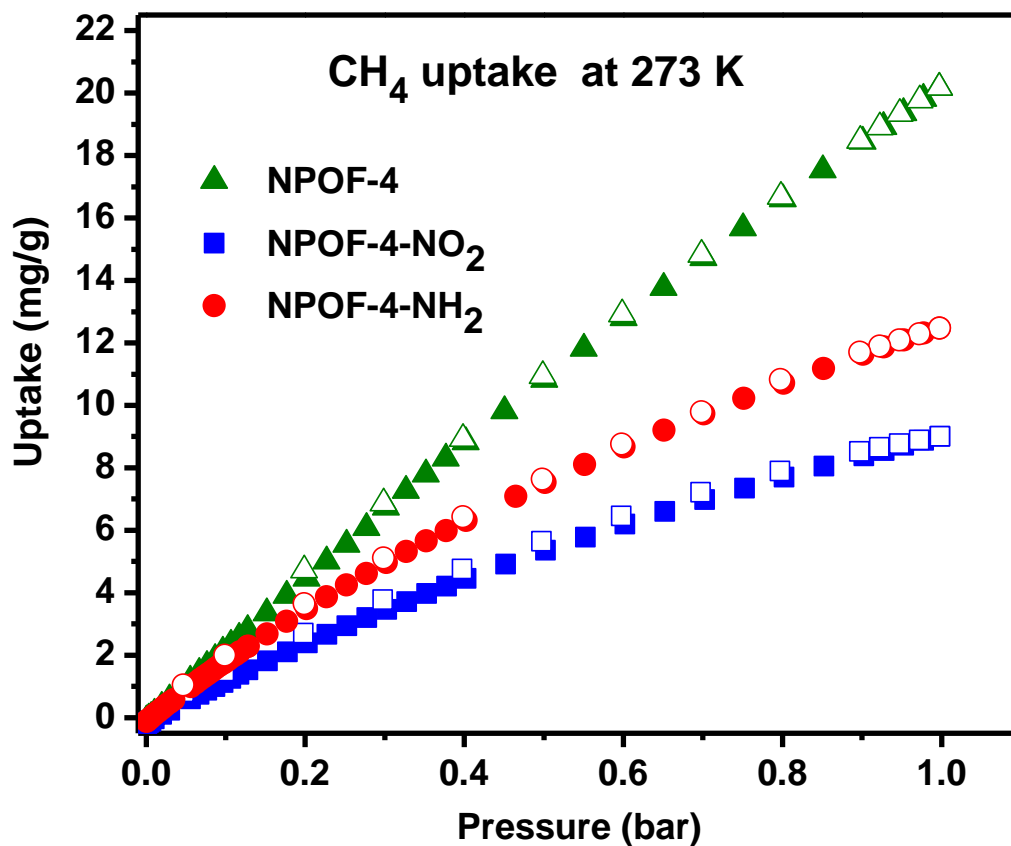


Figure 3.16: Methane isotherms for NPOFs at 298 K: adsorption (filled symbols) and desorption (empty symbols).

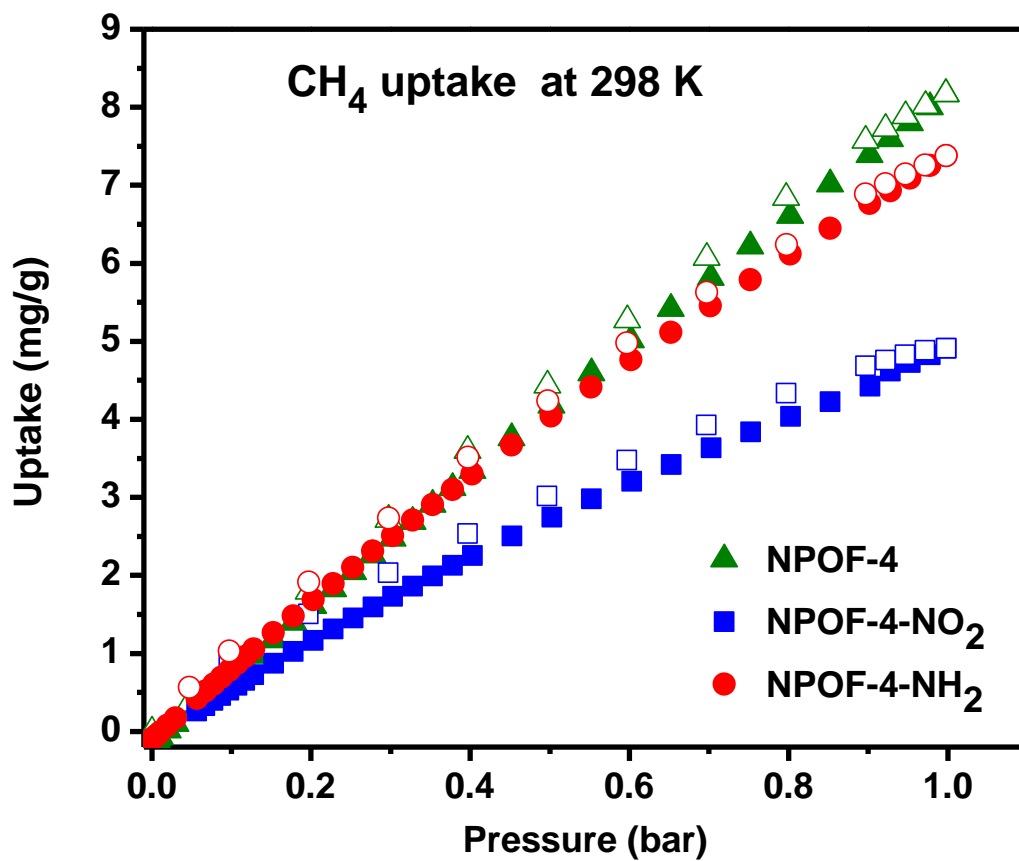


Figure 3.17: Hydrogen isotherms for NPOFs at 77 K: adsorption (filled symbols) and desorption (empty symbols).

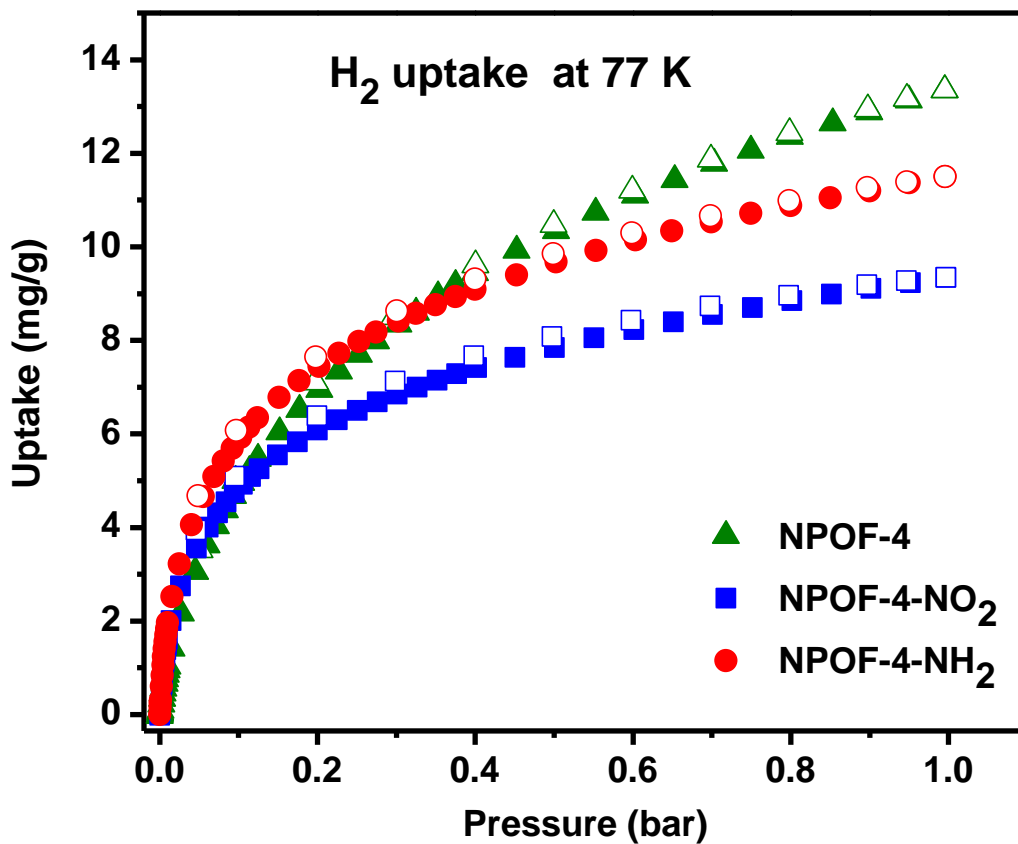
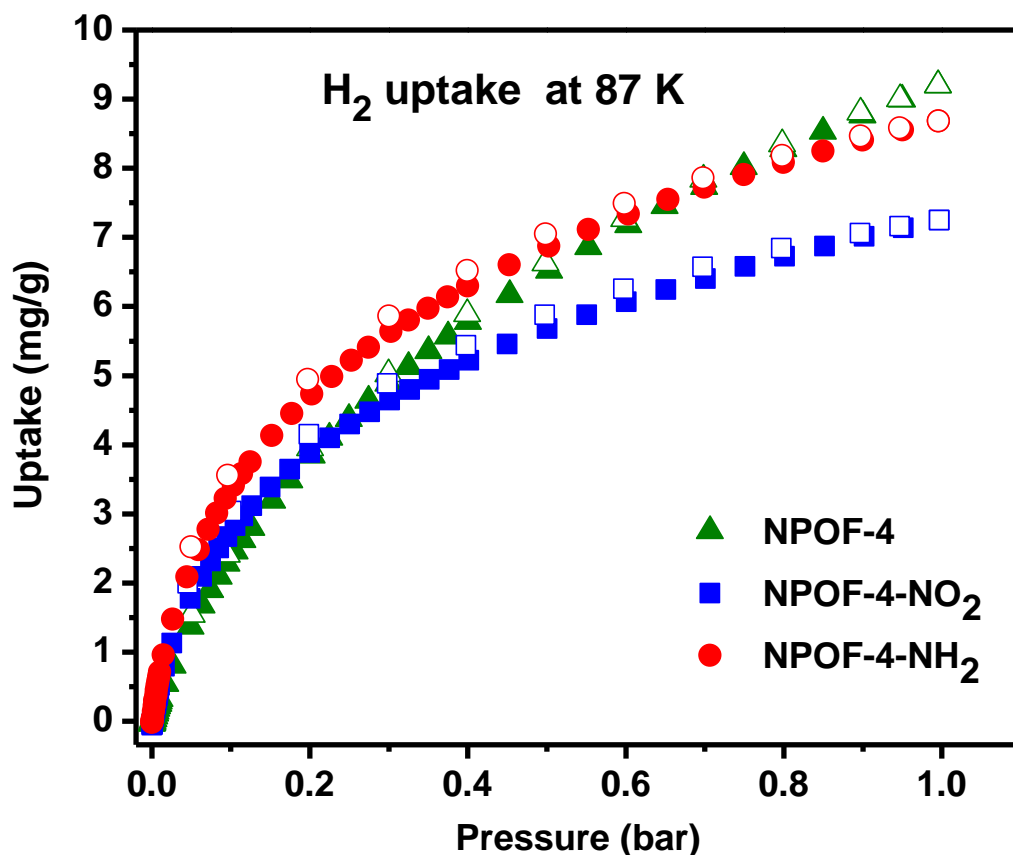


Figure 3.18: Hydrogen isotherms for NPOFs at 87 K: adsorption (filled symbols) and desorption (empty symbols).



Low-pressure gas sorption measurements for CO₂, H₂, CH₄, and N₂ were collected in order to investigate the impact of pore functionalization on gas storage and the preferential binding of CO₂ over CH₄ and N₂. The impact of pore functionalization on CO₂ uptake is depicted in Figure 3.13 which indicates that NPOF-4-NH₂ has the highest uptake of 12.78 wt% (2.9 mmol g⁻¹) at 1 bar and 273 K and is about 16% higher than the uptakes of NPOF-4-NO₂ and NPOF-4 despite of the latter's much higher surface area. These observations originate from the polarizable nature of the CO₂ molecule and its large quadrupole moment. While pore functionalization with -NO₂ and -NH₂ has

drastic impact on the binding affinity of CO₂ (explained in Chapter 4), its impact on the CO₂ final gravimetric uptake at 1.0 bar was less significant. The microporous nature of NPOF-4 and its high surface area facilitate CO₂ uptake at ambient pressure. High CO₂ uptake at low pressure (0.15 bar) is desirable for low-pressure post-combustion application where the flue gas usually consists of ~15% CO₂, ~75% N₂ and ~10% of other gases.

To commensurate the pore size of functionalized NPOF-4 for CO₂ separation from N₂ and CH₄, introduction of chemical heterogeneity to the pore walls which polarizes the CO₂ molecule have significant effect on CO₂ uptake at low pressures. At 0.2 bar and 273 K NPOF-4-NO₂ adsorbs 1.15 mmol g⁻¹ (5.08 wt%) of CO₂ and NPOF-4-NH₂ adsorbs 1.32 mmol g⁻¹ (5.80 wt%) which corresponds to an increase of gravimetric capacity of 54% and 76%, respectively, with respect to that of the non-functionalized NPOF-4 which takes 0.75 mmol g⁻¹ (3.30 wt%) of CO₂. The relatively large dipole moment of NO₂ and NH₂ results in dipole-quadrupole interactions with CO₂, and remarkably increase the initial CO₂ uptake at low pressure range. At 1.0 bar and 273 K NPOF-4-NO₂ adsorbs 2.41 mmol g⁻¹ (10.63 wt%) and NPOF-4-NH₂ adsorbs 2.9 mmol g⁻¹ (12.78 wt%) of CO₂ which exceed functionalized CMPs (1.6-1.8 mmol g⁻¹),⁵⁶ triptycene-based cage compounds (2.1 mmol g⁻¹),⁵² and functionalized amidoxime-PIM-1 (2.74 mmol g⁻¹).⁵⁸ At 1.0 bar and 298 K NPOF-4-NH₂ adsorbs 1.88 mmol g⁻¹ (12.78 wt%) of CO₂ which is comparable to BPL carbon (SA_{BET}= 1150 m² g⁻¹; a common reference material for CO₂ uptake) that shows an uptake of 1.90 mmol g⁻¹ under the same conditions.^{59,60}

We have also studied the H₂ and CH₄ uptake in order to evaluate the impact of -NO₂ and -NH₂ functionalities on the binding affinity of H₂ and CH₄. Both gases are being considered as an alternative fuel for automotive applications because of their abundance and clean nature. The H₂ uptakes by NPOF-4 (1.33 wt%) and its functionalized frameworks were modest (NPOF-NO₂: 0.93 wt% and NPOF-NH₂: 1.15 wt%) at 273 K/1 bar although the functionalized materials have higher binding affinities as depicted in Figure 4.3.

In a similar fashion, the CH₄ uptakes at 273 K and 298 K and 1 bar were collected for all materials and the results are presented in Figure 3.15 and Figure 3.16. A comparison of the methane uptake capacities for NPOF-4 and its functionalized derivatives suggests that surface area is the predominant factor in attaining high H₂ and CH₄ storage capacities at low pressure (1.0 bar), while surface functionality plays a more important role for CO₂ capture.

Chapter 4

Isosteric Heat of Adsorption of Carbon Dioxide, Methane, and Hydrogen with Nanoporous Organic Frameworks

4.1 Introduction

The process of adsorption is exothermic, i.e. heat is usually released when a gas molecule is adsorbed on a surface due to the loss of molecular motion of the gas molecules when they get adsorbed on a surface. As a consequence of that, the stronger adsorbent-adsorbate interactions are, the larger the amounts of heat released will be. The amount of the heat released also depends on the surface which is already covered with adsorbate. Presumably, as the surface is covered by adsorbate molecules, the heat of adsorption reduces. Therefore, it is more convenient to represent the heat as an isosteric heat of adsorption (Q_{st}), that is, at constant surface coverage for different temperatures. As a result, at least two isotherms are needed at different temperature in order to evaluate Q_{st} .

Calculation of isosteric heat of adsorption is based on experimental isotherms. Often, these isotherms are fitted to mathematical models that are intended to describe the data. In some cases, more than one isotherm is required to calculate Q_{st} . In the rest of the cases using more than one isotherm is encouraged to ensure that isotherm fitting parameters are reasonably accurate.

The virial method has been extensively employed to determine isosteric heat of adsorption of porous materials.⁶¹⁻⁶⁴ A virial expansion is a summation equation for which, in this case, the number of summation iterations is unknown:

$$\ln P = \ln N + (1/T) \sum_{i=0}^m a_i N^i + \sum_{i=0}^n b_i N^i$$

In this equation, P is pressure in torr, T is temperature in Kelvin, and N is the mmol of gas adsorbed per gram of sample. The values for m and n are undefined (hence, the unknown number of summation iterations) and are varied such that $m \geq n$ and result in the best fit as determined by the sum of the squares of the errors. The values for a_0, a_1, \dots, a_m and b_0, b_1, \dots, b_n are fitting parameters for the virial expansion. Following the appropriate fitting, the values for a_0, a_1, \dots, a_m are used in the calculation for the isosteric heat of adsorption, Q_{st} :

$$Q_{st} = -R \sum_{i=0}^m a_i N^i$$

The value of m in this case matches the value found for the preceding equation such that all a_i values are used. The calculated values are then plotted as they relate to the surface coverage, N , while the isosteric heat of adsorption at the point of zero-coverage is typically reported as a means of comparison.

In the case of the virial-type calculation for the isosteric heat of adsorption, only one temperature is necessary to perform the full calculation. However, the large combination of a_i and b_i values for varying m and n values results in a very subjective approach from the researcher's perspective. In order to mitigate, the subjective human element in these calculations, a minimum of two isotherms taken at different

temperatures should be performed when utilizing the virial method. This practice of multiple temperature-isotherms would drop the subjectivity of the calculations for the virial method, however, it should be noted that a base level of subjectivity still exists.

4.2 Experimental Calculations for the Isothermic Heat of Adsorption of Carbon Dioxide, Methane, and Hydrogen

Isothermic heats of adsorption of CO₂, CH₄ and H₂ were calculated for the networks by using virial method. Q_{st} values showed that both functionalized NPOFs networks gave higher heat of adsorption for CO₂ over non-functionalized NPOF-4 for the entire coverage range. Virial equation is fitted to isotherms which were taken at two different temperatures. The Q_{st} values and gas uptakes for networks are summarized in Table 4.1.

Table 4.1: Gas uptakes for NPOFs. Gas uptake in mg g⁻¹ and the isosteric enthalpies of adsorption (Q_{st}) in kJ mol⁻¹.

Network	H ₂ at 1 bar			CO ₂ at 1 bar			CH ₄ at 1 bar			
	S _A _{BET}	77 K	87 K	Q _{st}	273 K	298 K	Q _{st}	273 K	298 K	Q _{st}
NPOF-4	1249	13.3	9.2	7.2	109.9	61.6	23.2	20.2	8.2	24.6
NPOF-4-NO₂	337	9.3	7.2	8.3	106.3	68.8	32.5	9.0	5.4	20.8
NPOF-4-NH₂	554	11.5	8.7	8.1	127.8	82.8	30.1	12.5	7.4	20.7

The pore modification also increases the CO₂ bonding affinity from 23.2 kJ mol⁻¹ to 32.2 and 30.1 kJ mol⁻¹. These observations are again due to the polarizable nature of the CO₂ molecule and its large quadrupole moment. The enhanced Q_{st} values are expected due to both chemical and physical pore modifications. In addition to the electronic nature of -NH₂ and -NO₂, upon framework functionalization, the pore size of

NPOF-4 is reduced and this reduction provides higher adsorption potentials for CO₂ and thus higher uptake and bonding affinity were observed. The Q_{st} drops with higher CO₂ loading for functionalized NPOFs and clearly indicates the significant interactions between the CO₂ molecules and the functionalized pore surface. In contrast to this observation, the chemically homogeneous and non-functionalized pore surface of NPOF-4 leads to a non-notable change in Q_{st} upon increased CO₂ loading. The Q_{st} values for functionalized NPOFs exceeds most of the organic polymers such as BILPs,³⁷ functionalized CPMs⁵⁶ but are much lower than polyamine-tethered PPNs⁴⁰ and PAFs,⁶⁵ alkylamine appended MOF⁶⁶ which feature short-chain aliphatic amines having binding affinities similar to those of amine solutions being employed in CO₂ scrubbing (50-100 kJ mol⁻¹). It should be noted that PSM of PAF-1 with alkylmethylamine (PAF-1-CH₂NH₂) showed CO₂ uptake of 98 cc g⁻¹ which is almost double that of parent PAF-1 (55 cc g⁻¹) at 273 K / 1 bar even though the latter has a surface area three times higher. This dramatic increase in CO₂ uptake can be attributed to the much higher binding affinity of PAF-1-CH₂NH₂ compared to parent PAF-1 (15.6 kJ mol⁻¹). The notable difference in the binding affinity for CO₂ is most likely caused by the more reactive nature of the alkylamine employed for the functionalization of PAF-1 and PPN-6 as evidenced by the large initial Q_{st} values at lower coverage. Tailoring the binding affinity for selective CO₂ separation is essential because high heats of adsorption can lead to a major drawback wherein regeneration processes of adsorbents require heating as in the case of amine solutions (ca. 50-100 kJ mol⁻¹) that are associated with considerable energy penalty. Recent findings by Wilmer, et al. have suggested that these high binding affinities are less desirable when hypothetical MOFs

were screened for CO₂ capture from flue gas or natural gas, and that only moderate surface areas would be needed (1000 to 1500 m² g⁻¹).⁶⁷ Ironically, the Q_{st} of NPOF-4-NO₂ (32.5 kJ mol⁻¹) and NPOF-4-NH₂ (30.1 kJ mol⁻¹) are within the desirable range and suggest that both materials can have novel properties for use in selective CO₂ separation from natural gas or flue gas. Additionally, the fully reversible nature of the CO₂ isotherms of both samples at ambient conditions (Figure 3.13 and Figure 3.14) also indicates that CO₂-adsorbent interactions are weak enough to allow for adsorbents regeneration without applying heat.

The Q_{st} values for H₂ were calculated from adsorption data collected at 77 and 87 K by the virial method. At zero-coverage, the Q_{st} values are 7.17, 8.3 and 8.09 kJ mol⁻¹ for NPOF-4, NPOF-4-NO₂ and NPOF-NH₂, respectively (Figure 4.3). These values are higher than the values reported for organic polymers in general and similar to those having functionalized pores. In a similar fashion, the CH₄ uptakes at 273 K and 298 K and 1 bar were collected for all materials and the corresponding heats of adsorption was again calculated by using the virial method and the results are presented in Figure 4.2. The methane Q_{st} values suggest that pore functionalization with polar functionalities reduces the interaction with methane as a result of the non-polar nature of the CH₄ molecule which is consistent with recent reports on methane storage by non-functionalized PAFs.

Figure 4.1: Carbon dioxide isosteric heat of adsorption curves of NPOFs.

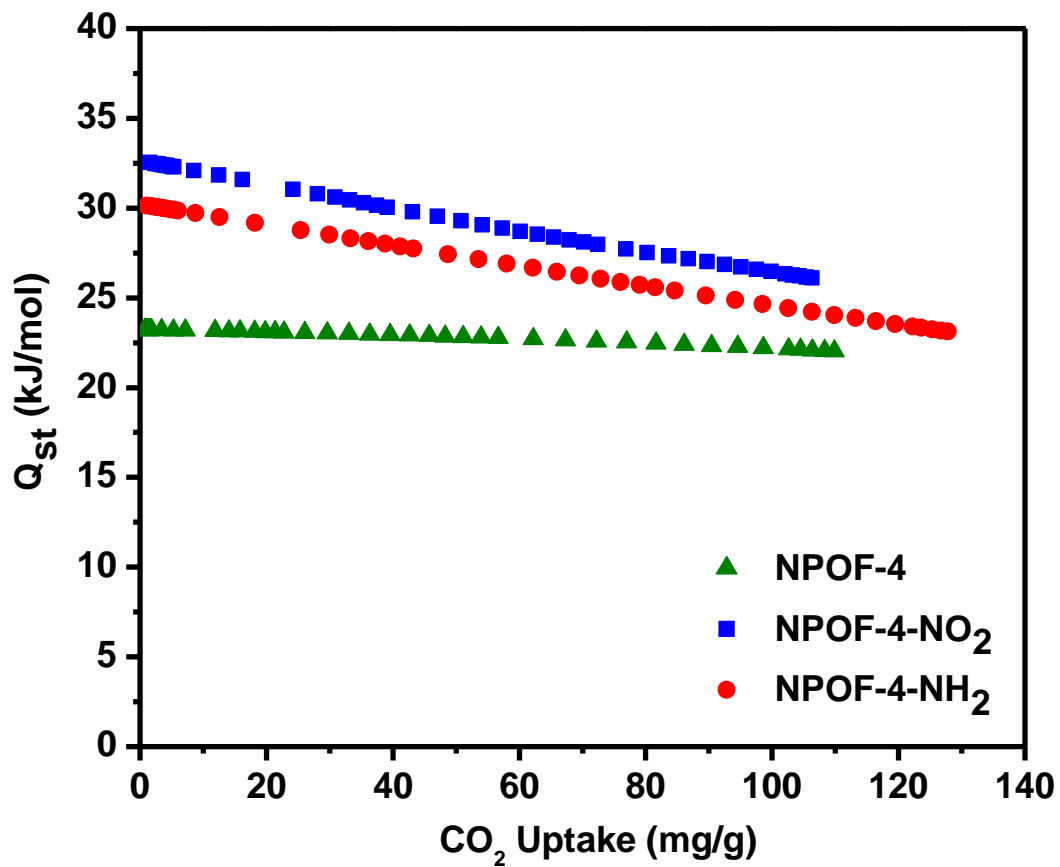


Figure 4.2: Methane isosteric heat of adsorption curves of NPOFs.

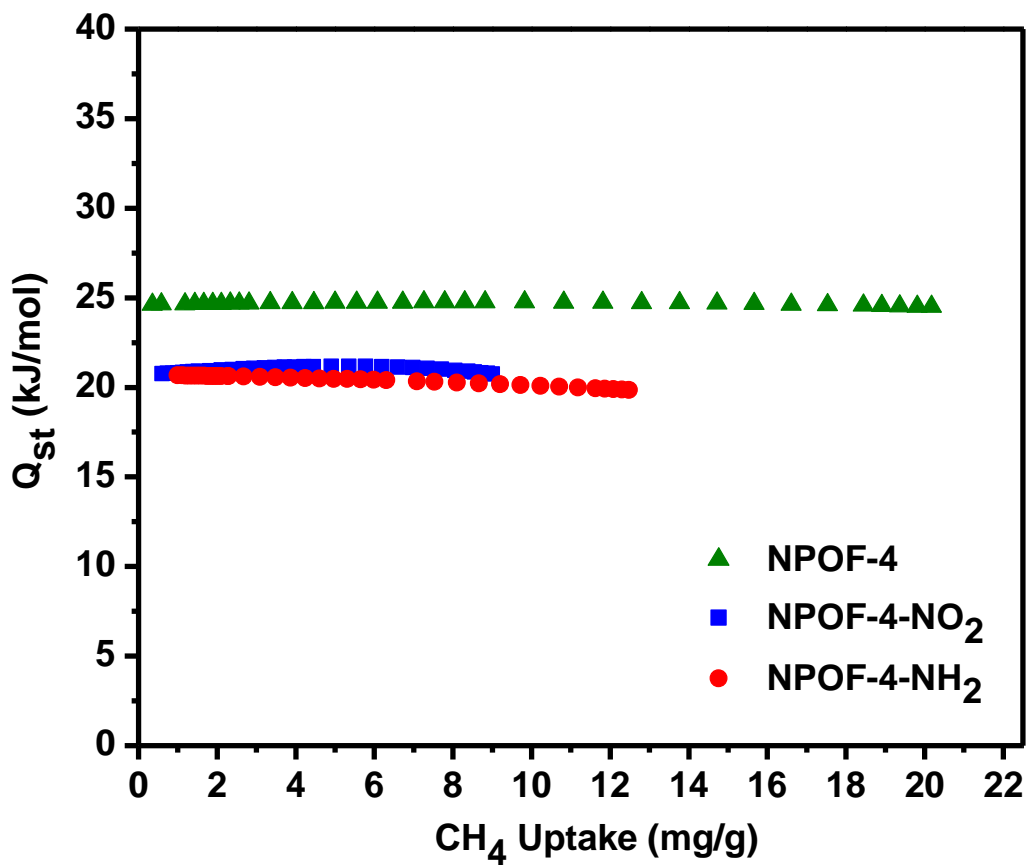


Figure 4.3: Hydrogen isosteric heat of adsorption curves of NPOFs.

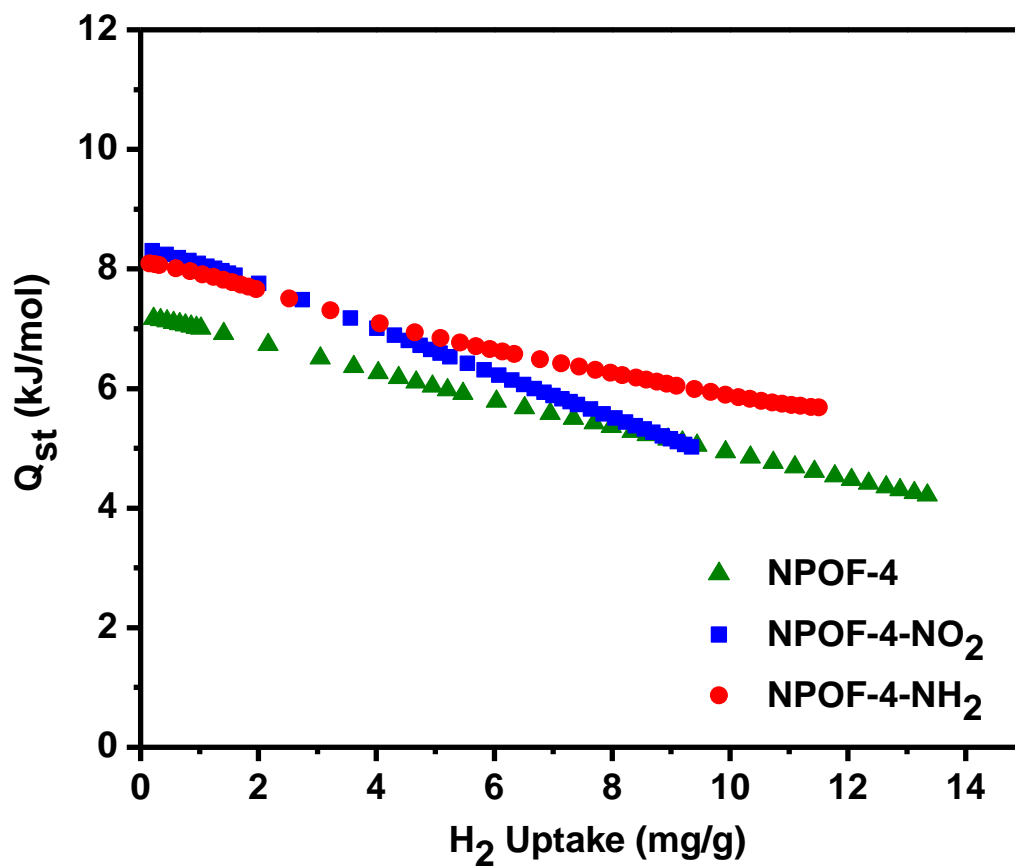


Figure 4.4: Virial analysis curve fitting of CO₂ adsorption isotherms for NPOF-4, NPOF-4-NO₂ and NPOF-4-NH₂ (blue circles: 273 K, olive squares: 298 K).

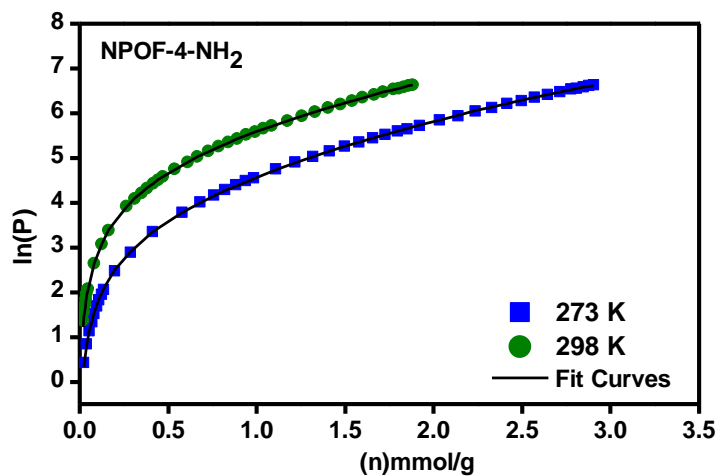
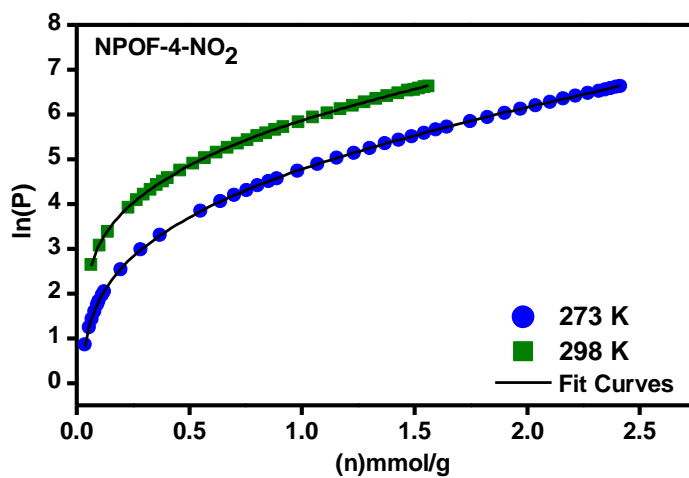
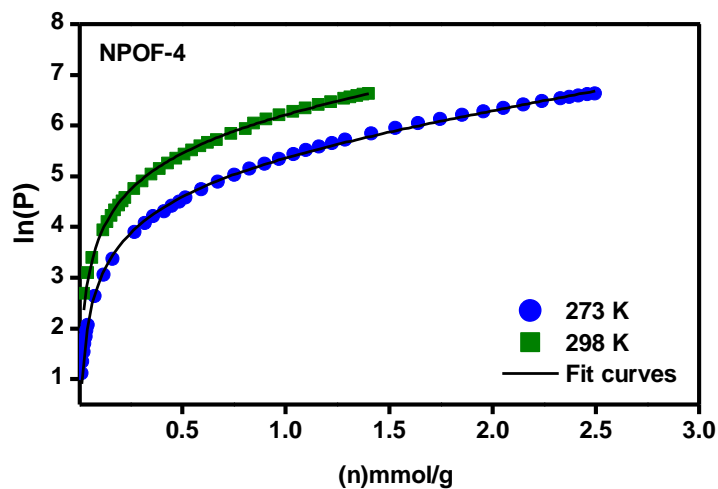


Figure 4.5: Virial analysis curve fitting of CH₄ adsorption isotherms for NPOF-4, NPOF-4-NO₂ and NPOF-4-NH₂ (blue circles: 273 K, olive squares: 298 K).

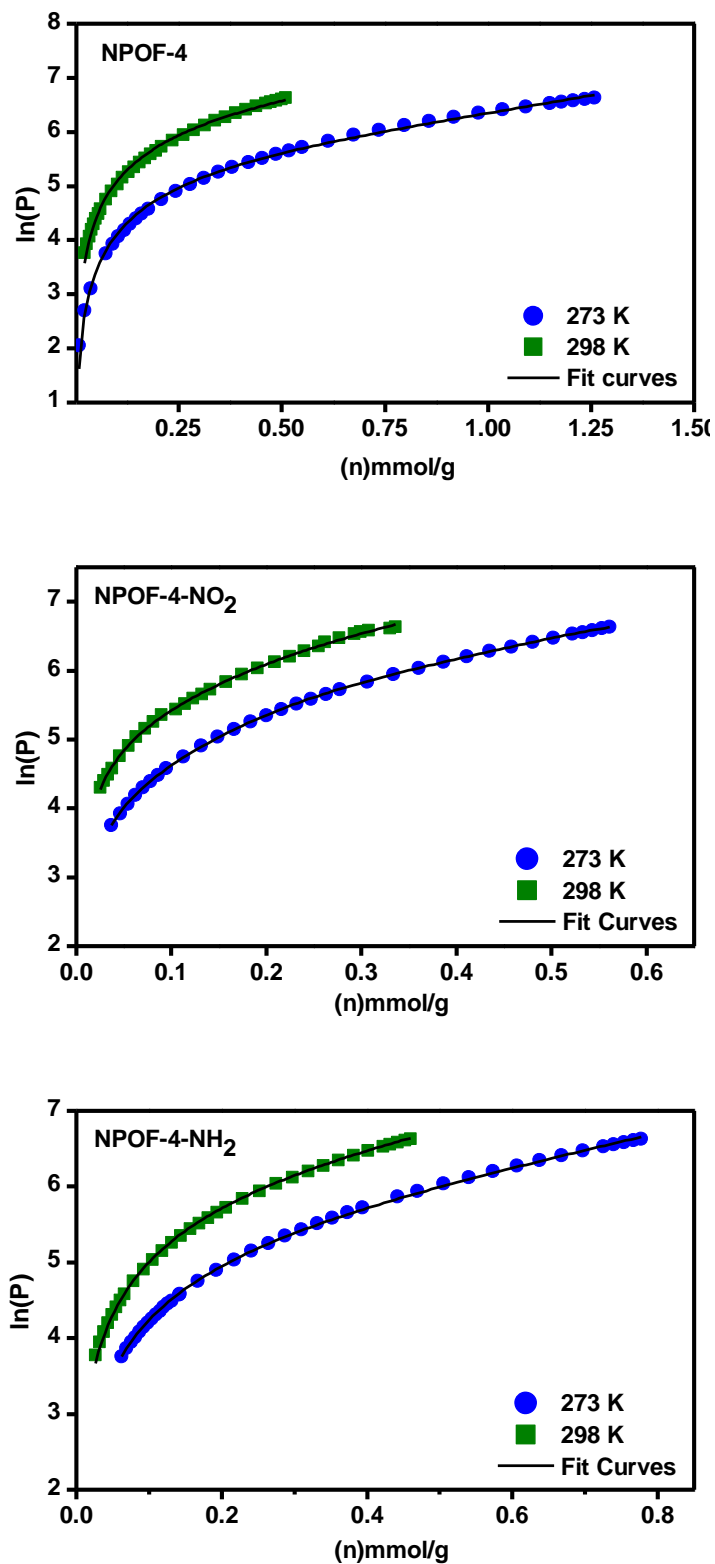
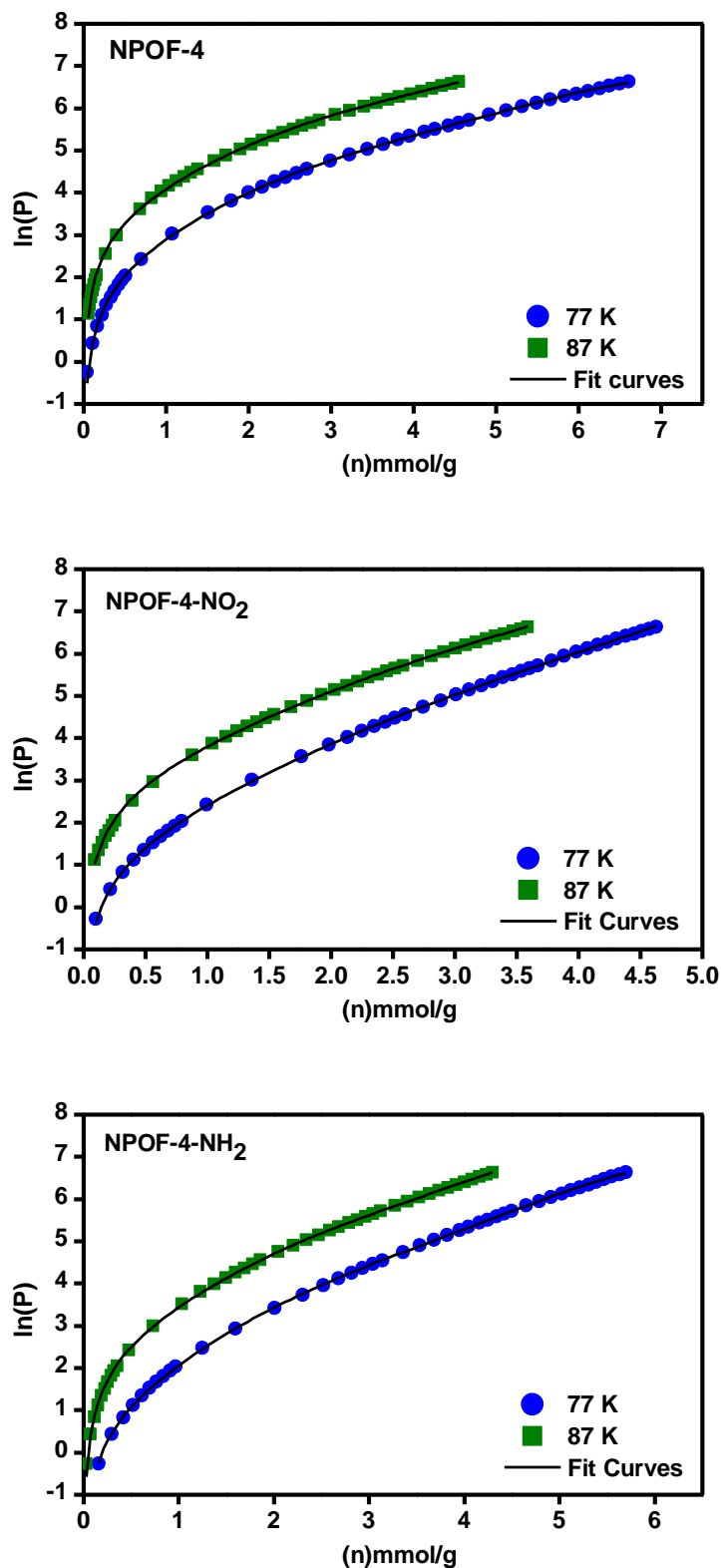


Figure 4.6: Virial analysis curve fitting of H₂ adsorption isotherms for NPOF-4, NPOF-4-NO₂ and NPOF-4-NH₂ (blue circles: 77 K, olive squares: 87 K).



Chapter 5

Gas Separation and Selectivity Capabilities for Nanoporous Organic Frameworks

5.1 Introduction

As a result of the economical and environmental impacts of gaseous impurities, selective gas separation continues to gain great attention by the scientific community.^{62,68-96} In particular, the separation of CO₂ from N₂, CH₄ has become a global concern since carbon dioxide exists as an impurity in flue gases as well as in natural gas. New technologies and material design in this area can result in a reduction in CO₂ concentration in the atmosphere and can provide a facile approach to the production of high purity natural gas. Owing to their tunable properties to capture targeted gases, porous organic polymers are an attractive method for this purification process. Calculations for the separation and selective capture capabilities of a porous polymer media are performed based on the polymer's pure gas isotherms. Typically, there are three different methods for calculating selectivity: (1) initial slopes method,⁹⁷ (2) Henry's Law constants where experimental isotherms are fitted to the virial-type expansion that was mentioned in Chapter 4 for the calculation of isosteric heat of adsorption,^{63,98} and (3) ideal adsorbed solution theory (IAST) where single-component isotherms is used to predict the mixture adsorption equilibria.^{98,99} The latter two methods will not be

discussed here and we have used the initial slopes method to carry out selectivity studies.

The initial slopes method for calculating selectivity employs the varying levels of gas uptake in the low pressure range (typically from 0 to about 0.1 bar). In this pressure range, the isotherms are assumed to be linear. As such, data points in this range are fit according to the linear equation: $y = mx + b$, where y is the gas uptake in mmol g^{-1} , and x is the pressure in bar, m is the slope of the curve, and b is the y -intercept of the curve. Selectivity is then calculated based on the ratio of the slopes of the curves for the respective gases. Selectivities based on this method are pursued based on the fact that it represents the simplest and fastest method of the three methods listed above. Nevertheless, the assumption that the isotherms are linear in the low pressure range can affect selectivity levels. Additionally, the applicable pressure range is very subjective and may hinder the calculation's reliability. As a result, utilizing the initial slopes method is typically performed as a quick assessment to pursue selectivity for the polymer or as a confirmation of one of the other two calculation methods.

In addition to this method, recent reports have reported selectivity studies using the equation:

$$S = \frac{q_1/q_2}{p_1/p_2} \quad \text{Equation 1}$$

where S is the selectivity factor, q_i represents the quantity adsorbed of component i , and p_i represents the partial pressure of component i .⁸ For post-combustion CO_2 capture, the partial pressure of CO_2 and N_2 are 0.15 bar and 0.75 bar, respectively. We have used both methods to study the selectivity of NPOFs.

5.2 Results and Discussion

Effective CO₂ adsorbents are expected to have high selectivity for CO₂ over other gases such as N₂ (~75 % in flue gas) and CH₄ (~95% in natural gas) along with high CO₂ capacity for gas separation application. Therefore, we carried out CO₂/N₂ and CO₂/CH₄ selectivity studies for NPOF-4 before and after framework functionalization to evaluate the preferential CO₂ adsorption at 273 and 298 K (Figure 5.1 - Figure 5.6). The general observation was that all materials show very low N₂ uptake and tangible CO₂ amounts at 0.15 bar (partial CO₂ pressure in flue gas) especially for the functionalized NPOFs. The same trend was also noticed for the CH₄ isotherms that show markedly lower CH₄ uptakes than CO₂ by all NPOFs. Selectivity studies were first calculated according to Equation 1.

For post-combustion CO₂ capture, the partial pressure of CO₂ and N₂ are 0.15 bar and 0.75 bar, respectively. The CO₂/N₂ selectivity studies resulted in very high values for NPOF-4-NO₂ (133) and NPOF-NH₂ (81), while NPOF-4 exhibited much lower selectivity (49) at 273 K (Table 5.1). Upon increasing the temperature to 298 K, the selectivity drops significantly to 14 (NPOF-4), 62 (NPOF-4-NO₂), and 29 (NPOF-4-NH₂). Furthermore, CO₂/N₂ selectivity studies were determined by using the ratios of Henry law constants for which the constants can be calculated from the initial slopes of pure gas isotherms. This simple and convenient method has been widely employed to investigate the gas selective nature of a wide range of porous adsorbents including porous organic materials as we have reported recently for BILPs. According to initial slope calculations presented in Table 5.1, the CO₂/N₂ selectivity levels for functionalized NPOFs are again much higher than the value calculated for NPOF-4 and are somewhat

higher than the values obtained from Equation 1. Nevertheless, both methods revealed the highly selective nature of NPOF-4-NO₂ and NPOF-4-NH₂ towards CO₂ over N₂. Noteworthy, these selectivity levels are among the highest by porous materials. For comparison, the most selective materials, NPOF-4-NO₂, outperforms other selective adsorbents at 273 K including BILPs (59-113),³⁷ PECONF-2 (109),⁵⁷ BPL carbon (17.8)⁶⁰ and ZIFs (17-50),⁵⁹ Bio-MOF-11 (81)⁹⁷ and noncovalent porous materials (NPMs) (74).¹⁰⁰

By following the same methods described above, we calculated the CO₂/CH₄ selectivity of NPOFs at 273 K and 298 K (Table 5.1). In a typical natural gas purification process, the mole fractions of CO₂ and CH₄ are 0.05 and 0.95, respectively, resulting in CO₂ having a partial pressure of only 0.1 bar. The CO₂/CH₄ selectivity values from both methods; initial slope calculations and Equation 1, provided consistent data for each framework. The selectivity trend is in line with those observed for CO₂/N₂ studies and reveal that NPOF-4-NO₂ is the most selective material with selectivity levels in the range of 16-15 at 273 K that again outperforms the parent framework (NPOF-4 : 3-3) and its amine-functionalized derivative (NPOF-4-NH₂ : 13-11) (Table 5.1). The latter values fall within the range of recently reported porous materials such as diimide-based organic polymers, BPL carbon, ZIFs, and most MOFs. The outcome of selectivity studies surprisingly indicates that introducing the –NO₂ functionality into the pore walls of microporous organic frameworks is very advantageous for CO₂ separation applications. Most likely the higher selectivity of NPOF-4-NO₂ originates from the polar nature of the nitro functionality and due to its larger size when compared to –NH₂ which reduces pore size and induces dipole-dipole interactions involving CO₂. Although NPOF-4-NO₂ and

NPOF-4-NH₂ have remarkable selectivities, their capacity for CO₂ at the practical partial pressure of this gas in flue gas (0.15 bar) remains below the desired level (3.0 mmol g⁻¹) which can limit their applications as adsorbents. Our results again highlight the considerable challenge of attaining high selectivity levels without compromising adsorption capacity for CO₂ adsorbents. Selectivity results are summarized in the following tables.

Table 5.1: Selectivity results for NPOFs. ^aSelectivity was calculated from the Equation 1 at 273 K and 298 K. ^bSelectivity (mol mol⁻¹) was calculated from initial slope calculations at 273 and 298 K.

	Selectivity ^a				Selectivity ^b			
	CO ₂ /N ₂		CO ₂ /CH ₄		CO ₂ /N ₂		CO ₂ /CH ₄	
Network	273 K	298 K	273 K	298 K	273 K	298 K	273 K	298 K
NPOF-4	49	14	3	3	27	16	3	3
NPOF-4-NO₂	133	62	16	11	139	66	15	10
NPOF-4-NH₂	81	29	13	9	101	40	11	8

Figure 5.1: Gas uptake selectivity studies for NPOF-4 at 273 K.

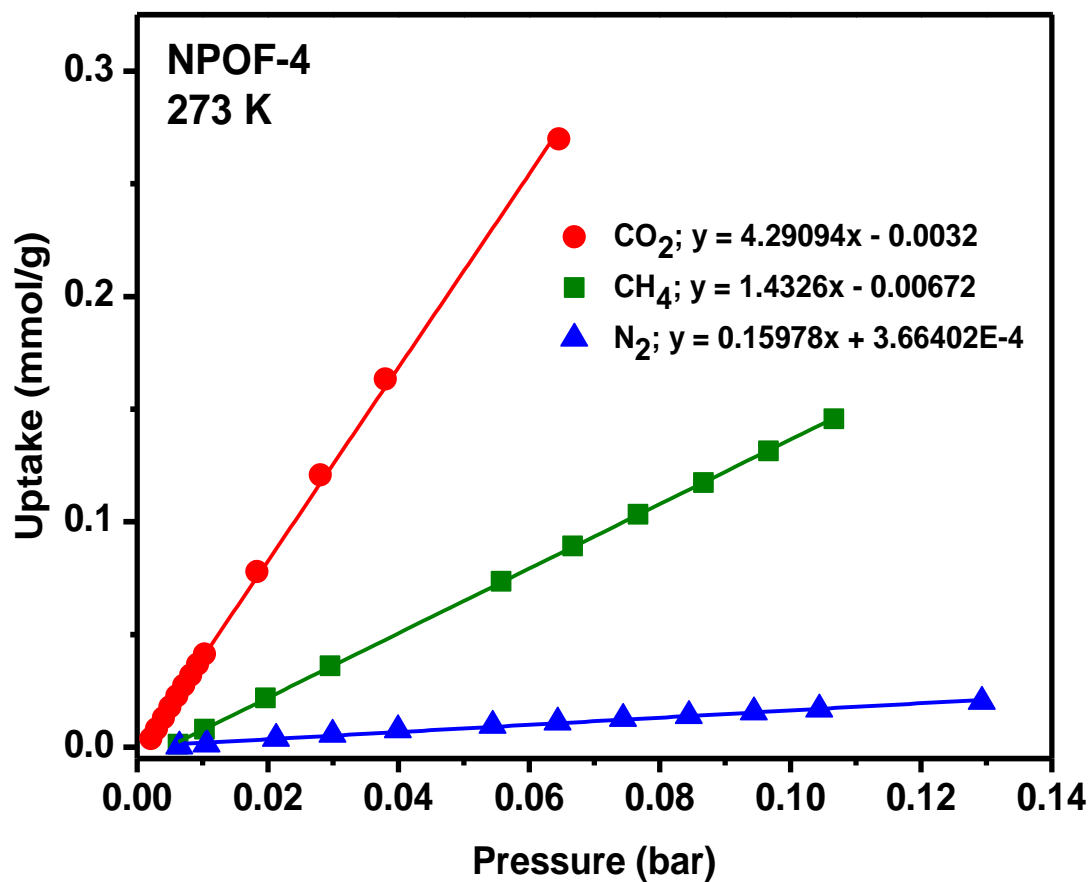


Figure 5.2: Gas uptake selectivity studies for NPOF-4 at 298 K.

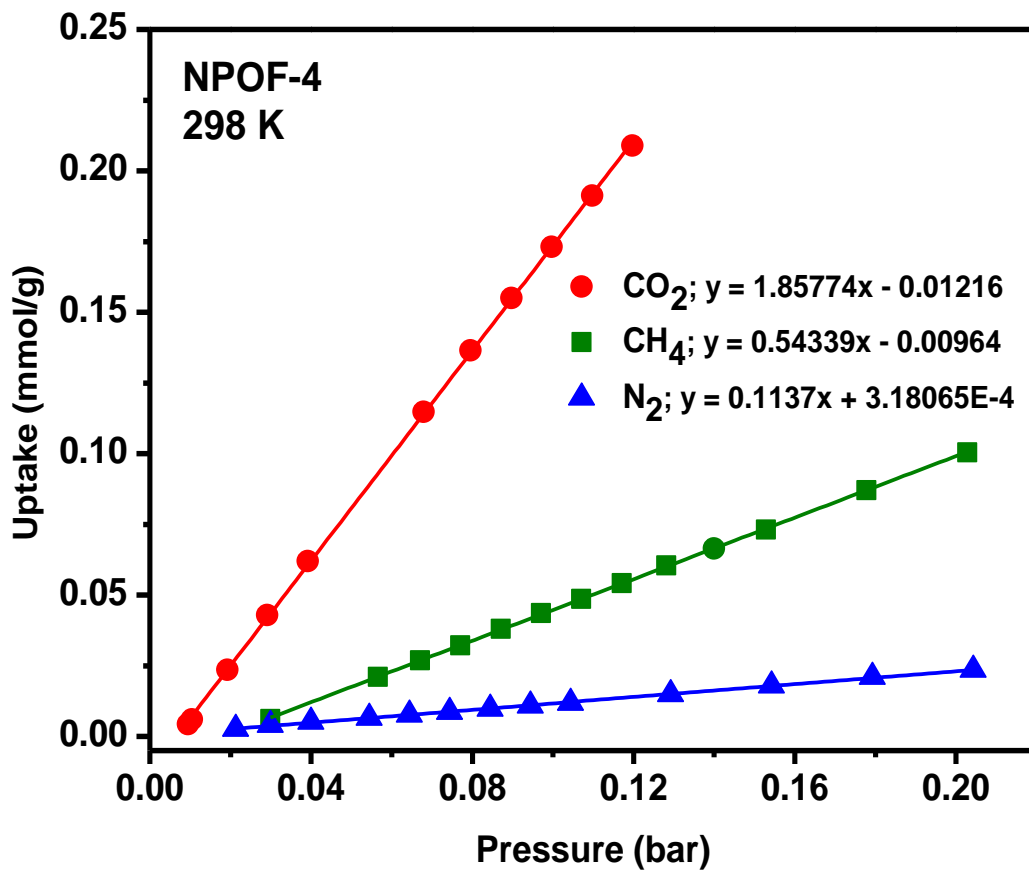


Figure 5.3: Gas uptake selectivity studies for NPOF-4-NO₂ at 273 K.

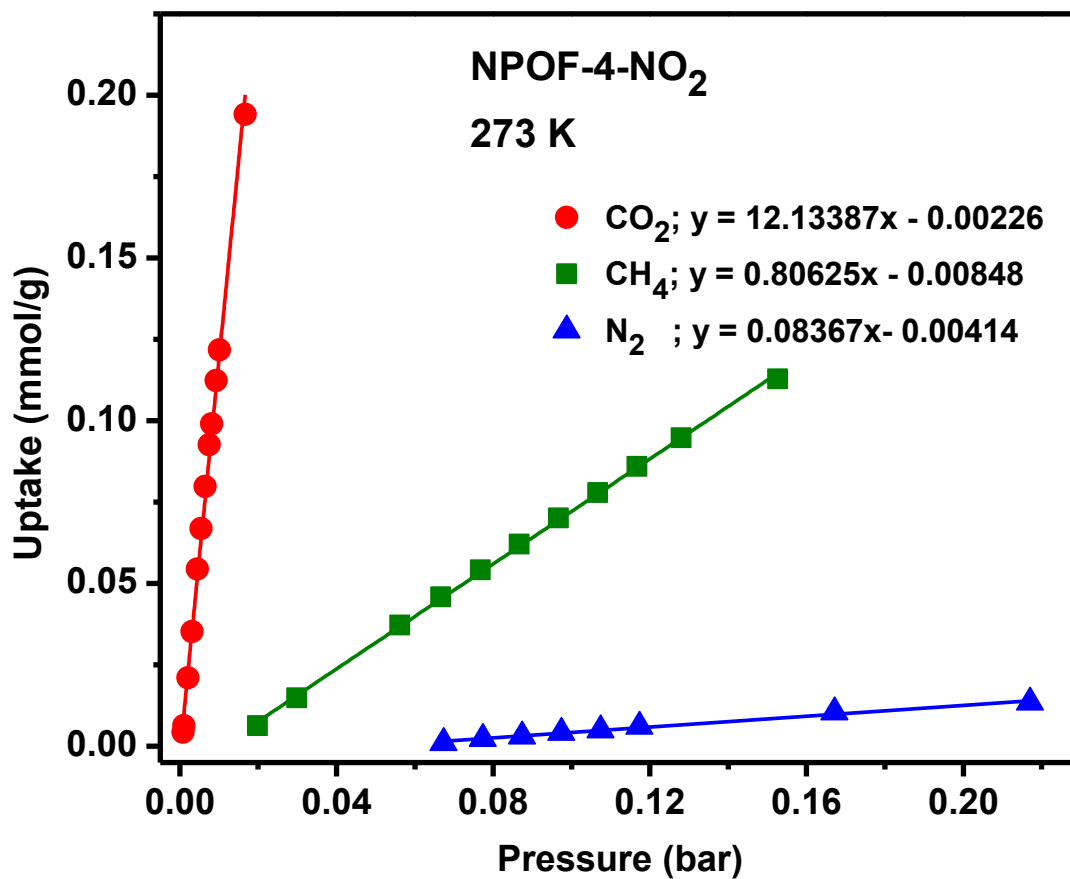


Figure 5.4: Gas uptake selectivity studies for NPOF-4-NO₂ at 298 K.

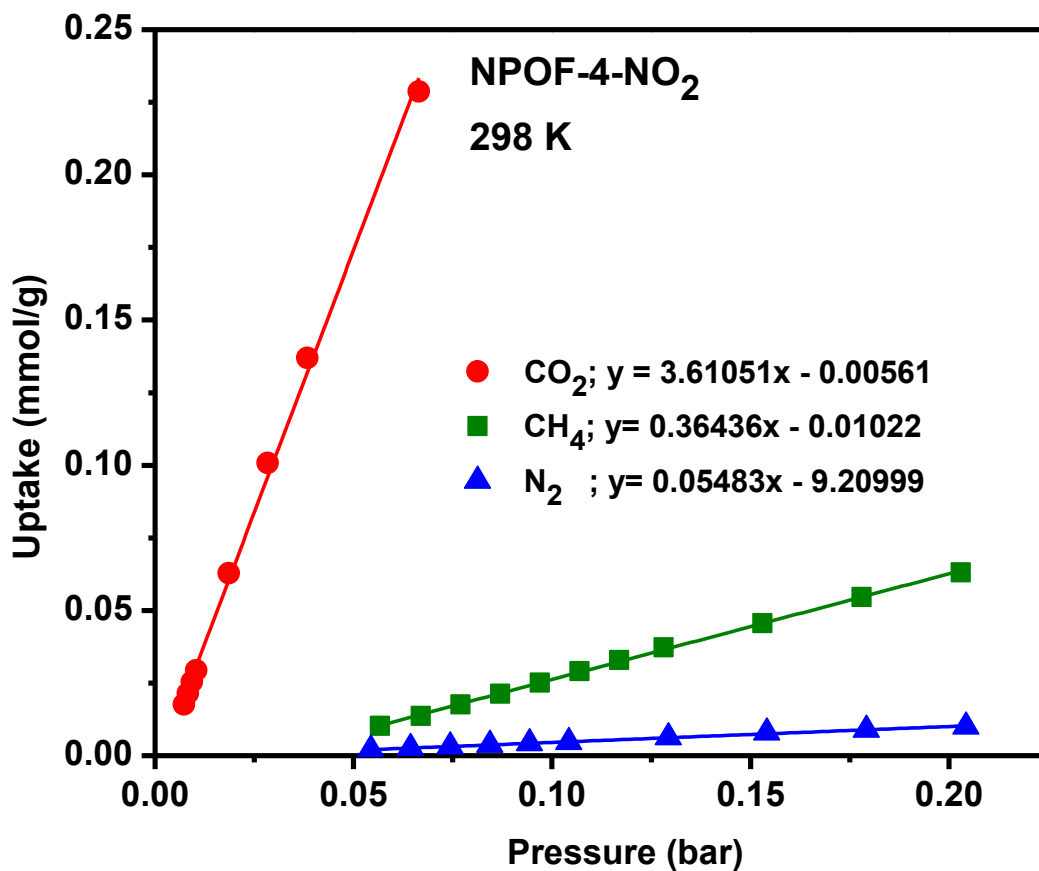


Figure 5.5: Gas uptake selectivity studies for NPOF-4-NH₂ at 273 K.

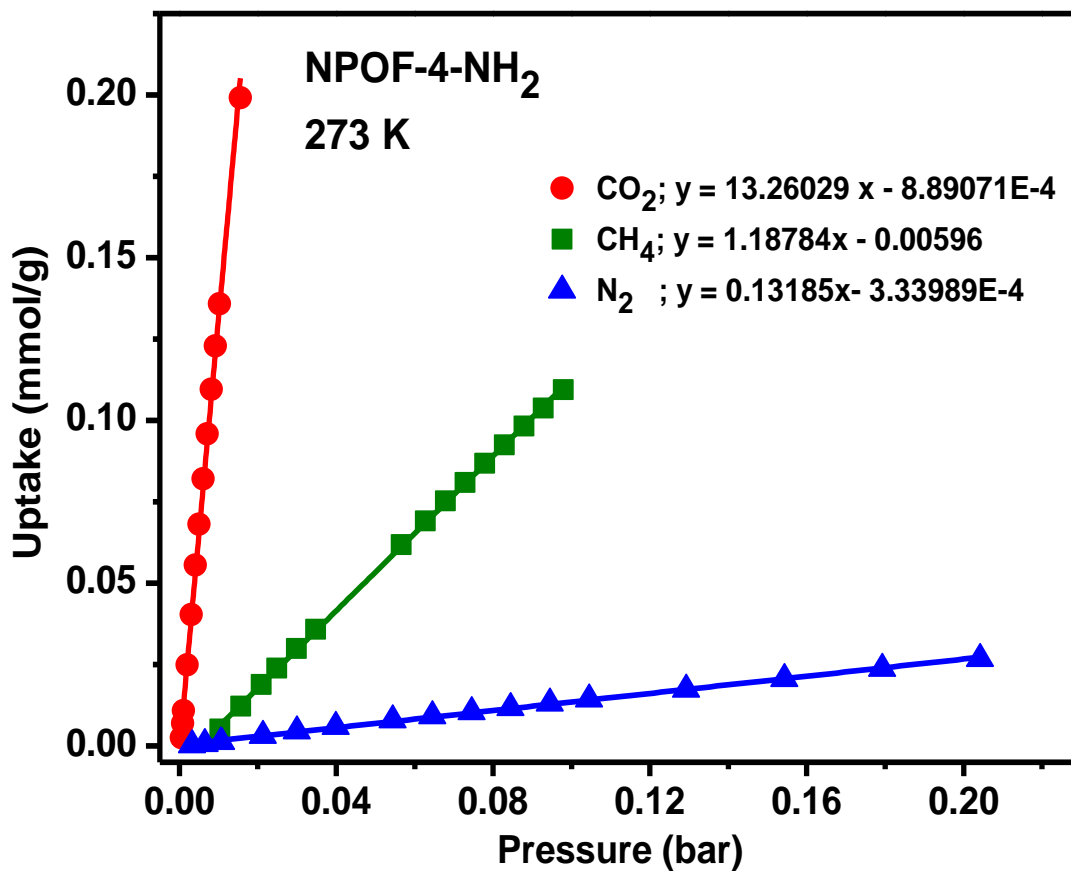


Figure 5.6: Gas uptake selectivity studies for NPOF-4-NH₂ at 298 K.

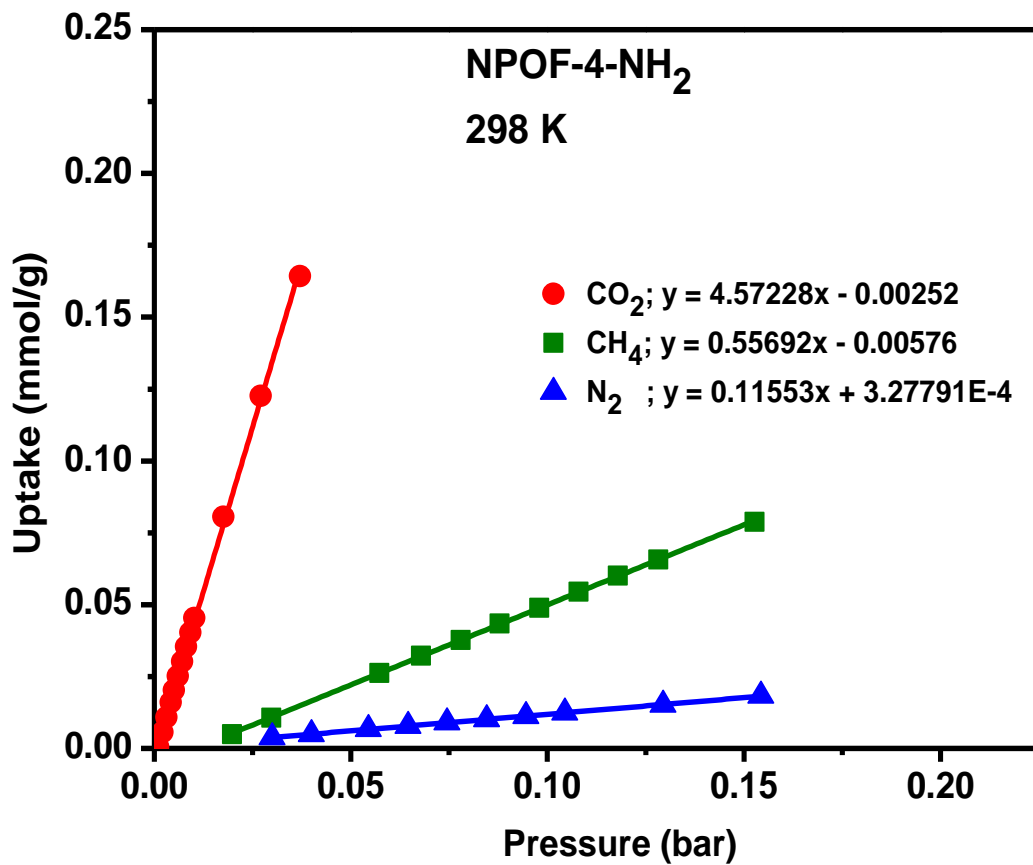


Table 5.2: CO₂ and N₂ uptakes at 273 and 298 K for CO₂/N₂ selectivity studies by using Equation 1.

	273 K				298 K			
	CO ₂		N ₂		CO ₂		N ₂	
Network	Pressure (bar)	Uptake (mmol/g)	Pressure (bar)	Uptake (mmol/g)	Pressure (bar)	Uptake (mmol/g)	Pressure (bar)	Uptake (mmol/g)
NPOF-4	0.15	0.59	0.75	0.06	0.15	0.26	0.75	0.10
NPOF-4-NO₂	0.15	0.97	0.75	0.04	0.15	0.45	0.75	0.04
NPOF-4-NH₂	0.15	1.09	0.75	0.07	0.15	0.53	0.75	0.09

Table 5.3: CO₂ and CH₄ uptakes at 273 and 298 K for CO₂/CH₄ selectivity studies by using Equation 1.

	273 K				298 K			
	CO ₂		CH ₄		CO ₂		CH ₄	
Network	Pressure (bar)	Uptake (mmol/g)	Pressure (bar)	Uptake (mmol/g)	Pressure (bar)	Uptake (mmol/g)	Pressure (bar)	Uptake (mmol/g)
NPOF-4	0.05	0.21	0.95	1.20	0.05	0.09	0.95	0.48
NPOF-4-NO₂	0.05	0.47	0.95	0.54	0.05	0.18	0.95	0.31
NPOF-4-NH₂	0.05	0.51	0.95	0.75	0.05	0.22	0.95	0.44

Chapter 6

Concluding Remarks

The research presented in this thesis comprises the design, synthesis and post-synthetic modifications of functional Nanoporous Organic Frameworks (NPOFs). We have successfully synthesized a new NPOF from a novel building block, 1,3,5,7-tetrakis(4-acetylphenyl)adamantane (TAPA) by employing a metal-free synthesis approach. Subsequently, we have successfully used post-synthesis modification processes to functionalize the framework with $-\text{NO}_2$ and $-\text{NH}_2$ functionalities to investigate their effect on CO_2 uptake and the potential use of functionalized NPOFs in small gas storage and separation applications. The metal-free synthesis of NPOF-4 and its convenient pore surface modification resulted in a significant enhancement in CO_2 binding affinity: 32.5 and 30.1 kJ mol^{-1} and selective binding over nitrogen and methane: CO_2/N_2 (139) and CO_2/CH_4 (15) at 273 K. These results confirmed that surface functionality outweighs the high surface area with regards to high CO_2 uptakes and binding affinity. Therefore, we conclude that having polar groups ($-\text{NO}_2$ and $-\text{NH}_2$) on pore walls notably enhances the initial CO_2 uptake and overall selectivity. These results highlight the potential use of functionalized NPOFs in post-combustion CO_2 separation and in natural gas purification processes. The functionalized NPOFs are also capable of storing up to 1.15 wt% H_2 at 77 K and 1 bar with high isosteric hydrogen heats of adsorption (8.1 and 8.3 kJ mol^{-1}). The relatively high initial uptake of H_2 by

functionalized NPOFs also indicates the significance of the physical and electronic nature of the pores in the design of future hydrogen storage sorbents.

List of References

- (1) ESRL, Trends in Atmospheric Carbon Dioxide. *ESRL's Global Monitoring Division* **2010**.
- (2) Rubin, E. S.; Mantripragada, H.; Marks, A.; Versteeg, P.; Kitchin, J., The Outlook for Improved Carbon Capture Technology. *Prog. Energy Combust. Sci.* **2012**, *38*, 630.
- (3) D'Alessandro, D. M.; Smit, B.; Long, J. R., Carbon Dioxide Capture: Prospects for New Materials. *Angew Chem Int Edit* **2010**, *49*, 6058.
- (4) Ma, S. Q.; Zhou, H. C., Gas Storage in Porous Metal-Organic Frameworks for Clean Energy Applications. *Chem. Commun.* **2010**, *46*, 44.
- (5) Keskin, S.; van Heest, T. M.; Sholl, D. S., Can Metal-Organic Framework Materials Play a Useful Role in Large-Scale Carbon Dioxide Separations? *ChemSusChem* **2010**, *3*, 879.
- (6) Liu, Y.; Wang, Z. U.; Zhou, H.-C., Recent Advances in Carbon Dioxide Capture with Metal-Organic Frameworks. *Greenhouse Gases: Science and Technology* **2012**, *2*, 239.
- (7) Hoff, K. A.; Juliussen, O.; Falk-Pedersen, O.; Svendsen, H. F., Modeling and Experimental Study of Carbon Dioxide Absorption in Aqueous Alkanolamine Solutions Using a Membrane Contactor. *Ind. Eng. Chem. Res.* **2004**, *43*, 4908.

- (8) Rao, A. B.; Rubin, E. S., A Technical, Economic, and Environmental Assessment of Amine-Based CO₂ Capture Technology for Power Plant Greenhouse Gas Control. *Environ. Sci. Technol.* **2002**, *36*, 4467.
- (9) Lepaumier, H.; Picq, D.; Carrette, P.-L., New Amines for CO₂ Capture. I. Mechanisms of Amine Degradation in the Presence of CO₂. *Ind. Eng. Chem. Res.* **2009**, *48*, 9061.
- (10) Mondal, M. K.; Balsora, H. K.; Varshney, P., Progress and Trends in CO₂ Capture/Separation Technologies: A Review. *Energy* **2012**, *46*, 431.
- (11) Brunetti, A.; Scura, F.; Barbieri, G.; Drioli, E., Membrane Technologies for CO₂ Separation. *J. Membr. Sci.* **2010**, *359*, 115.
- (12) Siriwardane, R. V.; Shen, M.-S.; Fisher, E. P.; Poston, J. A., Adsorption of CO₂ on Molecular Sieves and Activated Carbon. *Energy Fuels* **2001**, *15*, 279.
- (13) Díaz, E.; Muñoz, E.; Vega, A.; Ordóñez, S., Enhancement of the CO₂ Retention Capacity of X Zeolites by Na- and Cs-Treatments. *Chemosphere* **2008**, *70*, 1375.
- (14) Zhang, J.; Webley, P. A.; Xiao, P., Effect of Process Parameters on Power Requirements of Vacuum Swing Adsorption Technology for CO₂ Capture from Flue Gas. *Energy Convers. Manage.* **2008**, *49*, 346.
- (15) El-Kaderi, H. M.; Hunt, J. R.; Mendoza-Cortes, J. L.; Cote, A. P.; Taylor, R. E.; O'Keeffe, M.; Yaghi, O. M., Designed Synthesis of 3D Covalent Organic Frameworks. *Science* **2007**, *316*, 268.
- (16) Jackson, K., Synthesis and Characterization of Highly Porous Borazine-Linked Polymers Via Dehydrogenation/Dehydrocoupling of Borane-Amine Adducts and

- Their Applications to Gas Storage. PhD. Dissertation, Virginia Commonwealth University, Richmond, VA, **2011**.
- (17) Kahveci, Z.; Islamoglu, T.; Shar, G. A.; Ding, R.; El-Kaderi, H. M., Targeted Synthesis of a Mesoporous Triptycene-Derived Covalent Organic Framework. *CrystEngComm* **2013**.
- (18) Reporting Physisorption Data for Gas/Solid Systems with Special Reference to the Determination of Surface Area and Porosity. *Pure Appl. Chem* **1985**, *57*, 16.
- (19) Wu, D.; Xu, F.; Sun, B.; Fu, R.; He, H.; Matyjaszewski, K., Design and Preparation of Porous Polymers. *Chem. Rev.* **2012**, *112*, 3959.
- (20) Rabbani, M. G.; El-Kaderi, H. M., Template-Free Synthesis of a Highly Porous Benzimidazole-Linked Polymer for CO₂ Capture and H₂ Storage. *Chem. Mater.* **2011**, *23*, 1650.
- (21) Jackson, K. T.; Rabbani, M. G.; Reich, T. E.; El-Kaderi, H. M., Synthesis of Highly Porous Borazine-Linked Polymers and Their Application to H₂, CO₂, and CH₄ Storage. *Polym. Chem.* **2011**, *2*, 2775.
- (22) Reich, T. E.; Jackson, K. T.; Li, S.; Jena, P.; El-Kaderi, H. M., Synthesis and Characterization of Highly Porous Borazine-Linked Polymers and Their Performance in Hydrogen Storage Application. *J. Mater. Chem.* **2011**, *21*, 10629.
- (23) Kassab, R. M.; Jackson, K. T.; El-Kadri, O. M.; El-Kaderi, H. M., Nickel-Catalyzed Synthesis of Nanoporous Organic Frameworks and Their Potential Use in Gas Storage Applications. *Res. Chem. Intermed.* **2011**, *37*, 747.
- (24) Ben, T.; Ren, H.; Ma, S. Q.; Cao, D. P.; Lan, J. H.; Jing, X. F.; Wang, W. C.; Xu, J.; Deng, F.; Simmons, J. M.; Qiu, S. L.; Zhu, G. S., Targeted Synthesis of a

- Porous Aromatic Framework with High Stability and Exceptionally High Surface Area. *Angew. Chem., Int. Ed.* **2009**, *48*, 9457.
- (25) Lu, W. G.; Yuan, D. Q.; Zhao, D.; Schilling, C. I.; Plietzsch, O.; Muller, T.; Brase, S.; Guenther, J.; Blumel, J.; Krishna, R.; Li, Z.; Zhou, H. C., Porous Polymer Networks: Synthesis, Porosity, and Applications in Gas Storage/Separation. *Chem. Mater.* **2010**, *22*, 5964.
- (26) McKeown, N. B.; Budd, P. M.; Msayib, K. J.; Ghanem, B. S.; Kingston, H. J.; Tattershall, C. E.; Makhseed, S.; Reynolds, K. J.; Fritsch, D., Polymers of Intrinsic Microporosity (Pims): Bridging the Void between Microporous and Polymeric Materials. *Chem. Eur. J.* **2005**, *11*, 2610.
- (27) Kuhn, P.; Antonietti, M.; Thomas, A., Porous, Covalent Triazine-Based Frameworks Prepared by Ionothermal Synthesis. *Angew. Chem., Int. Ed.* **2008**, *47*, 3450.
- (28) Jiang, J.-X.; Su, F.; Trewin, A.; Wood, C. D.; Campbell, N. L.; Niu, H.; Dickinson, C.; Ganin, A. Y.; Rosseinsky, M. J.; Khimiyak, Y. Z.; Cooper, A. I., Conjugated Microporous Poly(Aryleneethynylene) Networks. *Angew. Chem., Int. Ed.* **2007**, *46*, 8574.
- (29) Rose, M.; Klein, N.; Bohlmann, W.; Bohringer, B.; Fichtner, S.; Kaskel, S., New Element Organic Frameworks Via Suzuki Coupling with High Adsorption Capacity for Hydrophobic Molecules. *Soft Matter* **2010**, *6*, 3918.
- (30) Rabbani, M. G.; Reich, T. E.; Kassab, R. M.; Jackson, K. T.; El-Kaderi, H. M., High CO₂ Uptake and Selectivity by Triptycene-Derived Benzimidazole-Linked Polymers. *Chem. Commun.* **2012**, *48*, 1141.

- (31) Dawson, R.; Ratvijitvech, T.; Corker, M.; Laybourn, A.; Khimyak, Y. Z.; Cooper, A. I.; Adams, D. J., Microporous Copolymers for Increased Gas Selectivity. *Polym. Chem.* **2012**, *3*, 2034.
- (32) Budd, P. M.; Ghanem, B. S.; Makhseed, S.; McKeown, N. B.; Msayib, K. J.; Tattershall, C. E., Polymers of Intrinsic Microporosity (PIMs): Robust, Solution-Processable, Organic Nanoporous Materials. *Chem. Commun.* **2004**, *0*, 230.
- (33) Weber, J.; Su, Q.; Antonietti, M.; Thomas, A., Exploring Polymers of Intrinsic Microporosity – Microporous, Soluble Polyamide and Polyimide. *Macromol. Rapid Commun.* **2007**, *28*, 1871.
- (34) Pandey, P.; Katsoulidis, A. P.; Eryazici, I.; Wu, Y.; Kanatzidis, M. G.; Nguyen, S. T., Imine-Linked Microporous Polymer Organic Frameworks. *Chem. Mater.* **2010**, *22*, 4974.
- (35) Rose, M.; Klein, N.; Senkovska, I.; Schrage, C.; Wollmann, P.; Bohlmann, W.; Bohringer, B.; Fichtner, S.; Kaskel, S., A New Route to Porous Monolithic Organic Frameworks via Cyclotrimerization. *J. Mater. Chem.* **2011**, *21*, 711.
- (36) Yuan, D.; Lu, W.; Zhao, D.; Zhou, H.-C., Highly Stable Porous Polymer Networks with Exceptionally High Gas-Uptake Capacities. *Adv. Mater.* **2011**, *23*, 3723.
- (37) Rabbani, M. G.; El-Kaderi, H. M., Synthesis and Characterization of Porous Benzimidazole-Linked Polymers and Their Performance in Small Gas Storage and Selective Uptake. *Chem. Mater.* **2012**, *24*, 1511.
- (38) Tanabe, K. K.; Cohen, S. M., Postsynthetic Modification of Metal-Organic Frameworks-a Progress Report. *Chem. Soc. Rev.* **2011**, *40*, 498.

- (39) Lu, W. G.; Yuan, D. Q.; Sculley, J. L.; Zhao, D.; Krishna, R.; Zhou, H. C., Sulfonate-Grafted Porous Polymer Networks for Preferential CO₂ Adsorption at Low Pressure. *J. Am. Chem. Soc.* **2011**, *133*, 18126.
- (40) Lu, W.; Sculley, J. P.; Yuan, D.; Krishna, R.; Wei, Z.; Zhou, H.-C., Polyamine-Tethered Porous Polymer Networks for Carbon Dioxide Capture from Flue Gas. *Angew. Chem., Int. Ed.* **2012**, *51*, 7480.
- (41) Xu, X.; Song, C.; Wincek, R.; Andresen, J. M.; Miller, B. G.; Scaroni, A. W., Separation of CO₂ from Power Plant Flue Gas Using a Novel CO₂ “Molecular Basket” Adsorbent. *Fuel Chem. Div. Prepr.* **2003**, *48*, 162.
- (42) Reichert, V. R.; Mathias, L. J., Expanded Tetrahedral Molecules from 1,3,5,7-Tetraphenyladamantane. *Macromolecules* **1994**, *27*, 7015.
- (43) Choi, S. B.; Seo, M. J.; Cho, M.; Kim, Y.; Jin, M. K.; Jung, D. Y.; Choi, J. S.; Ahn, W. S.; Rowsell, J. L. C.; Kim, J., A Porous and Interpenetrated Metal-Organic Framework Comprising Tetranuclear Iron(III)-Oxo Clusters and Tripodal Organic Carboxylates and Its Implications for (3,8)-Coordinated Networks. *Cryst. Growth Des.* **2007**, *7*, 2290.
- (44) Bernt, S.; Guillerme, V.; Serre, C.; Stock, N., Direct Covalent Post-Synthetic Chemical Modification of Cr-Mil 101 Using Nitrating Acid. *Chem. Commun.* **2011**, *47*, 2838.
- (45) Moellmer, J.; Celer, E. B.; Luebke, R.; Cairns, A. J.; Staudt, R.; Eddaoudi, M.; Thommes, M., Insights on Adsorption Characterization of Metal-Organic Frameworks: A Benchmark Study on the Novel soc-MOF. *Microporous Mesoporous Mater.* **2010**, *129*, 345.

- (46) Lowell, S. *Characterization of Porous Solids and Powders : Surface Area, Pore Size, and Density*; Kluwer Academic Publishers: Dordrecht ; Boston, 2004.
- (47) Dombrowski, R. J.; Hyduke, D. R.; Lastoskie, C. M., Pore Size Analysis of Activated Carbons from Argon and Nitrogen Porosimetry Using Density Functional Theory. *Langmuir* **2000**, *16*, 5041.
- (48) Schumacher, K.; Ravikovitch, P. I.; Du Chesne, A.; Neimark, A. V.; Unger, K. K., Characterization of MCM-48 Materials. *Langmuir* **2000**, *16*, 4648.
- (49) Cote, A. P.; Benin, A. I.; Ockwig, N. W.; O'Keeffe, M.; Matzger, A. J.; Yaghi, O. M., Porous, Crystalline, Covalent Organic Frameworks. *Science* **2005**, *310*, 1166.
- (50) Ravikovitch, P. I.; Vishnyakov, A.; Russo, R.; Neimark, A. V., Unified Approach to Pore Size Characterization of Microporous Carbonaceous Materials from N₂, Ar, and CO₂ Adsorption Isotherms. *Langmuir* **2000**, *16*, 2311.
- (51) Ghanem, B. S.; Hashem, M.; Harris, K. D. M.; Msayib, K. J.; Xu, M. C.; Budd, P. M.; Chaukura, N.; Book, D.; Tedds, S.; Walton, A.; McKeown, N. B., Triptycene-Based Polymers of Intrinsic Microporosity: Organic Materials That Can Be Tailored for Gas Adsorption. *Macromolecules* **2010**, *43*, 5287.
- (52) Mastalerz, M.; Schneider, M. W.; Oppel, I. M.; Presly, O., A Salicylbisimine Cage Compound with High Surface Area and Selective CO₂/CH₄ Adsorption. *Angew. Chem., Int. Ed.* **2011**, *50*, 1046.
- (53) Pandey, P.; Katsoulidis, A. P.; Eryazici, I.; Wu, Y. Y.; Kanatzidis, M. G.; Nguyen, S. T., Imine-Linked Microporous Polymer Organic Frameworks. *Chem. Mater.* **2010**, *22*, 4974.

- (54) Uribe-Romo, F. J.; Hunt, J. R.; Furukawa, H.; Klock, C.; O'Keeffe, M.; Yaghi, O. M., A Crystalline Imine-Linked 3-D Porous Covalent Organic Framework. *J. Am. Chem. Soc.* **2009**, *131*, 4570.
- (55) Farha, O. K.; Spokoyny, A. M.; Hauser, B. G.; Bae, Y. S.; Brown, S. E.; Snurr, R. Q.; Mirkin, C. A.; Hupp, J. T., Synthesis, Properties, and Gas Separation Studies of a Robust Diimide-Based Microporous Organic Polymer. *Chem. Mater.* **2009**, *21*, 3033.
- (56) Dawson, R.; Adams, D. J.; Cooper, A. I., Chemical Tuning of CO₂ Sorption in Robust Nanoporous Organic Polymers. *Chem. Sci.* **2011**, *2*, 1173.
- (57) Mohanty, P.; Kull, L. D.; Landskron, K., Porous Covalent Electron-Rich Organonitridic Frameworks as Highly Selective Sorbents for Methane and Carbon Dioxide. *Nat. Commun.* **2011**, *2*, 401.
- (58) Patel, H. A.; Yavuz, C. T., Noninvasive Functionalization of Polymers of Intrinsic Microporosity for Enhanced CO₂ Capture. *Chem. Commun.* **2012**, *48*, 9989.
- (59) Phan, A.; Doonan, C. J.; Uribe-Romo, F. J.; Knobler, C. B.; O'Keeffe, M.; Yaghi, O. M., Synthesis, Structure, and Carbon Dioxide Capture Properties of Zeolitic Imidazolate Frameworks. *Acc. Chem. Res.* **2009**, *43*, 58.
- (60) Banerjee, R.; Furukawa, H.; Britt, D.; Knobler, C.; O'Keeffe, M.; Yaghi, O. M., Control of Pore Size and Functionality in Isoreticular Zeolitic Imidazolate Frameworks and Their Carbon Dioxide Selective Capture Properties. *J. Am. Chem. Soc.* **2009**, *131*, 3875.
- (61) Rowsell, J. L. C.; Yaghi, O. M., Effects of Functionalization, Catenation, and Variation of the Metal Oxide and Organic Linking Units on the Low-Pressure

- Hydrogen Adsorption Properties of Metal-Organic Frameworks. *J. Am. Chem. Soc.* **2006**, *128*, 1304.
- (62) Britt, D.; Furukawa, H.; Wang, B.; Glover, T. G.; Yaghi, O. M., From the Cover: Highly Efficient Separation of Carbon Dioxide by a Metal-Organic Framework Replete with Open Metal Sites. *Proc. Natl. Acad. Sci. U. S. A.* **2009**, *106*, 20637.
- (63) Jagiello, J.; Bandosz, T. J.; Putyera, K.; Schwarz, J. A., Adsorption near-Ambient Temperatures of Methane, Carbon Tetrafluoride, and Sulfur-Hexafluoride on Commercial Activated Carbons. *J. Chem. Eng. Data* **1995**, *40*, 1288.
- (64) Czepirski, L.; Jagiello, J., Virial-Type Thermal Equation of Gas Solid Adsorption. *Chem. Eng. Sci.* **1989**, *44*, 797.
- (65) Garibay, S. J.; Weston, M. H.; Mondloch, J. E.; Colon, Y. J.; Farha, O. K.; Hupp, J. T.; Nguyen, S. T., Accessing Functionalized Porous Aromatic Frameworks (PAFs) through a De Novo Approach. *CrystEngComm* **2013**.
- (66) McDonald, T. M.; Lee, W. R.; Mason, J. A.; Wiers, B. M.; Hong, C. S.; Long, J. R., Capture of Carbon Dioxide from Air and Flue Gas in the Alkylamine-Appended Metal–Organic Framework Mmen-Mg₂(Dobpdc). *J. Am. Chem. Soc.* **2012**, *134*, 7056.
- (67) Wilmer, C. E.; Farha, O. K.; Bae, Y.-S.; Hupp, J. T.; Snurr, R. Q., Structure-Property Relationships of Porous Materials for Carbon Dioxide Separation and Capture. *Energy Environ. Sci.* **2012**, *5*, 9849.
- (68) Keith, D. W.; Minh, H.-D.; Stolaroff, J. K., Climate Strategy with CO₂ Capture from the Air. *Clim. Change* **2006**, *74*, 17.

- (69) Lee, K. B.; Beaver, M. G.; Caram, H. S.; Sircar, S., Reversible Chemisorbents for Carbon Dioxide and Their Potential Applications. *Ind. Eng. Chem. Res.* **2008**, *47*, 8048.
- (70) Cheon, Y. E.; Suh, M. P., Multifunctional Fourfold Interpenetrating Diamondoid Network: Gas Separation and Fabrication of Palladium Nanoparticles. *Chem. Eur. J.* **2008**, *14*, 3961.
- (71) Xue, M.; Liu, Y.; Schaffino, R. M.; Xiang, S. C.; Zhao, X. J.; Zhu, G. S.; Qiu, S. L.; Chen, B. L., New Prototype Isoreticular Metal-Organic Framework Zn(4)O(Fma)(3) for Gas Storage. *Inorg. Chem.* **2009**, *48*, 4649.
- (72) Miller, S. R.; Wright, P. A.; Devic, T.; Serre, C.; Ferey, G.; Llewellyn, P. L.; Denoyel, R.; Gaberova, L.; Filinchuk, Y., Single Crystal X-Ray Diffraction Studies of Carbon Dioxide and Fuel-Related Gases Adsorbed on the Small Pore Scandium Terephthalate Metal Organic Framework, $\text{Sc}_2(\text{O}_2\text{CC}_6\text{H}_4\text{CO}_2)_3$. *Langmuir* **2009**, *25*, 3618.
- (73) Comotti, A.; Bracco, S.; Sozzani, P.; Horike, S.; Matsuda, R.; Chen, J.; Takata, M.; Kubota, Y.; Kitagawa, S., Nanochannels of Two Distinct Cross-Sections in a Porous Al-Based Coordination Polymer. *J. Am. Chem. Soc.* **2008**, *130*, 13664.
- (74) Ma, B. Q.; Mulfort, K. L.; Hupp, J. T., Microporous Pillared Paddle-Wheel Frameworks Based on Mixed-Ligand Coordination of Zinc Ions. *Inorg. Chem.* **2005**, *44*, 4912.
- (75) Bae, Y. S.; Mulfort, K. L.; Frost, H.; Ryan, P.; Punnathanam, S.; Broadbelt, L. J.; Hupp, J. T.; Snurr, R. Q., Separation of CO_2 from CH_4 Using Mixed-Ligand Metal-Organic Frameworks. *Langmuir* **2008**, *24*, 8592.

- (76) Wang, Q. M.; Shen, D. M.; Bulow, M.; Lau, M. L.; Deng, S. G.; Fitch, F. R.; Lemcoff, N. O.; Semanscin, J., Metallo-Organic Molecular Sieve for Gas Separation and Purification. *Microporous Mesoporous Mater.* **2002**, *55*, 217.
- (77) Chowdhury, P.; Bikkina, C.; Meister, D.; Dreisbach, F.; Gumma, S., Comparison of Adsorption Isotherms on Cu-Btc Metal Organic Frameworks Synthesized from Different Routes. *Microporous Mesoporous Mater.* **2009**, *117*, 406.
- (78) Liang, Z. J.; Marshall, M.; Chaffee, A. L., CO₂ Adsorption-Based Separation by Metal Organic Framework (Cu-Btc) Versus Zeolite (13x). *Energy Fuels* **2009**, *23*, 2785.
- (79) Llewellyn, P. L.; Bourrelly, S.; Serre, C.; Vimont, A.; Daturi, M.; Hamon, L.; De Weireld, G.; Chang, J. S.; Hong, D. Y.; Hwang, Y. K.; Jhung, S. H.; Ferey, G., High Uptakes of CO₂ and CH₄ in Mesoporous Metal-Organic Frameworks MIL-100 and MIL-101. *Langmuir* **2008**, *24*, 7245.
- (80) Miller, S. R.; Pearce, G. M.; Wright, P. A.; Bonino, F.; Chavan, S.; Bordiga, S.; Margiolaki, I.; Guillou, N.; Feerey, G.; Bourrelly, S.; Llewellyn, P. L., Structural Transformations and Adsorption of Fuel-Related Gases of a Structurally Responsive Nickel Phosphonate Metal-Organic Framework, Ni-Sta-12. *J. Am. Chem. Soc.* **2008**, *130*, 15967.
- (81) Dietzel, P. D. C.; Besikiotis, V.; Blom, R., Application of Metal-Organic Frameworks with Coordinatively Unsaturated Metal Sites in Storage and Separation of Methane and Carbon Dioxide. *J. Mater. Chem.* **2009**, *19*, 7362.

- (82) Caskey, S. R.; Wong-Foy, A. G.; Matzger, A. J., Dramatic Tuning of Carbon Dioxide Uptake Via Metal Substitution in a Coordination Polymer with Cylindrical Pores. *J. Am. Chem. Soc.* **2008**, *130*, 10870.
- (83) Bae, Y. S.; Farha, O. K.; Spokoyny, A. M.; Mirkin, C. A.; Hupp, J. T.; Snurr, R. Q., Carborane-Based Metal-Organic Frameworks as Highly Selective Sorbents for CO₂ over Methane. *Chem. Commun.* **2008**, 4135.
- (84) Cheon, Y. E.; Suh, M. P., Selective Gas Adsorption in a Microporous Metal-Organic Framework Constructed of Co(4)(II) Clusters. *Chem. Commun.* **2009**, 2296.
- (85) Chen, B. L.; Ma, S. Q.; Hurtado, E. J.; Lobkovsky, E. B.; Zhou, H. C., A Triply Interpenetrated Microporous Metal-Organic Framework for Selective Sorption of Gas Molecules. *Inorg. Chem.* **2007**, *46*, 8490.
- (86) Bastin, L.; Barcia, P. S.; Hurtado, E. J.; Silva, J. A. C.; Rodrigues, A. E.; Chen, B., A Microporous Metal-Organic Framework for Separation of CO₂/N₂ and CO₂/CH₄ by Fixed-Bed Adsorption. *J. Phys. Chem. C* **2008**, *112*, 1575.
- (87) Cheon, Y. E.; Park, J.; Suh, M. P., Selective Gas Adsorption in a Magnesium-Based Metal-Organic Framework. *Chem. Commun.* **2009**, 5436.
- (88) Bourrelly, S.; Llewellyn, P. L.; Serre, C.; Millange, F.; Loiseau, T.; Férey, G., Different Adsorption Behaviors of Methane and Carbon Dioxide in the Isotypic Nanoporous Metal Terephthalates Mil-53 and Mil-47. *J. Am. Chem. Soc.* **2005**, *127*, 13519.

- (89) Llewellyn, P. L.; Bourrelly, S.; Serre, C.; Filinchuk, Y.; Ferey, G., How Hydration Drastically Improves Adsorption Selectivity for CO₂ over CH₄ in the Flexible Chromium Terephthalate Mil-53. *Angew. Chem., Int. Ed.* **2006**, *45*, 7751.
- (90) Galli, S.; Masciocchi, N.; Tagliabue, G.; Sironi, A.; Navarro, J. A. R.; Salas, J. M.; Mendez-Linan, L.; Domingo, M.; Perez-Mendoza, M.; Barea, E., Polymorphic Coordination Networks Responsive to CO₂, Moisture, and Thermal Stimuli: Porous Cobalt(II) and Zinc(II) Fluoropyrimidinolates. *Chem. Eur. J.* **2008**, *14*, 9890.
- (91) Choi, H. S.; Suh, M. P., Highly Selective CO₂ Capture in Flexible 3D Coordination Polymer Networks. *Angew. Chem., Int. Ed.* **2009**, *48*, 6865.
- (92) Bae, Y. S.; Farha, O. K.; Hupp, J. T.; Snurr, R. Q., Enhancement of CO₂/N₂ Selectivity in a Metal-Organic Framework by Cavity Modification. *J. Mater. Chem.* **2009**, *19*, 2131.
- (93) Neofotistou, E.; Malliakas, C. D.; Trikalitis, P. N., Unprecedented Sulfone-Functionalized Metal-Organic Frameworks and Gas-Sorption Properties. *Chem. Eur. J.* **2009**, *15*, 4523.
- (94) Couck, S.; Denayer, J. F. M.; Baron, G. V.; Remy, T.; Gascon, J.; Kapteijn, F., An Amine-Functionalized Mil-53 Metal-Organic Framework with Large Separation Power for CO₂ and CH₄. *J. Am. Chem. Soc.* **2009**, *131*, 6326.
- (95) Dreisbach, F.; Staudt, R.; Keller, J. U., High Pressure Adsorption Data of Methane, Nitrogen, Carbon Dioxide and Their Binary and Ternary Mixtures on Activated Carbon. *Adsorption* **1999**, *5*, 215.

- (96) Babarao, R.; Dai, S.; Jiang, D. E., Functionalizing Porous Aromatic Frameworks with Polar Organic Groups for High-Capacity and Selective CO₂ Separation: A Molecular Simulation Study. *Langmuir* **2011**, *27*, 3451.
- (97) An, J.; Geib, S. J.; Rosi, N. L., High and Selective CO₂ Uptake in a Cobalt Adeninate Metal-Organic Framework Exhibiting Pyrimidine- and Amino-Decorated Pores. *J. Am. Chem. Soc.* **2010**, *132*, 38.
- (98) Reich, T. E., Designed Synthesis of Halogenated Borazine-Linked Polymers and Their Applications in Gas Storage and Separation. PhD. Dissertation, Virginia Commonwealth University, Richmond, VA, **2011**.
- (99) Myers, A. L.; Prausnitz, J. M., Thermodynamics of Mixed-Gas Adsorption. *AIChE J.* **1965**, *11*, 121.
- (100) Lewiński, J.; Kaczorowski, T.; Prochowicz, D.; Lipińska, T.; Justyniak, I.; Kaszkur, Z.; Lipkowski, J., Cinchona Alkaloid–Metal Complexes: Noncovalent Porous Materials with Unique Gas Separation Properties. *Angew. Chem., Int. Ed.* **2010**, *49*, 7035.

Vita

Timur İslamoğlu

2359 Hickory Creek Ct. Apt. 3C

Richmond, VA 23294

islamoglut@vcu.edu, tmrislamoglu@gmail.com

Date and Place of Birth:

August 30, 1985; İkizdere, Rize, Turkey

Academic Preparation:

Dumlupınar University, Kutahya, Turkey Chemistry B.Sc., 2008

Dumlupınar University, Kutahya, Turkey Mathematics (Double Major) B.Sc., 2009

Virginia Commonwealth University, Richmond, VA USA Chemistry M.Sc, 2013

Professional Appointments

Sept 2009 – Jan 2010 Research Assistant, Department of Chemistry, Mehmet Akif Ersoy University, Burdur, Turkey.

Publications

İslamoğlu, T.; Rabbani, M. G.; El-Kaderi, H. M. "Impact of post-synthesis modification of nanoporous organic frameworks on small gas uptake and selective CO₂ capture"

(in preparation).

Kahveci, Z.; **Islamoglu, T.**; Shar, G. A.; Ding, R.; El-Kaderi, H. M., Targeted synthesis of a mesoporous triptycene-derived covalent organic framework. *CrystEngComm* **2013** (DOI: 10.1039/C2CE26487K).

Oral Presentations

Islamoglu, T “Catalytic Incorporation of Carbon Dioxide into Biodegradable Polymers”, Virginia Commonwealth University (Richmond, VA), November 1, **2012**.

Poster Presentations

Islamoglu, T.; Rabbani, M. G.; El-Kaderi, H. M. “Post-Synthesis Modification of Nanoporous Organic Framework for Highly Selective CO₂ Capture.” Virginia Commonwealth University (Richmond, VA), October 12, **2012**.

Participated Meetings & Expositions

243rd American Chemical Society National Meeting & Exposition, San Diego, CA
March 25-29, 2012

Awards, Scholarships, and Honors

2008 Undergraduate Honor Degree in Chemistry, Dumlupinar University, Turkey

2008 Full - Scholarship granted by Prime Minister for graduate education at Dumlupinar University

2009 Full - Scholarship granted by Republic of Turkey Ministry of National Education for English Learning Program in the Marmara University, Istanbul, Turkey

2009 Full - Scholarship granted by Republic of Turkey Ministry of National Education for graduate education at Virginia Commonwealth University

Professional Affiliations

American Chemical Society